

THE UNIVERSITY OF CALGARY

THE RECOVERY OF METALS FROM COAL ASH
BY HIGH TEMPERATURE CHLORINATION
IN A FLUIDIZED BED REACTOR

by

ANIL KUMAR MEHROTRA

A THESIS

SUBMITTED TO THE FACULTY OF GRADUATE STUDIES
IN PARTIAL FULFILLMENT OF THE REQUIREMENTS FOR THE
DEGREE OF DOCTOR OF PHILOSOPHY IN ENGINEERING

DEPARTMENT OF CHEMICAL ENGINEERING

CALGARY, ALBERTA

APRIL, 1980

© ANIL K. MEHROTRA 1980

THE UNIVERSITY OF CALGARY
FACULTY OF GRADUATE STUDIES

The undersigned certify that they have read, and recommend to the Faculty of Graduate Studies for acceptance, a thesis entitled,

"THE RECOVERY OF METALS FROM COAL ASH BY HIGH TEMPERATURE CHLORINATION IN A FLUIDIZED BED REACTOR",

submitted by Anil Kumar Mehrotra in partial fulfillment of the requirements for the degree of Doctor of Philosophy in Engineering.

W. Svrcek

Supervisor, Dr. W. Y. Svrcek
Department of Chemical Engineering

P. R. Bishnoi

Co-supervisor, Dr. P. R. Bishnoi
Department of Chemical Engineering

L. A. Behie

Dr. L. A. Behie
Department of Chemical Engineering

R. Joshi

Dr. R. Joshi
Department of Civil Engineering

Maurice A. Bergougnon

External Examiner
Dr. M. A. Bergougnon
University of Western Ontario

April 15 , 1980.

ABSTRACT

Coal ash is identified as an important mineral source for a variety of metals. A chlorination route is suggested to transform metals into their chlorides. The feasibility of the chlorination route is demonstrated by equilibrium calculations using the minimization of Gibbs free energy technique. A total of 12 elements and more than 135 chemical species were included for the equilibrium computations. The presence of a reducing agent is found necessary in order for the chlorination of aluminum to take place.

High temperature chlorination of 4 metal fractions was investigated experimentally using an 8 cm diameter fluidized bed reactor. The extent of conversion is low when carbon monoxide is the only reducing agent. With the addition of carbon to the reacting ash, the chlorination of aluminum improved significantly. At temperatures above 900°C, about 25% of aluminum in ash could be chlorinated in 2 hours. Although the reactions are sufficiently fast initially, a sharp decline in the rates of reaction is observed after an initial 10 minute period.

The effect of temperature, particle diameter and gas composition are studied with a factorial design of experiments. The chlorination of aluminum above 900°C

is unaffected by a variation in temperature. Reducing the particle size and increasing Cl_2/CO ratio have beneficial effects on the extent of aluminum chlorination.

The initial global reaction rate for aluminum is at least 5 to 8 times faster than that for the later period. The chlorides of alkali and alkali earth metals retard further chlorination of aluminum and other metals. The presence of these chlorides after chlorination is confirmed by surface area measurements, the differential thermal analysis and the water solubility studies. The decline in reaction rates is due to the slow diffusion of gaseous components through a film of molten chlorides.

The study indicates a possibility of chlorinating metals in ash. Further attempts are needed to improve the conversion of aluminum. This study has provided an important insight into the process of ash chlorination.

ACKNOWLEDGEMENT

The author wishes to express his gratitude to Dr. W.Y. Svrcek and Dr. P.R. Bishnoi for their guidance, encouragement, support and supervision of this project. The many valuable suggestions made by Dr. L.A. Behie are gratefully acknowledged.

The author also wishes to thank Mr. Vince Kraus, Mr. Ron Marshall and other staff of the Chemical Engineering workshop for their assistance. The prompt and excellent analytical work of Mr. Larry Dornan and Mrs. Pat Towle deserves special mention. The cooperation of Dr. Nancy Cyer of Research Council of Alberta in connection with DTA studies is gratefully acknowledged. The assistance of Mr. D. Lindsay for the glass blowing work is deeply appreciated.

The financial support from the Izaak Walton Killam Scholarship Trust, Natural Sciences and Engineering Research Council of Canada and the Department of Chemical Engineering is gratefully appreciated.

The author also wishes to thank his fellow graduate students for their friendship and assistance. The author remains indebted to his wife and parents for their understanding and encouragement throughout the course of this work.

Dedicated
to my wife,
Rashmi,
and my parents.

TABLE OF CONTENTS

	Page
ABSTRACT.....	iii
ACKNOWLEDGEMENT.....	v
LIST OF TABLES.....	xi
LIST OF FIGURES.....	xiii
LIST OF PHOTOGRAPHS.....	xvi
NOMENCLATURE.....	xvii

Chapter

1. INTRODUCTION.....	1
1.1 General Introduction.....	1
1.2 Research Objectives and Scope.....	4
2. LITERATURE REVIEW.....	7
2.1 Formation of Coal Ash.....	7
2.2 Chemical Characteristics of Coal Ash.....	7
2.3 Chlorination of Pure Metal Oxides.....	11
2.4 Recovery of Alumina from Ash.....	18
2.5 Chemistry of Chlorination Reactions..	19
2.6 Aluminum Chloride from Ash.....	22
2.7 Summary.....	26
3. THERMODYNAMIC ANALYSIS BY FREE ENERGY MINIMIZATION.....	27
3.1 General Description.....	27
3.2 Purpose of the Equilibrium Calculations.....	29
3.3 System Description.....	29
3.4 Application of Gibbs Phase Rule.....	31
3.5 Fly Ash Composition.....	35
3.6 Discussion of Results.....	37
3.6.1 Oxides-Carbon-Chlorine System..	37
3.6.2 Oxides-Carbon monoxide- Chlorine System.....	41
3.6.3 Effect of Temperature.....	46
3.6.4 Oxides-Sulfur-Chlorine System..	46
3.7 Recycle of Silicon Tetrachloride.....	48
3.8 Summary and Conclusions.....	53

Chapter	Page
4. EXPERIMENTAL.....	55
4.1 Introduction.....	55
4.2 Description of Apparatus.....	56
4.3 Characteristics of the Fluid-bed Reactor.....	60
4.4 Procedure for Chlorination Experiments.....	66
4.4.1 Rotameter Calibration.....	66
4.4.2 Calibration of Thermocouples...	66
4.4.3 Preparations for Experimental Runs.....	67
4.4.4 Experimental Runs.....	68
4.5 Condensation of Metal Chlorides.....	71
4.6 Products of Chlorination.....	79
5. MATERIALS AND METHODS.....	82
5.1 Characteristics of Ash.....	82
5.1.1 Particle Size Distribution.....	82
5.1.2 Density.....	84
5.1.3 Volatile Fraction.....	84
5.1.4 Moisture Content.....	86
5.2 Chemical Analysis of Ash.....	86
5.3 Acid Leaching of Ash.....	88
5.4 Thermal Behaviour of Ash.....	90
5.4.1 The Differential Thermal Analysis.....	91
5.4.2 Thermograms for Ash Samples....	92
5.5 Surface Characteristics.....	95
5.5.1 Microscopic Studies.....	95
5.5.2 Surface Area Determination.....	101
5.5.3 Surface Loss During Chlorination.....	104
5.6 Factorial Design of Experiments.....	109
6. PRESENTATION OF RESULTS: CHLORINATION OF OF ASH WITH CARBON MONOXIDE.....	110
6.1 Exploratory Runs at Low Temperatures.	110
6.2 Effect of Temperature.....	111
6.3 Effect of Particle Diameter.....	113
6.4 Effect of Gas Composition.....	115
6.5 Effect of Ash Type.....	117
6.6 Reduction in Reaction Rate.....	117
6.6.1 Chlorination of Alkali Metals..	120
6.6.2 Generation of Liquid Melt.....	120
6.6.3 DTA Thermograms of Spent Ash..	121
6.6.4 Handling of Melt.....	121
6.7 Sources of Error.....	123
6.8 Summary.....	126

Chapter	Page
7. PRESENTATION OF RESULTS: CHLORINATION OF ASH WITH CARBON AND CARBON MONOXIDE.....	127
7.1 Carbon to Ash Ratio.....	127
7.2 Role of Each Reducing Agent.....	129
7.3 Effect of Temperature.....	134
7.4 Effect of Particle Size.....	139
7.5 Effect of Gas Composition.....	142
7.6 DTA Thermograms of Spent Ash-Coke Mixtures.....	146
7.7 Sources of Error.....	146
8. DISCUSSION OF RESULTS.....	149
8.1 Factorial Design of Experiments.....	149
8.1.1 Selection of Process Variables.....	149
8.2 Analysis of Variance Tables.....	150
8.3 Analysis of Temperature Variation.....	158
8.4 Analysis of Particle Diameter.....	159
8.5 Analysis of Cl ₂ /CO Gas Ratio.....	161
8.6 Two-Factor Interactions.....	162
8.7 Time Dependence of Reaction Rate.....	163
8.8 Significance of Chemical Kinetics Step.....	164
8.9 Reaction of Compounds with Varying Structures.....	168
8.10 Simultaneous Chlorination of Other Metals.....	171
8.10.1 Existence of Molten Chlorides in Bed.....	171
8.10.2 Reduction in Particle Surface Area.....	172
8.10.3 Gaseous Diffusion through Molten Salts.....	173
8.10.4 Rate of Diffusion Estimation..	173
8.10.5 Experimental Chlorine Consumption Rate.....	174
8.10.6 Validity of the Model.....	176
8.11 Comparison of Results with Published Data.....	177
8.11.1 Chlorination of Georgia Clay..	178
8.11.2 Chlorination of Ash in Packed Bed.....	179
8.12 Summary.....	181
9. CONCLUSIONS AND RECOMMENDATIONS.....	183
9.1 Conclusions.....	183
9.2 Recommendations for Future Research..	186

Chapter	Page
REFERENCES.....	188
APPENDICES.....	194
I. Mathematics of Free Energy Minimization..	195
I.1 The Derivation.....	195
I.2 Limitation on Number of Phases.....	197
II. Design of 3-Factor Experiments.....	201
II.1 3-Factor Complete Factorial Experiments.....	201
II.2 Interpretation of Experimental Data..	201
II.3 The Sum of Squares.....	202
II.3.1 Correction for the Mean.....	203
II.3.2 Main Effect.....	203
II.3.3 Two-Factor Interaction.....	203
II.3.4 Three-Factor Interaction.....	204
II.3.5 Total Sum of Squares.....	204
III. Experimental Data Tables.....	206
IV. Gaseous Diffusion in Molten Salts.....	220
IV.1 Physical Properties Estimation.....	220
IV.2 Rate of Diffusion.....	222
IV.3 Comparison with Experimental Rates...	224

LIST OF TABLES

Table	Title	Page
2.1	Major Metal Constituents in Fly Ash..	9
2.2	Minor Metal Constituents in Fly Ash..	12
3.1	Heat of Reaction for Chlorination Reactions.....	28
3.2	Important Compounds and their Melting and Sublimation Temperatures.....	34
3.3	Reactants for Average Ash Composition	36
4.1	Operating Conditions for Gas-Liquid Columns.....	61
4.2	Characteristics of the Fluid-bed Reactor.....	64
4.3	Correlation of Condensed to Total Metal Chlorides.....	73
4.4	Fraction of Metals Recovered by Condensation.....	77
4.5	Correlation of Fraction Condensed with Flow Rate.....	78
5.1	Physical Properties of Ash Fractions.	85
5.2	Metals in Coal Ash.....	87
5.3	Some Compounds Showing Phase Change in Temperature Range 400-1400°C...	96
5.4	Specific Surface Area Measurements...	102
5.5	Water Soluble Constituents in Ash Samples.....	106
5.6	Ionic Balance of Water Soluble Constituents in Ash.....	108

LIST OF TABLES
(continued)

Table	Title	Page
6.1	Summary of Chlorination Experiments with CO as the Reducing Agent.....	112
6.2	Estimates of Error by Material Balance Calculations.....	124
7.1	Summary of Chlorination Experiments with Carbon and CO as Reducing Agents.....	128
7.2	Estimates of Error by Material Balance Calculations.....	148
8.1	Arrangement for (2x2x2) Three Factor Complete Factorial Experiment.....	151
8.2	Sums of Squares for Aluminum, Iron and Silicon.....	152
8.3	Significance Test with F-distribution Points.....	154
8.4	Significance Test with one 2-factor Effect Pooled with the Error Estimate.....	155
8.5	Direction of Main Effect for Each Factor.....	157
8.6	Global Reaction Rate for Aluminum (Initial and Straight Line Sections).....	167
II.1	Analysis of Variance for Complete 3-Factor Factorial Experiments....	205
IV.1	Calculation of Chlorine Consumption Rate.....	226

LIST OF FIGURES

Figure	Title	Page
3.1	Computational Flow Scheme.....	32
3.2	Chlorination with Stoichiometric Amount of Carbon.....	38
3.3	Distribution of Aluminum Compounds with C and Cl ₂	40
3.4	Chlorination with Stoichiometric Amount of CO.....	42
3.5	Distribution of Aluminum Compounds with CO and Cl ₂	43
3.6	Chlorination with Limiting Amount of CO.....	45
3.7	Effect of Temperature on Equilibrium Composition.....	47
3.8	Chlorine Requirement with SiCl ₄ Recycle.....	50
3.9	Aluminum Chlorides with Recycle of SiCl ₄	52
4.1	Schematic of Experimental Apparatus..	57
4.2	Quartz Fluid-bed Reactor.....	58
4.3	Pressure drop across the Bed-support.	63
4.4	Pressure drop for Fluidized Bed.....	65
4.5	Temperature History of a Typical Chlorination Experiment.....	69
4.6	Condensation of Aluminum and Iron Chloride Vapours.....	74
4.7	Condensation of Silicon and Titanium Chloride Vapours.....	75
5.1	Particle Size Distribution of Ashes by Sieve Analysis.....	83

LIST OF FIGURES
(continued)

Figure	Title	Page
5.2	Dissolution of Metal Fractions in HCl solution.....	89
5.3	DTA Thermograms for Fly Ash Samples..	93
5.4	DTA Thermograms for Bottom Ash Samples.....	94
6.1	Effect of Particle Size on Chlorination of Aluminum.....	114
6.2	Effect of Particle Size on Chlorination of Iron.....	116
6.3	Effect of Gas Composition on Aluminum Chlorination.....	118
6.4	Effect of Gas Composition on Iron Chlorination.....	119
6.5	DTA Thermograms for Spent Ash Samples of Run Numbers 8 & 10.....	122
7.1	Effect of Reducing Agents Ratio on Chlorination of Aluminum.....	130
7.2	Effect of Reducing Agents Ratio on Chlorination of Iron.....	133
7.3	Effect of Temperature on Chlorination of Aluminum.....	135
7.4	Effect of Temperature on Chlorination of Iron.....	137
7.5	Effect of Temperature on Chlorination of Silicon & Titanium.....	138
7.6	Effect of Particle Size on Aluminum Yield (for Equimolar Gas Ratio of CO and Chlorine).....	140
7.7	Effect of Particle Size on Aluminum Yield (for Chlorine Rich Gas).....	141

LIST OF FIGURES
(continued)

Figure	Title	Page
7.8	Aggregate Effect of Gas Composition on Aluminum Yield.....	143
7.9	Aggregate Effect of Gas Composition on Silicon Yield.....	144
7.10	DTA Thermograms for Spent Ash-Coke Mixtures of Run Numbers 16 & 25...	147
8.1	Time Dependence of Reaction Rate for Aluminum Chlorination.....	165
8.2	Variation in the Rate of Chlorination for two Particle Sizes.....	166
8.3	Time Dependence of Reaction Rate for Iron, Silicon and Titanium.....	169
8.4	Diffusion through Molten Salt Film...	175

LIST OF PHOTOGRAPHS

Plate	Description	Page
5.1	Fly Ash < 75 μ m [X160]	98
5.2	Fly Ash 89 μ m [X200]	98
5.3	Fly Ash 125 μ m [X200]	99
5.4	Fluid Coke 163 μ m [X200]	99
5.5	Spent Ash (# 10) [X200]	100
5.6	Spent Ash + Coke (# 21) [X200]	100

NOMENCLATURE

a	intercept of a line on ordinate axis
a_{ji}	number of atoms of element j species i
b	slope of a straight line
B_j	total kmol of element j
c	gas solubility, g/cm^3
C	number of chemical species in the system
C_f	correction for rotameter
CM	correction for mean
d_p	geometric mean particle diameter, μm
D	diffusivity, cm^2/s
E	difference (L-J), mg
f	degrees of freedom
F	free energy function for minimization
g	number of species in gas phase
G	Gibbs molar free energy, MJ/kmol
GR	gas ratio, Cl_2/CO
H_r	heat of reaction, MJ/kmol
J	amount of solid condensed, mg
k	a constant
L	total solids, mg
M	number of elemental species
MW	molecular weight of solvent
n_i	moles of species i
n_r	number of ratios of elemental abundances

N_a	molar flux, mol/h/cm ²
P	pressure, Pascals
r	correlation coefficient
r	radius of particle, cm
R	ideal gas constant, 8.314 J/mol K
S	number of condensed species
S_{max}	maximum number of condensed species
t	time, second or minute or hour
T	temperature, °C or K
W_a	total flux, mol/h or mol/s
x	number of components
X	Concentration of Cl ₂ in NaCl, mol/cm ³
y	response at a level of any block
μ	overall population mean
μ_{cp}	viscosity, cp
ϕ	number of phases
π	Lagrangian multiplier
ρ	density, g/cm ³
σ	standard error
θ	correction to μ

CHAPTER 1

INTRODUCTION

1.1 General Introduction

A significant fraction of coal burnt in thermal power plants remains as coal ash. This fraction may vary from 8 to 20 percent depending on the type and source of coal employed. With an ever increasing dependence on coal, especially through the gasification and liquefaction routes being proposed and adopted, substantial quantities of coal residue will be generated. The disposal of coal ash in an environmentally compatible manner poses a formidable task. Conventionally the coal ash from coal-utilising facilities is disposed off by burial in either surface or deep mines, that is as landfill or backfill.

In the recent years there has been an increasing number of attempts made to explore productive usages of ash. The suggested applications vary widely in nature; as diverse as road paving to waste water treatment. Other possible means of ash utilization include applications in cement manufacture, brick making, as soil conditioner and as a rubber filling agent. However, the fraction of ash employed in such applications barely exceeds 10-15% of that generated.

Concurrently, a deterioration of the naturally occurring mineral supplies is being experienced throughout the industrialized world. The continually increasing demands for the minerals are causing severe problems for the supplying countries in meeting the demand. This shortage also creates large scale price escalation. Under these circumstances, it may be in the best interest of many countries importing raw materials to develop indigenous alternatives instead of relying largely on diminishing international resources. Canada, for instance, has to satisfy its aluminum needs by depending almost completely on imported bauxite ore. As present trends in the demand for minerals of all sorts continue, the processing of inferior ores will be essential at the expense of increased extraction costs. It is at this point where coal ash could become an important mineral source. The extraction of metals from coal ash could help resolve two potential problems with: (a) a decrease in the importation of minerals, such as bauxite, with a domestic substitute and (b) elimination of the disposal of coal ash and the environmental problems associated with it.

One distinct advantage in using fly ash for the extraction of metals is that as a raw material, it is available in the "mined" and "crushed" form. This ready access of ash as a feed-stock eliminates the

costs incurred in the mining and size-reduction steps necessary with conventional ores. This should help make the substitution of other ores by fly ash commercially more viable.

The concentration of aluminum in coal ash compares well with that found in several bauxite ores(1). Other metals of increasing commercial importance that could be extracted from coal ash are iron, titanium, gallium. Should the demand for silicon increase, it can be readily obtained from ash as a by-product. Coal ash also has the potential of becoming an important mineral source for germanium, selenium, uranium, antimony, beryllium, bismuth, cadmium, molybdenum, nickel, vanadium and magnesium (1).

One factor which may have deterred the exploitation of this vast mineral resource, coal ash, is the unavailability of sufficient amount of it from a single source. However, with the development of large coal gasification and liquefaction units this concern would be precluded. Under such favourable circumstances, one could envision a giant industrial complex producing aluminum and a series of other important metals and chemicals, in proximity of a coal-based facility.

Despite the fact that several studies have been made on the extraction of metals from coal ash, much of

the work aimed at obtaining metals in their oxide form. Such an approach, in reality, attempts to obtain concentrated ore from a low-grade source. Though high recoveries of various metals from coal ash have been claimed, the processes appear to be quite involved and employ techniques such as causticization, sintering, leaching and solute extraction (2). An alternate route to extract aluminum and other metals is to chlorinate ash in the presence of a strong reducing agent at high temperature. This would result in chlorination of a majority of constituents in ash, and the produced chlorides of importance can be condensed fractionally. To obtain aluminum metal, the condensed aluminum chloride fraction is decomposed electrolytically. The technology for this electrolysis-step is commercially available (3,4,5). Interestingly, only 70 per cent as much electrical energy is needed to obtain pure metal from aluminum chloride as from bauxite. Thus the chlorination route appears to be favourable from an overall economic viewpoint.

1.2 Research Objectives and Scope

The objective of this study was to examine the reductive-chlorination process for extracting metals, aluminum in particular, as their chlorides from coal ash. An important first step in studying any reaction route is to explore the thermodynamic feasibility of

the reaction system. This was achieved by employing the minimization of Gibbs free energy technique. It was found that the chlorination reactions would proceed favourably over a wide range of temperature, but only in the presence of a reducing agent (6). Beyond 1200 K, the chlorination of aluminum in ash is shown to be restricted due to predominance of the reverse reaction.

Coal ash samples were obtained from a power plant in Central Alberta. The results presented in this study are those that were obtained with the available ash samples. Several physical and chemical properties of the available ash samples were determined. Sieve analyses of the fly ash sample indicates that about 65% of the particles are smaller than 75 μ m. The chemical analyses show the aluminum content in all fractions to be about 15-16%. The Differential Thermal Analysis (DTA) tests were performed for a number of ash samples before and after the chlorination runs. The results, in general, indicate phase transformations that take place when ash is heated to about 1200 $^{\circ}$ C. Particle surface measurements and water solubility tests were performed to show the presence of alkali and alkali earth metals as their chlorides after chlorination.

The chlorination reactions over a wide temperature range were studied in a fluidized bed reactor made of

quartz. The overall rates of reaction were observed to be quite slow upto a temperature of about 800°C with carbon monoxide as the reducing agent. Increasing the temperature beyond 820°C resulted in the formation of a liquid melt which severely disrupted the operation of the fluid-bed. This occurrence was even more prominent with smaller diameter ash particles. In order to achieve higher reactor temperatures, ash was premixed with coke from the fluid-bed coking unit. This helped in maintaining fluidized conditions in the bed at temperatures upto 950°C. The effects of 3 reaction parameters were studied at 2 levels each according to a factorial design of experiments. The reaction parameters are temperature, ash particle size and chlorine/carbon monoxide ratio in the reaction gas.

The initial global reaction rates for aluminum are 5 to 8 times faster than that for the later period. The decline in reaction rates is due to the simultaneous chlorination of alkali and alkali earth metals. The chlorides of these metals exist as liquid at the reaction temperatures. The presence of the liquid over the reacting ash surface adds an additional mass transfer resistance. This results in a slow down of the chlorination reactions.

CHAPTER 2

LITERATURE REVIEW

2.1 Formation of Coal Ash

When pulverized coal is burned in the fire box of a boiler about two-thirds of the residual ash leaves the furnace with the exit flue gas (7). This ash is in the form of finely divided suspended particles which are mostly trapped by means of electrostatic precipitators, cyclones or collector bags (8). The remainder of ash leaves as bottom ash; the portion of ash which slags and falls into the pit below the furnace. Coal burns rapidly at a temperature of $1500+200^{\circ}\text{C}$, and as a result many of the minerals originally present in the coal undergo chemical and physical changes (8). The composition of ash varies considerably with the minerals originally present in coal, and it depends upon the combustion temperature and the residence time of ash at high temperatures. The specific reaction environment surrounding a burning coal particle may also affect the ash characteristics. Thus the formation of coal ash is influenced by several factors.

2.2 Chemical Characteristics of Coal Ash

Coal ash can be visualized as a mixture of particles of complex mineral composition (8;9,10). The

mineral fraction in coal can be either linked with the organic part of the light fraction or as individual formations well separated from it (11). The mineral content of fly ash, determined by X-ray diffraction, is primarily quartz, mullite ($3\text{Al}_2\text{O}_3 \cdot 2\text{SiO}_2$) with hematite ($\alpha\text{-Fe}_2\text{O}_3$), magnetite (Fe_3O_4), silica and gypsum (12,13,14). It is found that the particles are colourless to green, broken, hollow spheres, ellipsoids and teardrop along with irregular shapes.

Chemically, the glassy fly ash contains aluminum, silicon, calcium, magnesium, iron and several other minor and many trace elements as oxides, silicates, aluminates, sulfates and carbonates (12). Most of the iron in fly ash is not chemically bonded with aluminum or silicon (14). In general, bituminous type ash contains more iron oxide than calcium plus magnesium oxides, whereas lignite-type has more calcium plus magnesium than iron oxide (14). Bottom ash is chemically and physically similar to fly ash except for the larger diameter particles. The chemical composition of the sub-micron fraction, approximately 10% of fly ash, is found to be considerably different from the bulk (15). In Table 2.1, some of the analyses of coal ash available in the literature have been listed.

Aluminum and silicon are frequently referred to as the acidic constituents. Their origin is primarily as

Source Element	Metal Content in Ash, % by weight					
	Wright and Roffman (1)	Behie Alberta (18)	Tibbetts CANMET (16)	Fisher et al (17)	Chakrabarti India (13)	Abel and Rancitelli (42)
Silicon	9.4-21.5	25.3	20.9	28.4	22.3
Aluminum	9.2-21.5	12.8	15.9	14.1	13.8	12.6
Iron	5.3-23.0	3.1	3.0	2.9	7.0	6.5
Calcium	0.1- 4.4	6.2	9.7	2.3	2.9	...
Sodium	0.2- 0.6	2.0	1.4	1.8	...	0.4
Potassium	1.0- 2.0	0.5	0.3	0.8	...	1.7
Titanium	0.8- 1.2	0.4	0.3	0.7	...	0.8
Magnesium	0.2- 0.7	0.7	0.5	0.6	...	2.1

Table 2.1 Major Metal Constituents in Fly Ash.

extraneous ash and they are, to a large extent, responsible for the innocuous particle material in the flue gas (19). Iron, calcium and magnesium are also found in the extraneous portion of ash, but to lesser degrees. The latter three elements, together with sodium and potassium, constitute the basic portion of ash. As individual constituents, the two acidic ingredients have high melting points. The acidic and basic constituents could combine during combustion to produce low melting point compounds. Sodium and potassium generally volatilize in the furnace. The alkalies thus released, especially from high sulfur coals, tend to form complex aluminum or iron alkali sulfates. These sulfates have lower melting temperatures, in the vicinity of 810-977 K. An important thermochemical transformation takes place during ashing of coal at around 800°C. The ashing results in liberation of calcium oxide which combines with oxides of sulfur to form calcium sulfate (11). It is important to note that calcium sulfate is a low melting point substance, which would create a liquid phase when the ash is heated to high temperatures.

Fly and bottom ashes also contain a variety of trace elements. The smaller fly ash particles show a significant enrichment of several volatile trace elements. The enrichment of trace elements involves the

volatilization of these elements during combustion followed by condensation or adsorption over non-volatile oxides of aluminum, silicon and magnesium (20). The elements Ti, Al, Mg, K, Na have a smaller fraction volatilized during combustion. Also there is an inverse concentration dependence upon particle size for many trace elements (20). Several analyses for trace elements in coal ash are listed in Table 2.2.

2.3 Chlorination of Pure Metal Oxides

The chlorination reactions to obtain metal chlorides from the oxides have been studied quite extensively in the past. This route provides an efficient means of acquiring metals in pure form. Generally, chlorine alone is employed as the reaction medium at high temperature for a host of metals. But there are certain metals having high affinity for oxygen, and the presence of a strong reducing agent, such as carbon, is necessitated. In most instances, the product chlorides are volatile at the reaction temperatures, hence the metal chlorides are easily separable.

Piccolo et al (21) studied the chlorination of alumina in the presence of calcined petroleum coke in a fluidized bed reactor. The results were expressed in terms of the fraction of chlorine consumed in a tall fluid bed (height 85 cm). They found that increasing temperature and the particle surface area result in

Source Element	Metal Content in ash, ppm			
	Wright and Roffman (1)	Behie, Alberta (18)	Fisher et al (17)	Abel and Rancitelli (42)
Barium	10,000	5,000-10,000	1,680-4,090	3,400
Strontium	500	3,000	410-700	1,900
Manganese	300	100	209-309	489
Vanadium	200	300	86-327	220
Chromium	60	<50	28-71	131
Rubidium	51-57	124
Arsenic	11	..	14-132	61
Lanthanum	62-69	82
Cobalt	<10	..	9-21	40
Thorium	26-30	28

Table 2.2 Minor Metal Constituents in Fly Ash.

improved chlorine consumption. The optimum carbon-alumina ratio was close to the stoichiometric composition. The temperature range studied was between 900 to below 1100°C. However, neither the conversion of alumina nor the duration of experimental runs were mentioned. The heat released from the reactions was sufficient to maintain the process temperature.

In another study on chlorination of alumina (22), the reactions were reported to proceed according to the thermodynamic calculations to yield AlCl_3 . At 1200-1450°C, the partial formation of aluminum monochloride was predicted, but the reverse reaction dominated when the products were allowed to cool. Interestingly, beads of metallic aluminum were also observed to form inside the reaction tube at 1200°C. However, the thermodynamic calculations of Spinella et al (23) contradict the possibility of the formation of AlCl at the reaction temperatures. It was stated that the role of AlCl in vapour-phase transport of aluminum into the cooler zone is completely negligible. The main chlorination product, predicted thermodynamically, was AlCl_3 , with a much smaller fraction represented by AlCl_2 .

In an attempt to purify bauxite by removing the iron fraction, the chlorination with CO-Cl_2 mixture resulted in the removal of iron but only at the expense

of aluminum which also reacted with the chlorine. Holliday and Milne (24), however, found that sulfidization of iron to FeS prior to the chlorination step permits beneficiation of bauxite to final iron contents of 0.1 to 0.3%. With additional purification using molten aluminum or hydrogen gas, the resultant bauxite would be of ideal characteristics for aluminum production via AlCl_3 . An alternate way to remove iron oxides from bauxite was considered by Foley and Tittle (25), where the removal was carried out in two stages. The technique involved the chemical reduction of iron oxides by carbon as the first step. This was followed by the selective removal of iron species by chlorination. The reduction process was carried out with pre-calcined bauxite at 1040-1100°C. The chlorination was carried out at 500-750°C employing Cl_2 , Cl_2/N_2 , or $\text{Cl}_2/\text{N}_2/\text{CO}$ mixtures. At temperatures above 750°C the attack of alumina became significant, causing a loss of alumina and a decrease in chlorine efficiency. The final product was found to contain 0.5-1.0% Fe_2O_3 and 87-92% Al_2O_3 .

Geisser et al (26) obtained an intimate mixing of carbon and alumina prior to the alumina chlorination reactions. The combinations of reactants considered in their study were CO/Cl_2 , COCl_2 (phosgene) and C/Cl_2 in the temperature range 400-900°C. Of the three follow-

ing methods, only the cracking method produced a mixture which could be completely chlorinated:

- (a) thermo-catalytic cracking of gaseous hydrocarbons on the alumina surface at 800°C ,
- (b) carbonizing of alumina-glucose mixture, and
- (c) mechanical mixing of alumina and soot.

However, for a lower temperature chlorination in an industrial system, the CO/Cl_2 (particularly COCl_2) chlorination method would be a more attractive route. It was also indicated that the pore diffusion step could be the rate-controlling factor in determining the overall rate of reaction. The reaction times for the chlorination with CO/Cl_2 were shorter than those with carbon as the reducing agent.

The chlorination of aluminum oxide for the estimation of aluminum, titanium, chromium and iron was studied by Storozhenko (27). The product of chlorination of alumina samples was Al_2Cl_6 at about $500\text{-}550^{\circ}\text{C}$. The overall reaction rate was found to increase by approximately 10 per cent per 100°C increase in the temperature.

Landsberg (28) studied the chlorination kinetics of prepared γ -alumina and low-grade alumina source using a packed bed reactor. The rate of alumina chlorination increased gradually with an increase in reaction temperature. The reaction rates were found to

be slow when carbon was used as the reducing agent. The reactions progressed rapidly at the beginning, but much more slowly later on even though considerable amounts of bauxite had remained unreacted. This decrease in reaction rate was attributed to a reduction in surface area and the presence of less reactive components such as silicon. The initial rates for clay were also found to be high.

In an attempt to remove iron and titanium from kaolins by chlorination, Brin and Eremin (29) found that the rate of iron chlorination depended substantially on increased chlorine concentration. In the absence of any reducing agent, alumina and silica fractions did not react appreciably at 800-1000°C. Dunn (30) studied chlorination of titanium bearing minerals. The reaction rate in this case was found proportional to the partial pressures of CO and Cl₂. The chlorination with phosgene (COCl₂) was much faster than that with CO+Cl₂. The reaction rate increased with temperature, passed through a maximum, fell to a minimum and then rose with temperature as the CO+Cl₂ reaction dominated.

The chlorination route is applied to a variety of other metal oxides besides iron and aluminum. Mehra et al (31) studied the chlorination of niobium pentoxide in the presence of graphite powder. It was found that

the amount chlorinated is proportional to the partial pressure of chlorine and independent of chlorine flow. The range of temperature considered for the reactions was 600-750°C. In another study by the same group of researchers, the chlorination rate for tantalum pentoxide was found to be proportional to the square root of the partial pressure (32). In both cases, the rates were proportional to the geometric surface of the pellets.

Skeaff (33) studied the chlorination process for the extraction of uranium and thorium from their ores. The reducing agent used was carbon monoxide. He found that at higher temperatures for this case, the conversions were restricted by equilibrium considerations. The chlorination of other metals, such as silicon, iron and aluminum, was also observed to be occurring simultaneously.

Olsen and Black (34) studied the chlorination of columbite, containing niobium and tantalum fractions, in a fluidized-bed reactor. The reaction rate in the temperature range 550-650°C was independent of chlorine concentration and only a weak function of mineral concentration.

2.4 Recovery of Alumina from Ash

There have been several studies aimed at recovering aluminum as alumina from coal ash. An excellent bibliography of the work done in this direction was published by Condry (2). Out of the 24 references abstracted in this bibliography there appear to be two different approaches that have been adopted in the past. These are:

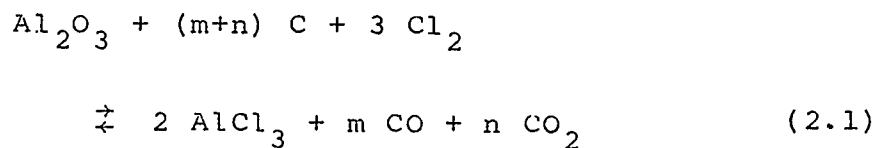
- (a) acid-leach process using sulfuric acid with other sulfates to give aluminum in ash as aluminum sulfate, and
- (b) causticization process using strong alkalies, such as KOH, NaOH, along with milder compounds such as Na_2CO_3 , $\text{Ca}(\text{OH})_2$. Aluminum hydroxide or alumina is the final form obtained with this approach.

The processes that were suggested are used frequently in extractive metallurgical operations. The steps employed include acid or caustic leaching, sintering, roasting, burning ash-caustic mixtures, etc. Though a large number of interesting options with varying success have been reported in the past, the wet-techniques required in such processes would make the separation of different metal fractions even more cumbersome. A detailed investigation into the aforementioned approaches is, however, beyond the scope

of this study.

2.5 Chemistry of Chlorination Reactions

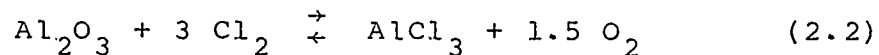
The overall process of reductive-chlorination of a metal oxide, particularly of alumina, can be summarized by the following equation:



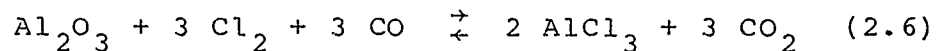
$$\text{where, } m + 2n = 3$$

Similar reactions will take place with other metallic constituents in ash. This equation can be the sum of different steps depending on the mechanism of the overall process.

Mechanism I



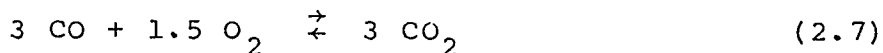
Mechanism II



Mechanism I consists of the equilibrium reaction (2.2) which, thermodynamically, strongly favours the formation of Al_2O_3 . To produce AlCl_3 it is necessary that the oxygen released be withdrawn by reactions such as (2.3) and (2.4). The heterogeneous gas-solid reaction (2.2) involves the adsorption of chlorine on ash surface, the reaction between the adsorbed chlorine with the oxide, and finally desorption of oxygen and the metal chloride from the surface of ash particles. The reaction (2.4) is homogeneous in the gas phase whereas reactions (2.3) and (2.5) are heterogeneous. Among these three reactions, reaction (2.4) is the fastest while reaction (2.5) appears to be the slowest.

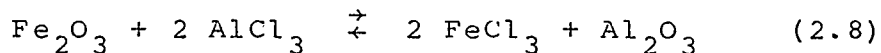
Mechanism II, on the other hand, consists only of two steps. The first step, given by equation (2.6), is a heterogeneous gas-solid reaction. According to this, CO and Cl_2 are absorbed on the ash surface giving rise to the formation of metal chlorides and CO_2 which are then desorbed. In the second step, reaction (2.5), CO_2 is reduced to CO at the expense of carbon added to the system. It is found for alumina chlorination with carbon that Mechanism II does not lead to the formation of AlCl_3 (21). However, if carbon monoxide is employed as the reducing agent, the reaction may very well progress according to this reaction mechanism.

With carbon monoxide as the reducing agent, the reaction may proceed according to the following equations:



An increase in the metal chlorination with increased chlorine partial pressure would indicate the dominance of reaction (2.2) on the overall reaction. The reaction (2.7) is a homogeneous reaction and the reaction rate is usually observed to be quite high (21).

It is of importance to note that if a mixture of gaseous chlorides is brought in contact with additional metal oxide, a series of disproportionation reactions will take place. The metals (or, their oxides) with a higher affinity for chlorine would react to form the chlorides. The chlorides of metals with the lower affinity will, subsequently, revert to the respective oxides. Equation 2.8 illustrates this situation with iron and aluminum. Iron oxide has a greater tendency to form chloride than aluminum.



During chlorination, metals can assume various valencies to give a variety of products. Aluminum, for instance, can react with chlorine to give AlCl , AlCl_2 ,

AlCl_3 , Al_2Cl_4 and also Al_2Cl_6 . The proportions in which these will form, will be dictated by thermodynamic equilibrium and influenced by the specific reaction environment. This particular aspect will be the subject of Chapter 3.

2.6 Aluminum Chloride from Ash

In general, the chlorination of pure metal oxides can be achieved relatively easily. However, chlorination of complex mixtures, such as coal ash, is inherently more involved. The presence of silicate materials further complicates the problem of ash chlorination. While recovering aluminum and other metals from minerals and ash as their chlorides, the concern is not merely to chlorinate the metals but also to avoid the chlorination of constituents of less value. Additionally, the complications can be due to the metal chlorides which do not appear as vapours below the reaction temperatures. These metal chlorides will remain within the reactor and, in particular, could hinder complete chlorination of aluminum. The metal chlorides with lower melting points but high vapourizing temperatures are those of calcium, sodium, potassium and magnesium. Thus it is evident that the chlorination of coal ash would be a lot more complex than the chlorination of metal oxides individually.

In a patented process (35), a technique was illustrated for the chlorination of aluminum rich ores. In the reaction zone of the suggested scheme, alumina and other metallic compounds are halogenated in the presence of carbon to form the corresponding chlorides. The chlorides and the inert gas are passed upward through an elongated compact gravitating bed where fractional condensation is effected. In another patent (36), the use of sulfur halide, such as S_2Cl_2 , was suggested as a means of producing $AlCl$. The disproportionment of $AlCl$ to $AlCl_3$ and aluminum is carried out in a flash condenser using $AlCl_3$ as a liquid coolant. A process for the selective recycle production of aluminum chloride required the condensation and recycle of sodium aluminum chloride to improve the chlorination of aluminum (37).

While studying the chlorination of Georgia clay with 39% Al_2O_3 , 44% SiO_2 and less than 1% Fe_2O_3 , Ujhidy et al (38) observed very slow reaction rates. As their objective was to recover aluminum as aluminum chloride, another source of concern was the simultaneous chlorination of silicon. At temperatures above $800^\circ C$, the conversion of aluminum to aluminum chloride was 25% in 2-hours. The effect of varying reaction parameters, such as temperature, alkali and alkali earth metal chlorides as catalyst, etc., was found to

be insignificant. Even the addition of solid reducing agent along with CO-Cl₂ mixture did not increase the conversion beyond 40%. However, the chlorination of granules of clay and coal at 850-930°C resulted in a yield of about 80%. But the usefulness of the process is doubtful for a large scale operation.

The chlorination of coal fly ash was investigated by Burnet et al (7). As a first step, the separation of the magnetic fraction of fly ash was suggested. This was able to isolate 10 to 25% of the high density (mostly submicron) magnetic fraction from ash (39,40). But about one-third of the iron was left with the non-magnetic fraction. The unseparated fraction represented the iron trapped in the interior of vitreous particles (39). Moreover, about 10% of the total aluminum in ash was also lost to the magnetic fraction (7).

In the chlorination step, the non-magnetic fraction of fly ash was mixed with carbon and chlorinated in a fixed bed. The remaining iron could be removed as iron chloride at lower temperatures between 400 to 600°C, at which very little silicon and aluminum reacted. By raising the temperature to 850-950°C, the aluminum and silicon fractions were chlorinated. They found that the amount of reducing agent, carbon, was not a controlling factor, but the rate of chlorine

flow had a major effect on the conversion suggesting the overall rate to be controlled by the gas phase diffusion (for their packed bed experiments). The conversion of aluminum to AlCl_3 was favoured by high temperatures. The final conversion, at the end of each run, varied from 40 to 80%. Although the exact duration of runs was not mentioned, it appears to be between 2 to 4-hours (calculated from the bulk rate data provided). The investigation with a fluidized-bed reactor, and the recycling of silicon tetrachloride along with CO were suggested.

From an experimental study, Milne (41) concluded that the addition of SiCl_4 to the chlorination gas resulted in some reduction in the amount of SiO_2 reacting. The reaction rates were also lowered significantly. The detrimental effect of SiCl_4 on the reaction rate of Al_2O_3 could be due to:

- (a) SiO_2 produced from Al_2O_3 - SiCl_4 deposited on the surface of alumina to hinder gaseous diffusion.
- (b) SiCl_4 selectively chemisorbed on alumina surface which effectively led to the poisoning of the reactive surface.

2.7 Summary

The difficulties that are anticipated while chlorinating the metals in coal ash are:

- (a) The refractory nature of ash particles may render the chlorination process very arduous.
- (b) The presence of several metals and their simultaneous chlorination may introduce complexities.
- (c) The formation of metal chlorides, such as NaCl, KCl, CaCl₂ etc., may result in a liquid phase at the reaction temperatures.

CHAPTER 3

THERMODYNAMIC ANALYSIS BY FREE ENERGY MINIMIZATION

3.1 General Description

For the estimation of equilibrium composition within a system of a number of reactive chemical substances, a convenient thermodynamic property to use is the Gibbs free energy. The procedure for arriving at a set of algebraic correlations is well documented in the literature (43,44,45,46,47). Hence only a brief description will be given here. A procedure to obtain the necessary equations is outlined in Appendix I.

The usefulness of the equilibrium composition predicted by the free energy minimization calculations is restricted largely by the role of reaction kinetics and the mass transport resistances. However, if it is presumed that at high temperatures (800-1000°C) anticipated for the chlorination reactions, the kinetic considerations do not dominate, then the thermodynamic aspect of the reactions would be the controlling factor. In fact, since the chlorination reactions are exothermic (Table 3.1), the high temperatures necessary for improved chlorination rates may very well limit the extent of conversion for the reversible chlorination reactions. Hence the feasibility of the chlorination

General Chlorination Reaction:		
$M_xO_y + \frac{y}{2} C + y Cl_2 \rightarrow x MCl_z + \frac{y}{2} CO_2$ $\text{and, } z = \frac{2y}{x}$		
Metal Oxide (M_xO_y)	Chlorinated form (MCl_z)	Heat of Reaction, ($-\Delta H_r$) _{298K} (MJ/kmol of MCl_z)
Al_2O_3	$AlCl_3$	145.6
CaO	$CaCl_2$	359.4
Fe_2O_3	$FeCl_3$	283.3
K_2O	KCl	354.8
MgO	$MgCl_2$	236.0
Na_2O	$NaCl$	301.7
SiO_2	$SiCl_4$	173.2
TiO_2	$TiCl_4$	211.3

Table 3.1 Heat of Reaction for Chlorination Reactions.

reaction route can be effectively tested with these calculations.

3.2 Purpose of the Equilibrium Calculations

The purpose of the outlined free energy minimization calculations is to explore the following important features (6):

- (i) the possibility of recovering aluminum and other important metals as chlorides from fly ash from a thermodynamic view-point,
- (ii) selective recovery of aluminum from chiefly a mixture containing oxides of silicon, aluminum, iron and calcium,
- (iii) ratio of fly ash and chlorine and/or other reactants necessary for complete recovery of aluminum,
- (iv) the effect of temperature in altering the equilibrium composition of products, and
- (v) the effect of variation in feed composition on the redistribution of reaction products.

3.3 System Description

The system for the minimization of free energy calculations is necessarily heterogeneous, consisting of "S" condensed species and "g" gaseous components. It is assumed that "S" condensed species (liquids and solids) are mutually insoluble, and that each of these exists as a pure independent phase. This assumption is

necessary due to the lack of information on solid-solid or solid-liquid solutions for many of the species under consideration. The assumption is reasonable for the fly ash system as most of the condensed species, such as aluminates, silicates, oxides, etc., exist as solids in the temperature range of interest. However, this assumption can be relaxed if sufficient thermodynamic data were to become available in future. It is further assumed that each species exists as either a condensed phase or a constituent of the gas phase mixture. This implies that the vapour pressure of a condensed species below its condensation temperature is neglected.

Assumption two avoids the requirement for consideration of component phase equilibria and thus the computational task is simplified. This, of course, may result in some inaccuracy when the calculations are performed in the vicinity of the condensation temperature of a species.

There are at least 8 metal elements, namely Si, Al, Fe, K, Na, Ca, Mg and Ti, which occur in significant concentrations in coal ash. In addition, chlorine, carbon and oxygen will be introduced to form the reaction environment. Sulfur was included to study the reaction path via S_2-Cl_2 , as suggested in the literature (48). Thus a total of 12 elements were chosen for compiling a data library. A total of over

140 non-ionic chemical species were selected with available free energy data in JANAF Tables (49,50,51). The free energy values for all of these species at 15 different temperatures (298-1700 K), and the phase transition temperatures were acquired.

In order to solve the set of $(M+S+1)$ equations given in Appendix I as Equations (I.6), (I.7) and (I.8) with $(M+S+1)$ unknowns, the following should be provided:

- (i) Non-zero initial molar amounts of all the species satisfying element balance as trial values.
- (ii) A suitable algorithm for the convergence of iterative computations.

The convergence scheme selected for this study is the method of steepest descent (52). The computational flow scheme is described as Figure 3.1. The calculations were performed on a CDC 6400 computer.

3.4 Application of Gibbs Phase Rule

Of all compounds listed for calculations, a large number of these appears as solids in the temperature range of interest. If the number of variables exceeds the degrees of freedom, the computation scheme will produce erroneous results. It is shown that the maximum number of condensed phases for one computation should be one more than the number of elemental species in the condensed phase (43,46). With temperature and

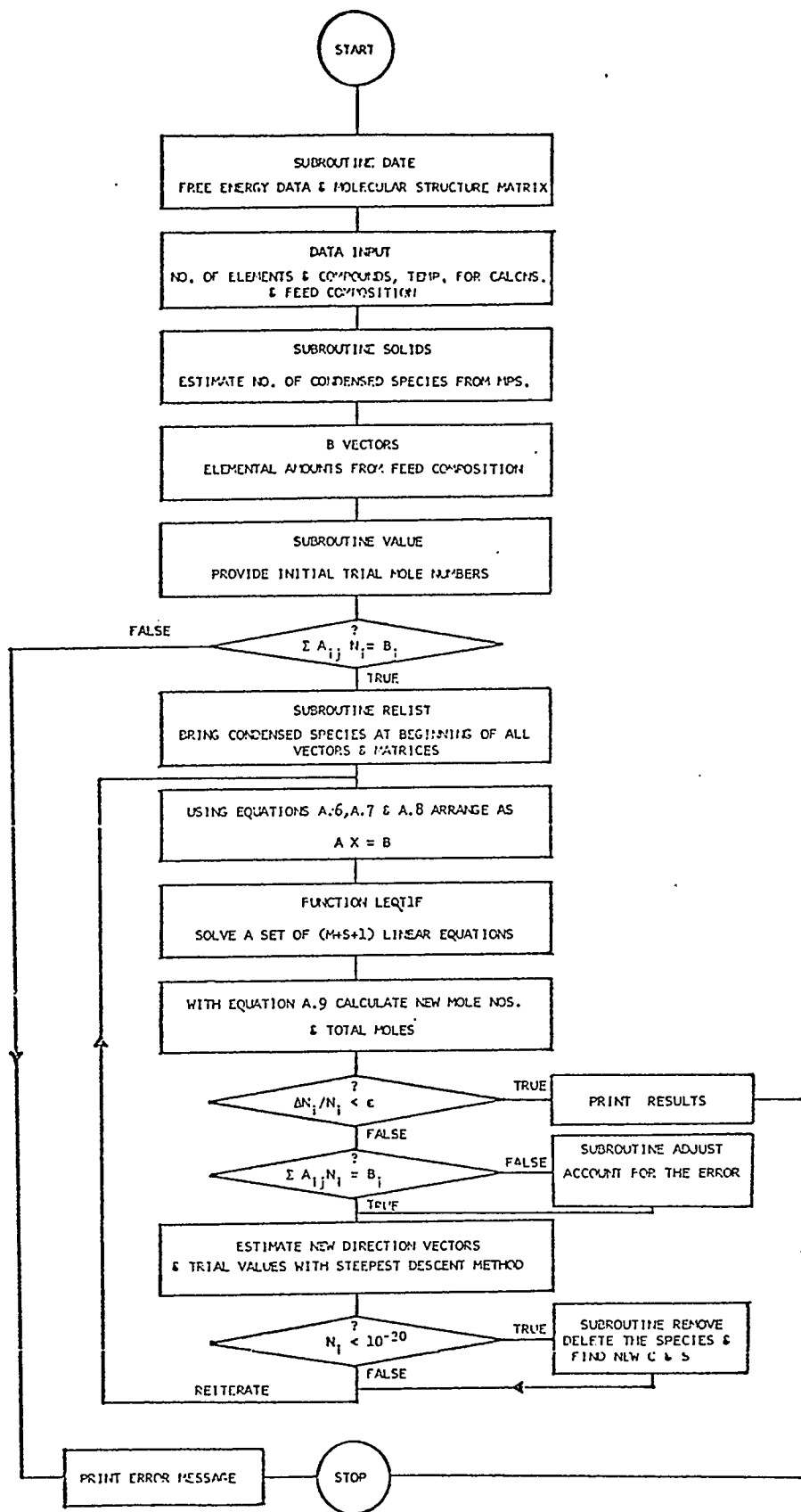


Figure 3.1 Computational Flow Scheme.

pressure of the system specified, the degrees of freedom are reduced by two. Hence the number of condensed phases that can be arbitrarily chosen is one less than the number of elements in condensed species. It is thus evident that not all the solids listed can be included in one calculation. It is also apparent that two or more condensed species with composition vectors linearly dependent of one another can not be considered in one calculation run as doing this would cause two equations within "S" equations to have identical row vectors resulting in a trivial solution (Appendix I). Thus the Gibbs phase rule has exposed some very important constraints for these free energy minimization calculations.

The restriction to include only a certain maximum number of solid phases for any one calculation can have significant effects on the computed equilibrium values. The selection of more probable condensed species for all the runs involved a large number of trial program runs. The preliminary calculations indicated that the complex silicate and aluminate compounds were usually absent at the equilibrium over the temperature range of interest. After a number of trial runs, the solid species that were retained are shown in Table 3.2.

Species	Melting/ Sublimation Temp.,K	Species	Melting/ Sublimation Temp.,K	Species	Melting/ Sublimation Temp.,K
Al	933	SiCl ₃	...	Ti ₃ O ₅	2047
AlCl	...	TiCl ₃	1104	NaAlCl ₄	424
AlCl ₂	...	SiCl ₃	...	Na ₃ AlCl ₆	780
AlCl ₃	466	TiCl ₄	249	NaAlO ₂	<1920
Al ₂ O ₃ (d)	2315*	Fe ₂ Cl ₆	...	Na ₂ CO ₃	1123
KAlCl ₄	529	Fe ²⁺	1809	Mg	920
Al ₂ Cl ₆	...	FeO	1650	MgO	3100*
Al ₂ SiO ₅	>3000	Fe ₂ O ₃	1735	Ca	1112
Al ₆ Si ₂ O ₁₃	2023	Fe ₂ (SO ₄) ₃	1451	NaCl	1074
C	>1700*	Fe ₃ O ₄	1870	CaCl ₂	1045*
K ₂ CO ₃	1175	K	336	MgCl ₂	987*
CO	...	K ₂ O	1154	MgSiO ₃	1850
CO ₂	...	FeSO ₄	944	MgTiO ₃	1950
CS ₂	...	TiO ₄	2023	MgTi ₂ O ₅	1960
SiC	3245	O ₂	...	Mg ₂ TiO ₄	2010
TiC	3290	SO ₂	...	Mg ₂ SiO ₄	2170
Cl	...	SiO ₂	1996*	Na ₂	...
KCl	1044	TiO ₂	2143*	Na ₂ O	1405
KClO ₄	798	O ₃	...	Na ₂ SiO ₃	1360
Cl ₂	...	SO ₃	...	Na ₂ S	1223
FeCl ₂	950	Ti ₂ O ₃	2112	Na ₂ SO ₄	1157
SiCl ₂	...	S	388	CaO	3220*
TiCl ₂	1582	Si	1685	K ₂ SO ₄	...
FeCl ₃	577	Ti	1933	Fe ₂ Cl ₄	...

* solids included for the final calculations.

Table 3.2 Important Compounds and their
Melting and Sublimation Temperatures.
(from JANAF Tables) (49,50,51)

3.5 Fly Ash Composition

Based on several ash analyses listed in Tables 2.1 and 2.2, an average ash composition was assumed. This ash composition, given in Table 3.3, was employed in all computations. It is realized that the metals in fly ash do not necessarily exist as simple oxides, but under the reacting conditions considered in this study the complex silicate compounds are unstable at equilibrium. Thus treating metals as their oxides should not affect the results obtained.

The stoichiometric amount of chlorine required to produce the highest chlorides of all metals was calculated. Similarly, the required stoichiometric amounts of C and CO to utilize the oxygen atoms liberated during reduction of metal oxides were calculated (Table 3.3). These estimates provided the basis for specifying reactant amounts. All calculations were performed at a constant total pressure of 1 atmosphere. The effect of the following variables on the conversion was studied:

- (i) amount of chlorine with the stoichiometric amounts of C and CO in the feed,
- (ii) amount of CO with the stoichiometric amount of chlorine in the feed, and
- (iii) system temperature with the stoichiometric amount

Element	Oxidized form in ash	Avg. Fraction in ash (% wt)	Moles as oxide Basis (100 wt)	Atoms of Cl ₂ needed	% Cl ₂ of total (%)	Atoms of C needed
Al	Al ₂ O ₃	13.0	0.2409	1.4455	33.3	0.3614
Ca	CaO	3.0	0.0749	0.1497	3.4	0.0374
Fe	Fe ₂ O ₃	7.0	0.0627	0.3761	8.6	0.0941
K	K ₂ O	1.5	0.0192	0.0384	0.9	0.0096
Mg	MgO	1.5	0.0617	0.1234	2.8	0.0308
Na	Na ₂ O	0.4	0.0087	0.0174	0.4	0.0043
Si	SiO ₂	15.0	0.5340	2.1360	49.1	0.5340
Ti	TiO ₂	0.8	0.0167	0.0668	1.5	0.0167
O	...	34.9	1.0883
Inerts	...	22.9
Total		100.0		4.3532	100.0	1.0883 (2.1766 with CO)

Table 3.3 Reactants for Average Ash Composition.

of CO and chlorine in the feed.

In addition, recycling silicon tetrachloride to suppress further chlorination of silicon in ash and to economize the reactants consumption was explored.

3.6 Discussion of Results

The results obtained from the free energy minimization calculations are discussed in this section. As stated previously, these results should be viewed as the maximum attainable conversions predicted by the thermodynamic considerations alone.

3.6.1 Oxides - Carbon - Chlorine System

The utilization of chlorine with a stoichiometric quantity of elemental carbon in the feed is illustrated in Figure 3.2. The temperature, 1200 K, falls in the range reported in the literature for the chlorination of metal oxides (21,22,23,24,40). Though not shown in the figure, sodium and potassium oxides are the first to be chlorinated. These are followed by calcium and magnesium. Iron oxide is chlorinated preferentially to the ferrous form (and its dimer) until almost 90% of the stoichiometric amount of chlorine is provided.

The behavior shown by the chlorination of titanium appears somewhat intriguing. Although virtually all titanium is chlorinated initially, it is the lower chlorides (mono and di-chlorides) which dominate under

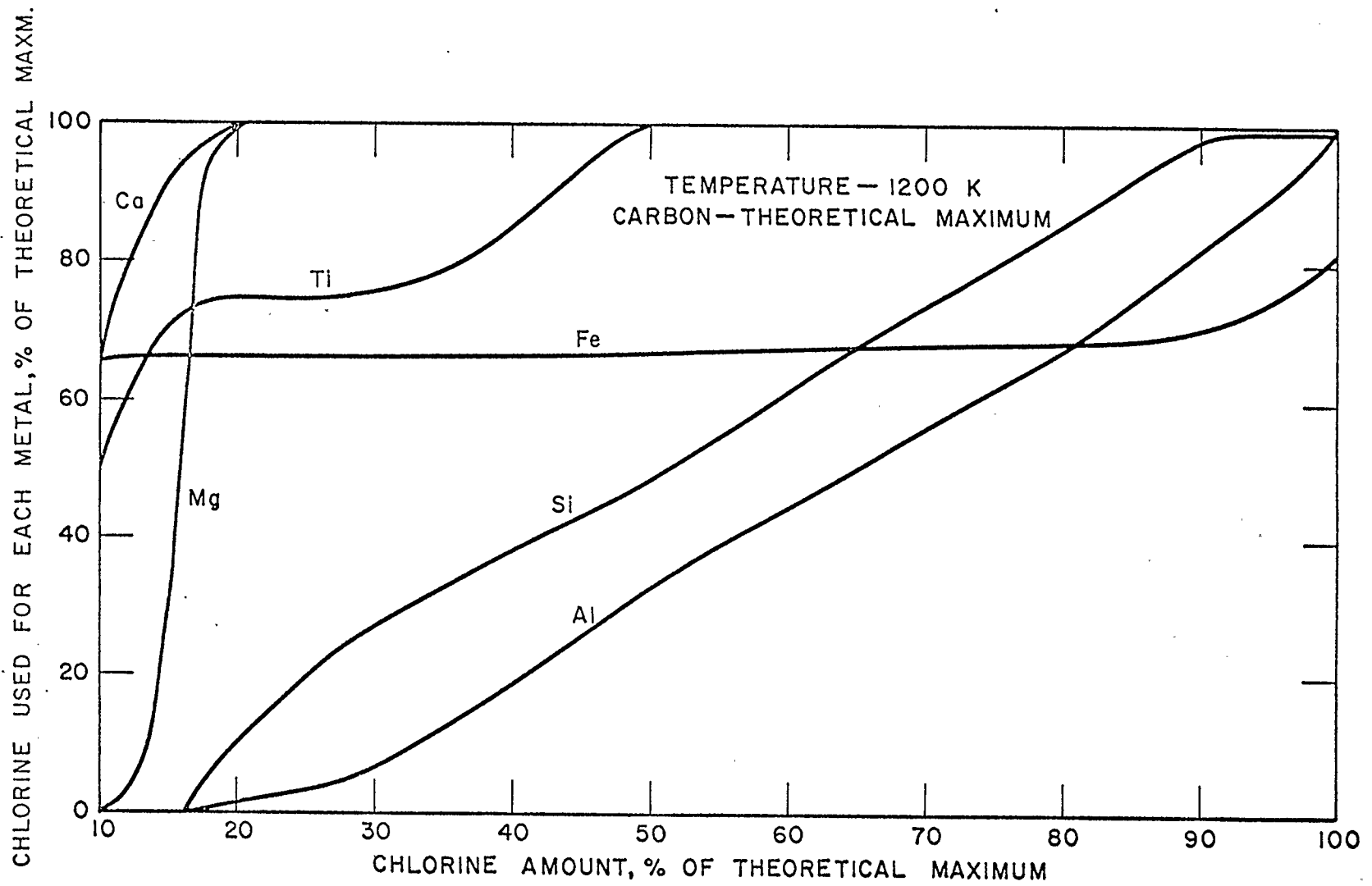


Figure 3.2 Chlorination with Stoichiometric Amount of Carbon.

the low chlorine supply situation. But these are gradually converted to trichloride when about a quarter of the total chlorine is provided. The tetrachloride form is ultimately produced as the chlorine amount is increased to about half. The seemingly persistent stability of titanium trichloride can be attributed to its occurrence as a solid at 1200 K, whereas the trichloride form exists as gas.

Silicon and aluminum oxides start chlorinating only after all other metal oxides have reacted. Silicon appears to be preferentially chlorinated than aluminum. In both cases, the highest chlorides essentially dominate. The redistribution of aluminum compounds shows that carbon alone is able to reduce aluminum oxide yielding aluminum metal (Figure 3.3). This would not seem plausible when the kinetic considerations are superimposed as it involves reaction between two solids. Hence not much practical significance should be attached to this observation. With the introduction of small amounts of chlorine, aluminum dichloride is formed. Further increases in chlorine amounts result in trichlorides (monomer and dimer). Finally when the stoichiometric amount of chlorine is available to the mixture, about 80% of aluminum appears as aluminum trichloride dimer and the rest as monomer.

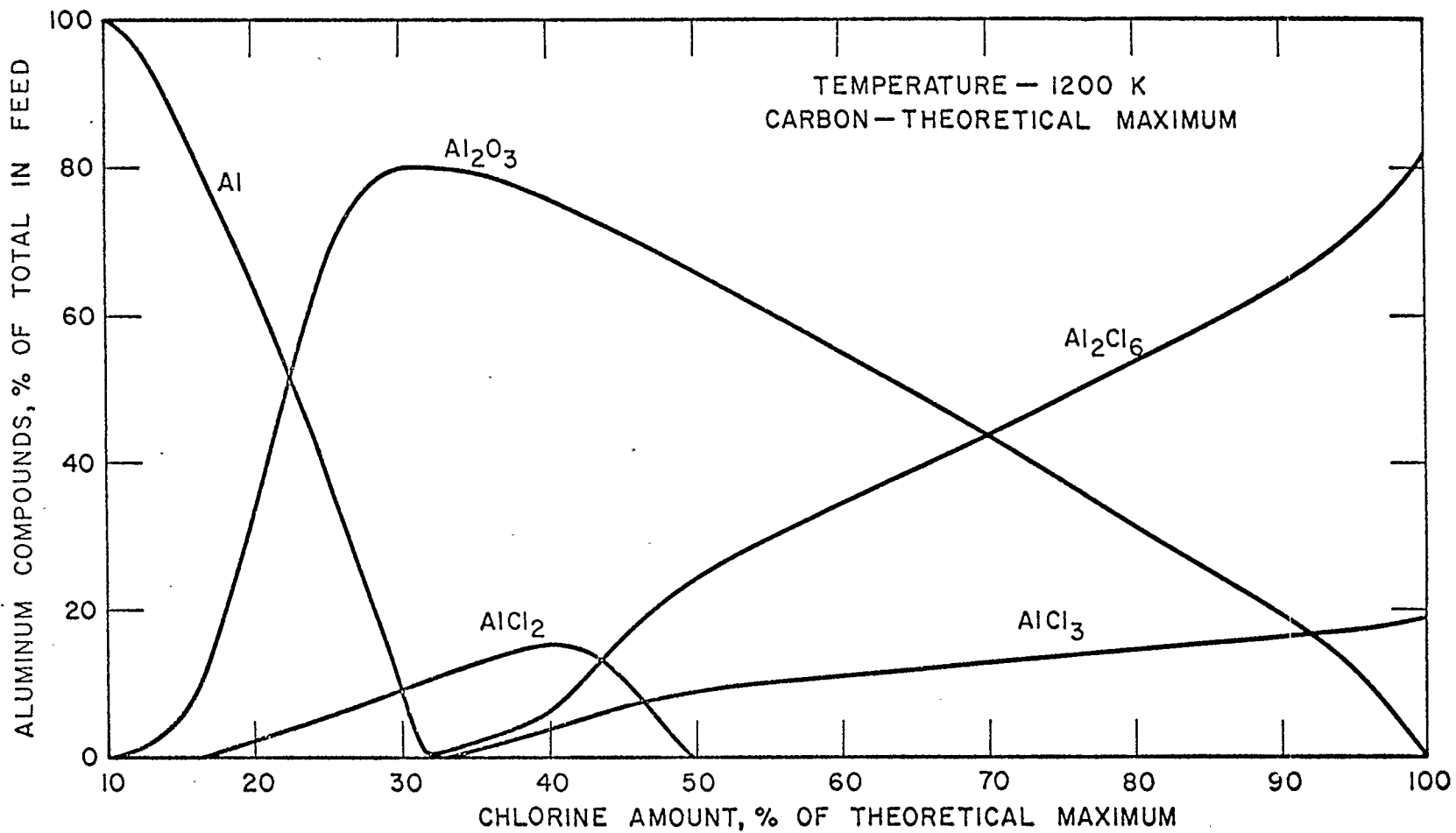


Figure 3.3 Distribution of Aluminum Compounds with C and Cl₂.

3.6.2 Oxides - Carbon monoxide - Chlorine System

The free energy calculations were also performed using carbon monoxide in place of carbon in the feed. The results of these calculations at 1200 K are shown in Figure 3.4. The results obtained with CO are quite similar to those in Figure 3.2, except that a different behavior is obtained for titanium chlorides. In the presence of CO, titanium oxide is completely chlorinated to titanium tetrachloride before the chlorination of calcium and magnesium. The overall minimum with gaseous CO for titanium compounds is found to be different than with solid carbon. The behavior of other constituents is not affected greatly as titanium represents only a small fraction of ash. The curves for iron, aluminum and silicon follow a pattern that is qualitatively similar to Figure 3.2. However, the curves for aluminum and silicon appear to be somewhat more spaced, indicating that silicon is chlorinated even more preferentially than aluminum when CO is the reducing agent.

The redistribution of aluminum compounds, shown as Figure 3.5, indicates the absence of elemental aluminum. This is different from the case with carbon as the reducing agent (Figure 3.3). Gradual chlorination of aluminum into its trichloride (both dimer and monomer) is observed. At almost total chlorination of

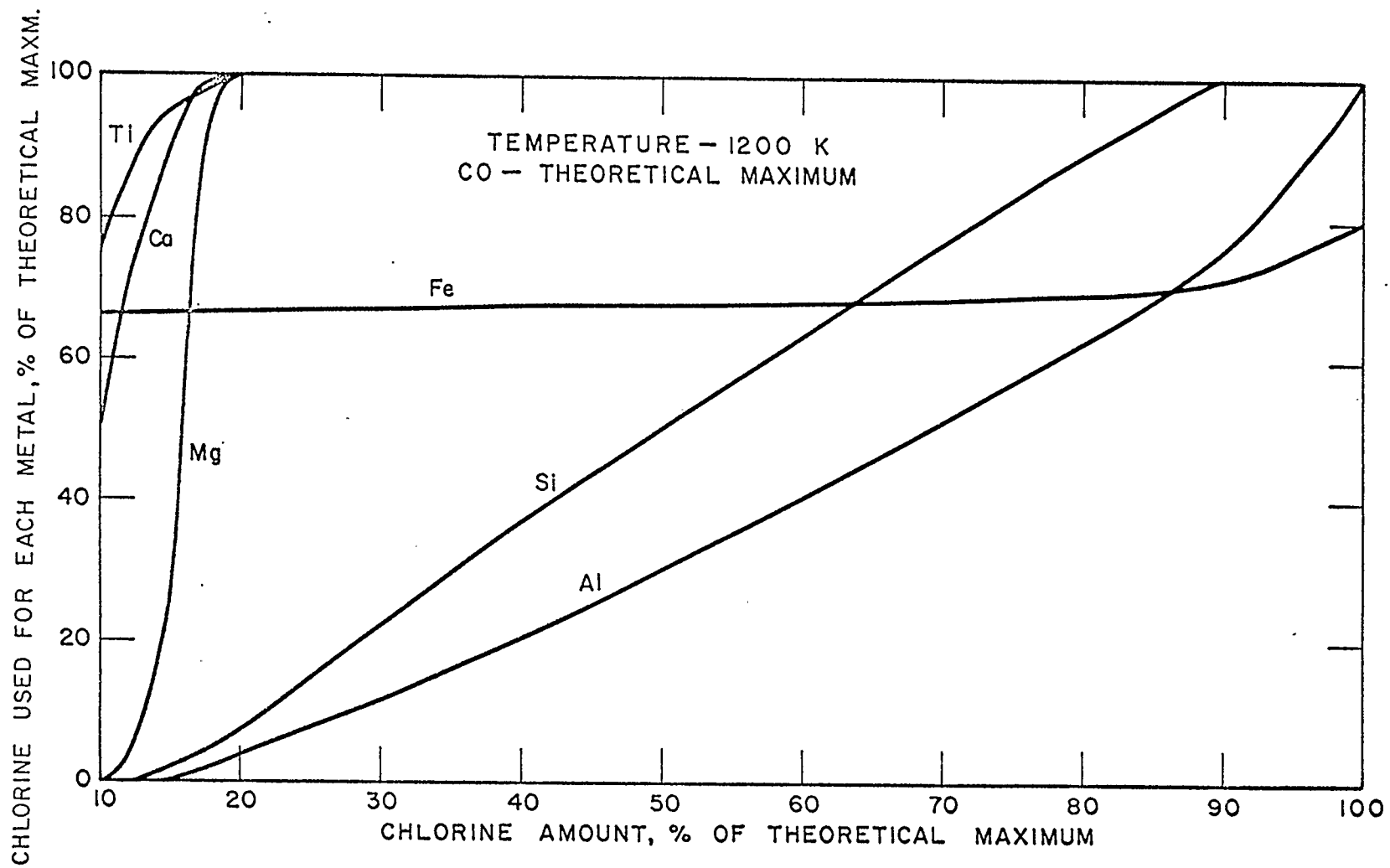


Figure 3.4 Chlorination with Stoichiometric Amount of CO.

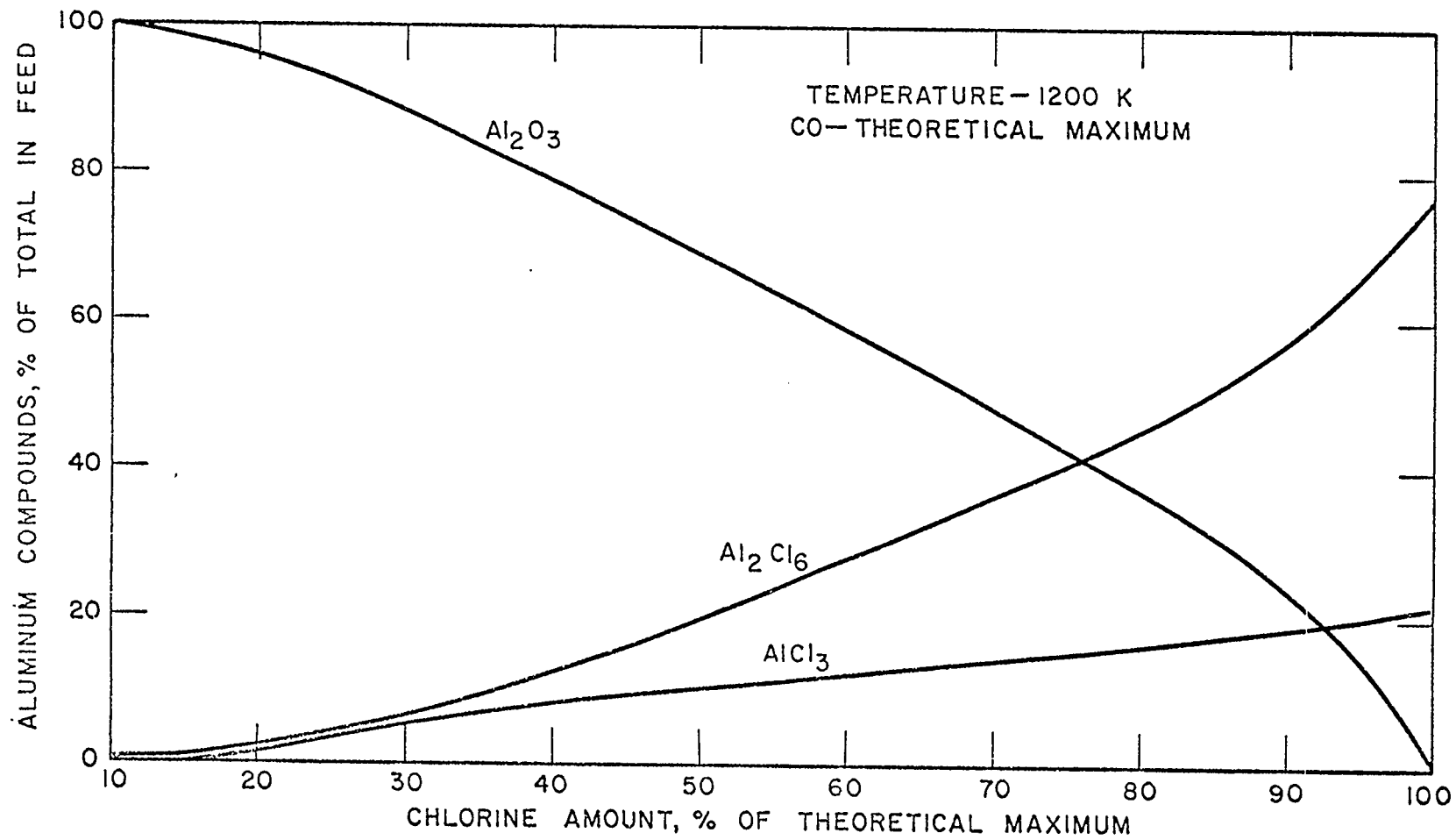


Figure 3.5 Distribution of Aluminum Compounds with CO and Cl₂.

aluminum, ratio of dimer to monomer is 3.3 compared to 4.3 for the case of carbon.

A series of program runs were made using the stoichiometric amount of chlorine but only a limited supply of carbon monoxide. This was done to identify the oxides which would chlorinate in absence of sufficient reducing agent (i.e. with chlorine alone). The computed equilibrium data at 1200 K are plotted in Figure 3.6. It was revealed that the oxides of sodium, potassium, titanium, iron, magnesium and calcium do not require the presence of a reducing agent. The resulting liberated oxygen was found to be present as free oxygen molecules. Silicon and aluminum oxides began chlorinating only after the free oxygen molecules were used up by the reducing agent, i.e. at about 20% of the stoichiometric amount. Though there was an excess of unreacted chlorine available at all times, the chlorination of aluminum and silicon fractions progressed with increased amounts of the reducing agent. This affected the distribution of iron chlorides too. With added amounts of the reducing agent in the mixture, ferrous chloride became the more prominent iron compound in the mixture.

From the results of these calculations, it is evident that oxides of aluminum and silicon need the presence of C or CO for their chlorination. Other major

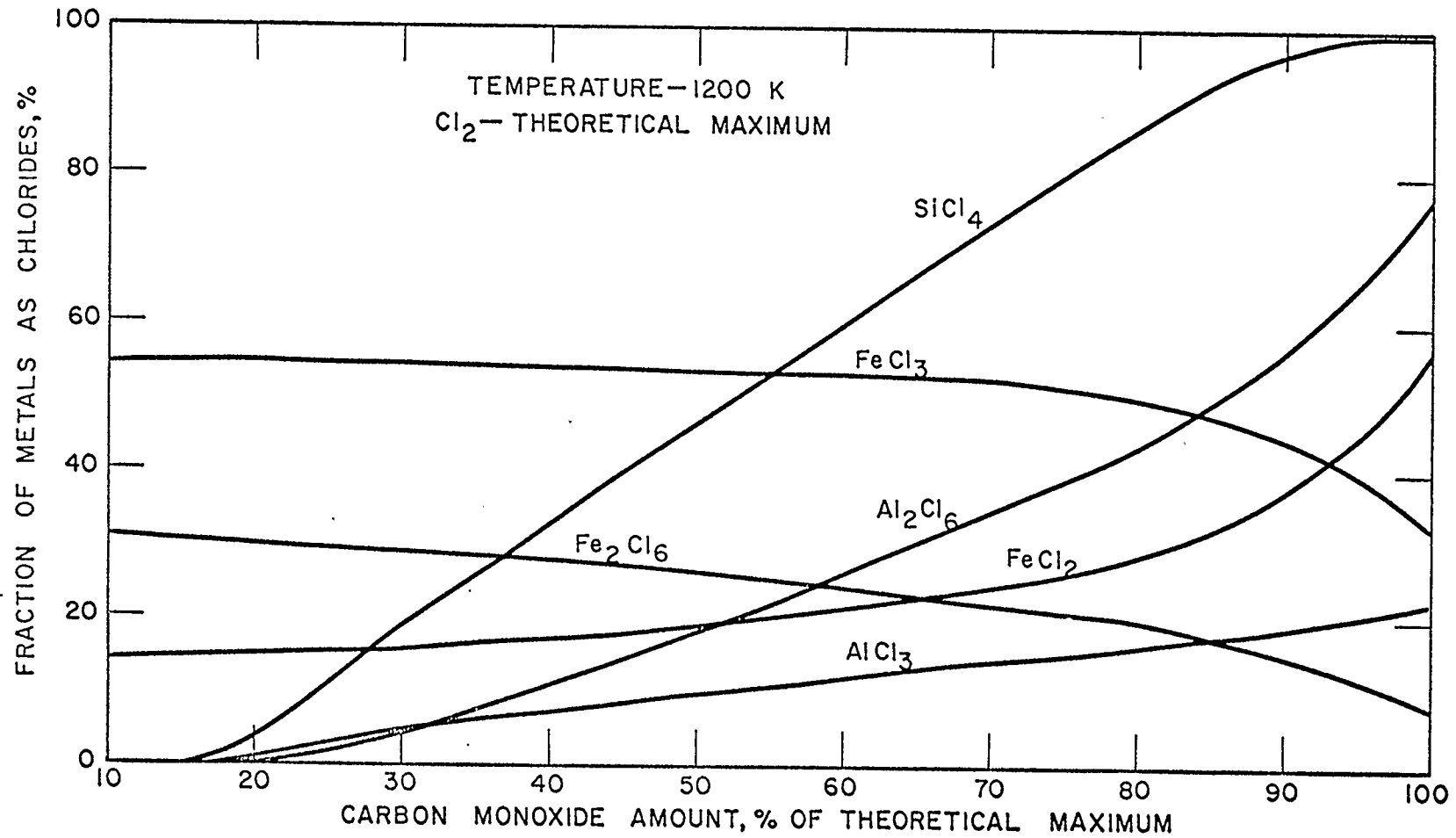


Figure 3.6 Chlorination with Limiting Amount of CO.

metal constituents in ash can be chlorinated with chlorine alone.

3.6.3 Effect of Temperature

The variation in the system temperature with stoichiometric amounts of CO and chlorine indicated no significant changes in the chlorination of all but iron and aluminum oxides. For aluminum and iron compounds, a significant redistribution was observed as shown in Figure 3.7. At lower temperatures the more stable chloride of aluminum is AlCl_3 , but Al_2Cl_6 is more stable at intermediate temperatures. About 8% of aluminum is used up in the formation of KAlCl_4 at all temperatures. More importantly, at temperatures beyond 1200-1300 K, the chlorination of aluminum oxide is suppressed to some extent. This could put an upper limit on actual chlorination temperatures to be studied experimentally.

Iron chlorides show an interesting redistribution pattern. The trichloride appears to be stable at lower temperatures, but is replaced by the dichlorides. Between 600 and 1200 K, Fe_2Cl_6 shows a limited stability with a maximum of 30% obtained at 900-1000 K.

3.6.4 Oxides - Sulfur - Chlorine System

The purpose of studying this system was to evaluate sulfur as a reducing agent in place of carbon or

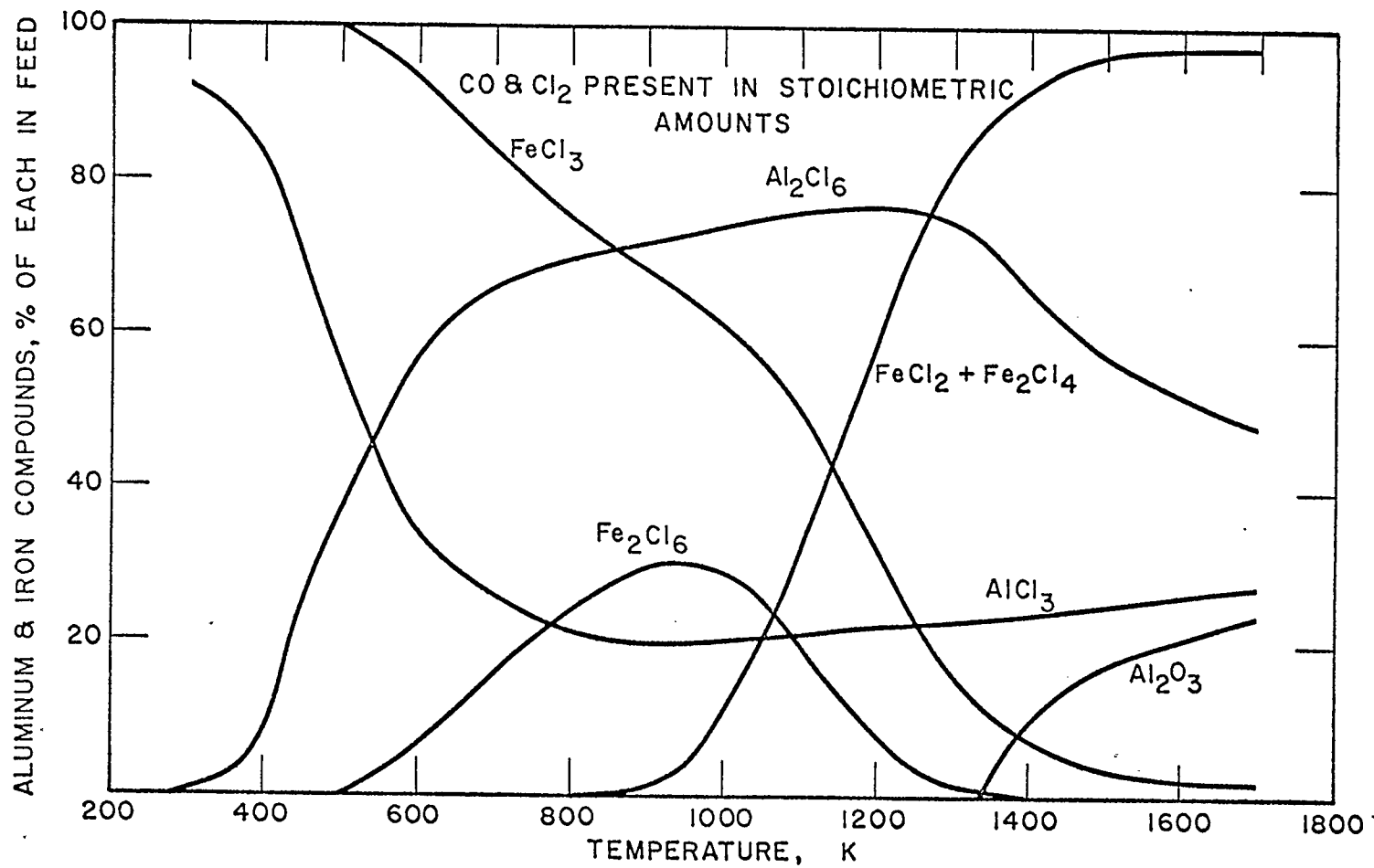


Figure 3.7 Effect of Temperature on Equilibrium Composition.

carbon monoxide. It also helped in testing the validity of the proposal that the presence of sulfur as S_2Cl_2 enhances the preferential formation of $FeCl_2$ (48). When carbon is replaced with sulfur, no significant difference in the equilibrium values was noticed (from those given in Figures 3.2 and 3.3). As carbon and sulfur have similar reactions with oxygen, the equilibrium values for the compounds of interest were found identical in two cases.

The use of sulfur over carbon as the reducing agent does not appear to offer any advantage. On the other hand the use of sulfur will present inherent design and severe environmental control problems. Therefore, its use as a reducing agent for the recovery of metals from ash seems unlikely.

3.7 Recycle of Silicon tetrachloride

In the previous sections, it was shown that for the two more abundant metals in ash, aluminum and silicon, the chlorination process requires the presence of a reducing agent. In addition, the calculations predict the chlorination of silicon to be marginally preferential over aluminum (53,54). Since the demand for silicon or silicon tetrachloride is not great, the production of large amounts of silicon tetrachloride would be a serious drawback. Thus unless the recovery of chlorine associated with $SiCl_4$ is practised, the

overall economics of the metal recovery process would be unattractive.

One possible means of accomplishing the recovery of chlorine from SiCl_4 is through its decomposition to form silica and hydrogen chloride (7). This scheme is quite involved requiring catalytic conversion of hydrogen chloride to produce chlorine. An alternative approach involves the recycling of SiCl_4 vapour. This idea needs investigation to establish if the recycle would provide an efficient means of suppressing the formation of the less desirable product. The effect of the recycle is examined by adding SiCl_4 to a stoichiometric mixture of ash, chlorine and carbon monoxide.

With increased addition of silicon tetrachloride to the stoichiometric mixture, any significant change in the product distribution at the equilibrium was not observed. However, by reducing the amount of chlorine in the mixture along with recycling SiCl_4 , further chlorination of silicon in ash was suppressed. The results of the equilibrium calculations for three ratios of chlorine supplied to the reaction mixture is shown in Figure 3.8. In this figure, the area above the dashed curve represents the region where complete chlorination of aluminum in ash is predicted. In order to totally suppress the chlorination of silicon in ash,

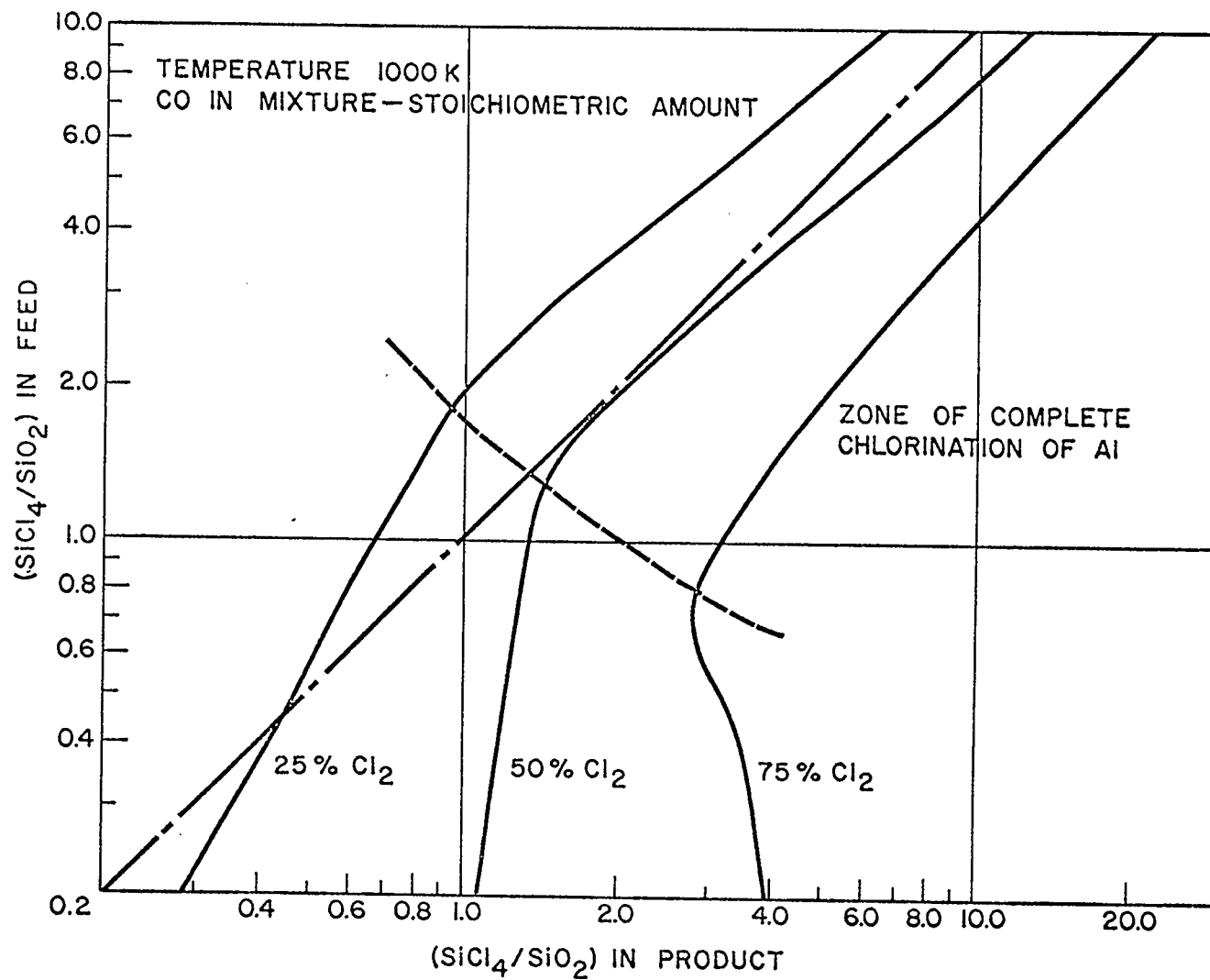


Figure 3.8 Chlorine Requirement with SiCl₄ Recycle.

the operating point of recycle should lie on the diagonal (chained line). This will make the ratio $(\text{SiCl}_4/\text{SiO}_2)$ in the feed and the product identical. For 25% chlorine supply situation, the process requires an external source of SiCl_4 whereas for 75% chlorine supply an excess of chlorine is predicted. It may be noted that at about 50% of the stoichiometric chlorine demand, neither an accumulation nor a depletion of SiCl_4 occurs. A satisfactory operating point of recycle is achieved when the ratio $(\text{SiCl}_4/\text{SiO}_2)$ assumes a value of 1.5 to 2.0.

It is important to bear in mind that the above mentioned set of conditions is optimum for the ash composition assumed initially for the calculations (Table 3.3). For an ash of different composition or at temperatures other than 1000 K, these operating conditions will change. In Table 3.3, it is also indicated that the fraction of chlorine required for silicon alone is 50% of the total stoichiometric amount. To achieve an optimum recycling of SiCl_4 , the chlorine amount should be sufficient to chlorinate all constituents in the ash except silicon.

The distribution of aluminum between aluminum trichloride dimer and monomer is also affected by the recycle of SiCl_4 . The effect of recycling SiCl_4 on the ratio $(\text{Al}_2\text{Cl}_6/\text{AlCl}_3)$ is shown in Figure 3.9. An

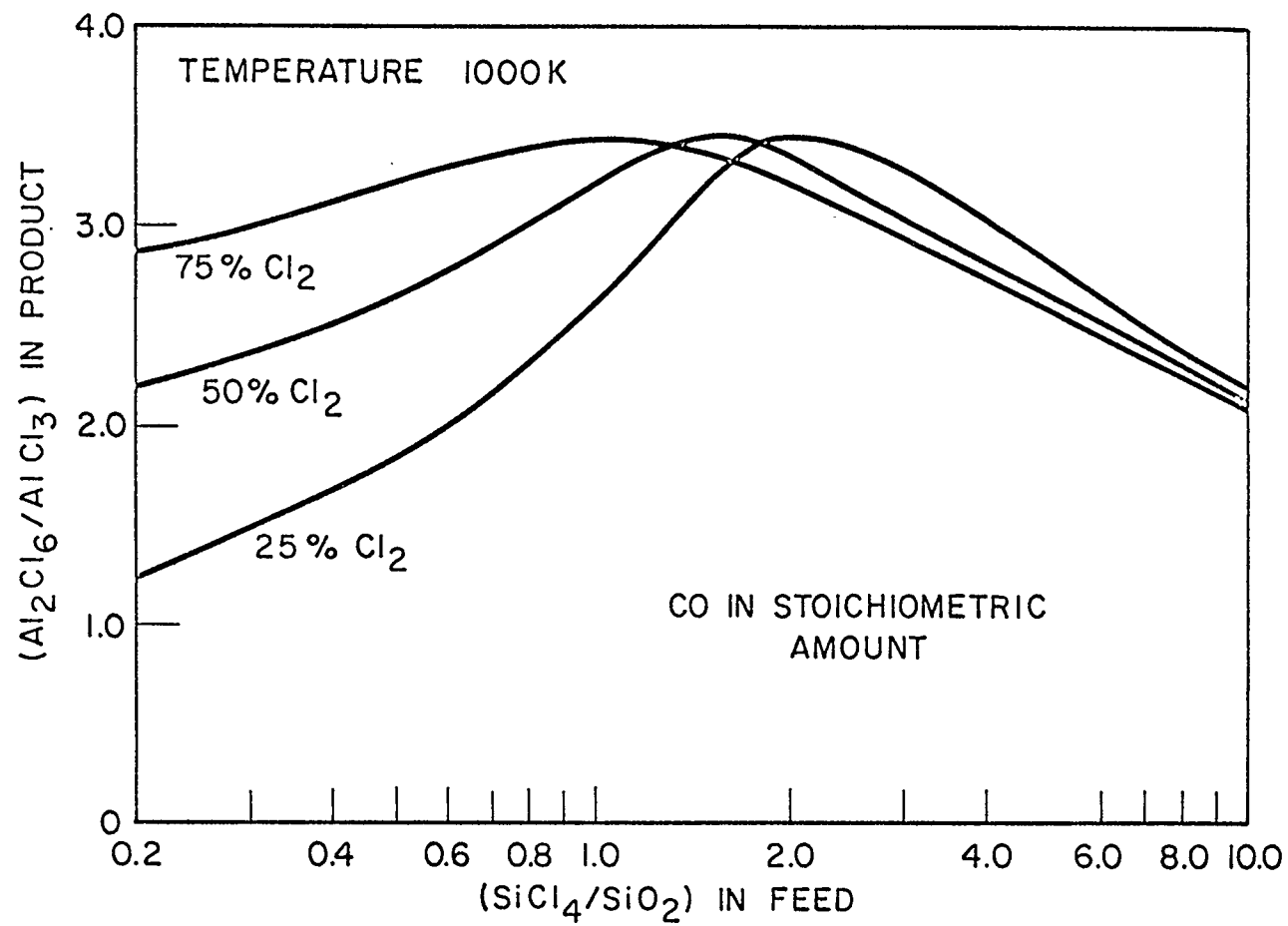


Figure 3.9 Aluminum Chlorides with Recycle of SiCl₄.

increase in the supply of chlorine to the reaction mixture with SiCl_4 recycle enhances the formation of Al_2Cl_6 when the chlorination of aluminum is incomplete. However, it is interesting to note that this trend is reversed when the total chlorination of aluminum has occurred. Further increases in the amount of recycled SiCl_4 lower the fraction of aluminum as aluminum chloride dimer.

Thus the thermodynamic feasibility of recycling silicon tetrachloride to suppress the chlorination of silicon in ash is demonstrated. The possibility of such a recycle introduces an effective means of improving the overall economics of the ash chlorination process.

3.8 Summary and Conclusions

The thermodynamic free energy minimization calculations have been very useful in providing an understanding of the overall chlorination process. The following can be concluded from this study:

- (i) Coal ash has the potential of becoming an important source of several metals through a reductive chlorination process. There does seem to be a clear reaction path for the chlorination of aluminum in particular. The use of chlorine alone will not result in chlorination of aluminum and silicon. For complete chlorination of aluminum in

ash, stoichiometric amounts of chlorine and carbon/carbon monoxide are required.

- (ii) Though the variation in system temperature has a dominant effect on the redistribution of aluminum compounds, total chlorination of aluminum is predicted up to 1300 K. Above this temperature, the stability of aluminum is enhanced.
- (iii) There is no apparent pathway for selective chlorination of aluminum. It is predicted that simultaneous chlorination of silicon will occur. However, it is shown that the recycle of silicon tetrachloride would suppress further chlorination of silicon in ash. This should give tremendous savings due to the reduced reactant consumption.

CHAPTER 4

EXPERIMENTAL

4.1 Introduction

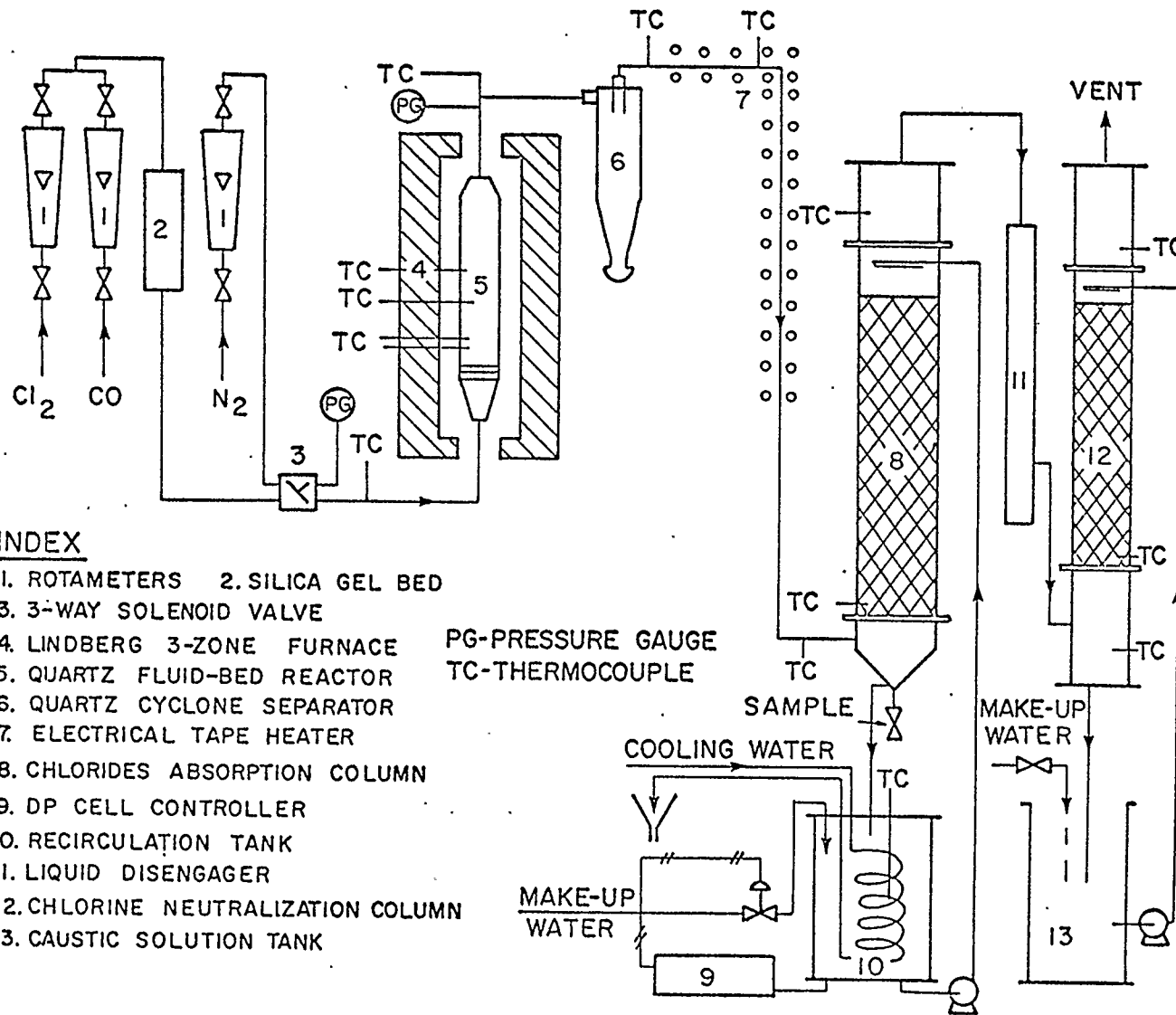
Experiments were conducted to evaluate the effect of selected process variables on chlorination of ash. The reduction chlorination reactions involved in extracting metals as their chlorides are exothermic in nature (Table 3.1). In order to achieve a rapid dissipation of the heat that is released during the reactions, a fluidized bed reactor offers several advantages. A fluid-bed as opposed to a fixed bed yields superior homogeneity and control over the reaction temperature. In addition, the gas-solid film resistance is relatively higher in the packed bed system. Due to the higher gas velocity, the film resistance is much smaller in magnitude for the fluidized bed reactor.

The fluid bed reactor was operated at 1.5 to 2 times the minimum fluidization velocity. It provided a means of controlling the solids entrainment. In addition, this aided in diminishing the extent of back mixing in gas phase that is encountered in fluidized bed reactors. Thus by keeping the reactor at slightly above the minimum fluidization velocity, an optimum operation of the fluid bed was achieved.

4.2 Description of Apparatus

A schematic of the experimental apparatus is shown in Figure 4.1. The parts exposed to high temperatures and corrosive gases were fabricated from quartz or pyrex glass. The reactions were carried out in a 8.0 cm diameter fluid bed reactor made of quartz. The reaction bed was supported on two porous frits, also of quartz. The reactor assembly was encased vertically in a 3-zone Lindberg Sola-basic tubular furnace. The furnace with an appropriate temperature controller was capable of attaining temperatures upto 1000°C with precise control. The temperature within the reactor was monitored with 4 thermocouples inserted into thermocouple wells provided at the wall of the reactor. Other important features of the reactor are shown in Figure 4.2.

The reacting gas mixture of chlorine and carbon monoxide was fed to the reactor through appropriate rotameters and a silica gel dryer. The entrained solid particles of ash were trapped in a cyclone separator of quartz. Since transporting the solids collected in the cyclone separator back to the reactor would have introduced serious operating difficulties, the experimental runs were conducted at slightly above the minimum fluidization conditions. The exit gas with metal chlorides in vapour form entered a scrubbing column



INDEX

- 1. ROTAMETERS
- 2. SILICA GEL BED
- 3. 3-WAY SOLENOID VALVE
- 4. LINDBERG 3-ZONE FURNACE
- 5. QUARTZ FLUID-BED REACTOR
- 6. QUARTZ CYCLONE SEPARATOR
- 7. ELECTRICAL TAPE HEATER
- 8. CHLORIDES ABSORPTION COLUMN
- 9. DP CELL CONTROLLER
- 10. RECIRCULATION TANK
- 11. LIQUID DISENGAGER
- 12. CHLORINE NEUTRALIZATION COLUMN
- 13. CAUSTIC SOLUTION TANK

PG-PRESSURE GAUGE
TC-THERMOCOUPLE

Figure 4.1 Schematic of Experimental Apparatus.

where metal chlorides were dissolved in a mild HCl solution.

From preliminary investigations, it was ascertained that in spite of added thermal insulation, significant cooling of the gas stream occurred in the pyrex tubing connecting the cyclone separator and the scrubber. This led to partial condensation of metal chlorides, especially of iron and aluminum, inside the tube. Since the main purpose of installing the scrubber was to monitor the concentration of metals on a continuous basis, such premature condensation of the chlorides had to be minimized. Sections of tube were wrapped with electrical heating tape. This worked satisfactorily and maintained the temperature above 300°C in the heated section. Due to the thermal stresses caused in the glass tubing, the section of tubing prior to the scrubber frequently broke. Hence, it became necessary to remove the heating tape from this particular section. All heated sections exposed to atmosphere were thoroughly insulated with a ceramic insulation material.

The metal chlorides produced from chlorination of ash were dissolved in a weak HCl solution, which was recirculated countercurrently in the scrubbing column. The column was filled with 12 mm multiple-turn helical packing of borosilicate glass. The design and

operating details are listed in Table 4.1. The purpose of using weak acidic medium was basically to ensure that metal ions remained in solution form. The recirculating solution was in turn cooled with tap water using a stainless steel cooling coil. Samples of recirculating solution were withdrawn from the bottom of the column for the determination of metals by an atomic absorption technique.

The gas exiting from the scrubber entered a second column for the removal of unreacted chlorine. In this column, a strong caustic solution reacted and neutralized the chlorine in the exit gas for safe discharge into the atmosphere.

The temperature history of all the experimental runs was recorded on a 24-point chart recorder.

4.3 Characteristics of the Fluid-bed Reactor

The selection of porous frits to serve as the bed support and inlet gas distributor was based primarily on achieving intimate gas-solid contacting without appreciable channelling of gas. It is also more effective in preventing the finer particles from falling through the bed support. The resultant high pressure drop across the porous frits also yields better gas distribution. The uniformity of gas distribution over the frit area was studied visually by passing nitrogen

Item	HCl Scrubber	Caustic Column
Column ID, cm	10.0	7.5
Total height, cm	100	105
Packed height, cm	35	85
Cross section area, cm ²	81	46
Liquid rates, l/m	3.0-4.0	4.0
Liquid velocity, cm/s	0.62-0.82	1.45
Gas velocity, cm/s	1.6	2.9
Liquid volume, l	14.0	32.0
HCl/NaOH concn.	0.1-0.2 N	125-150 g/l

Table 4.1 Operating Conditions for Gas-Liquid Columns.

gas through a thin bed of ash particles.

The pressure drop across the gas distributor was studied next. The two pressure taps were located before and after the reactor assembly. This limited the measurement of the pressure drop to a combined value for the bed and bed support. The pressure drop observations were recorded at several constant temperatures and varying gas flow rates. The data for the bed without any solids, i.e. only the bed support, are shown in Figure 4.3. The pressure drop is plotted against the actual gas flow rate, corrected for pressure and temperature of gas at conditions inside the reactor. The variation in slope of the lines with temperature is primarily due to change in viscosity of nitrogen with temperature. All curves give almost identical slopes once the viscosity effects have been taken into consideration (Table 4.2). The linear variation of (ΔP) initially with velocity is in accordance with Darcy's equation (57) for flow through porous media at low velocity and $\Delta P \ll P$.

The reactor was filled with 125 μ m bottom ash particles to a bed height of 10 cm. The pressure drop measurements were repeated at 3 temperatures. The results after subtracting the pressure drop across the frits are shown in Figure 4.4. The break in each line signifies the onset of fluidization as the flow rate is

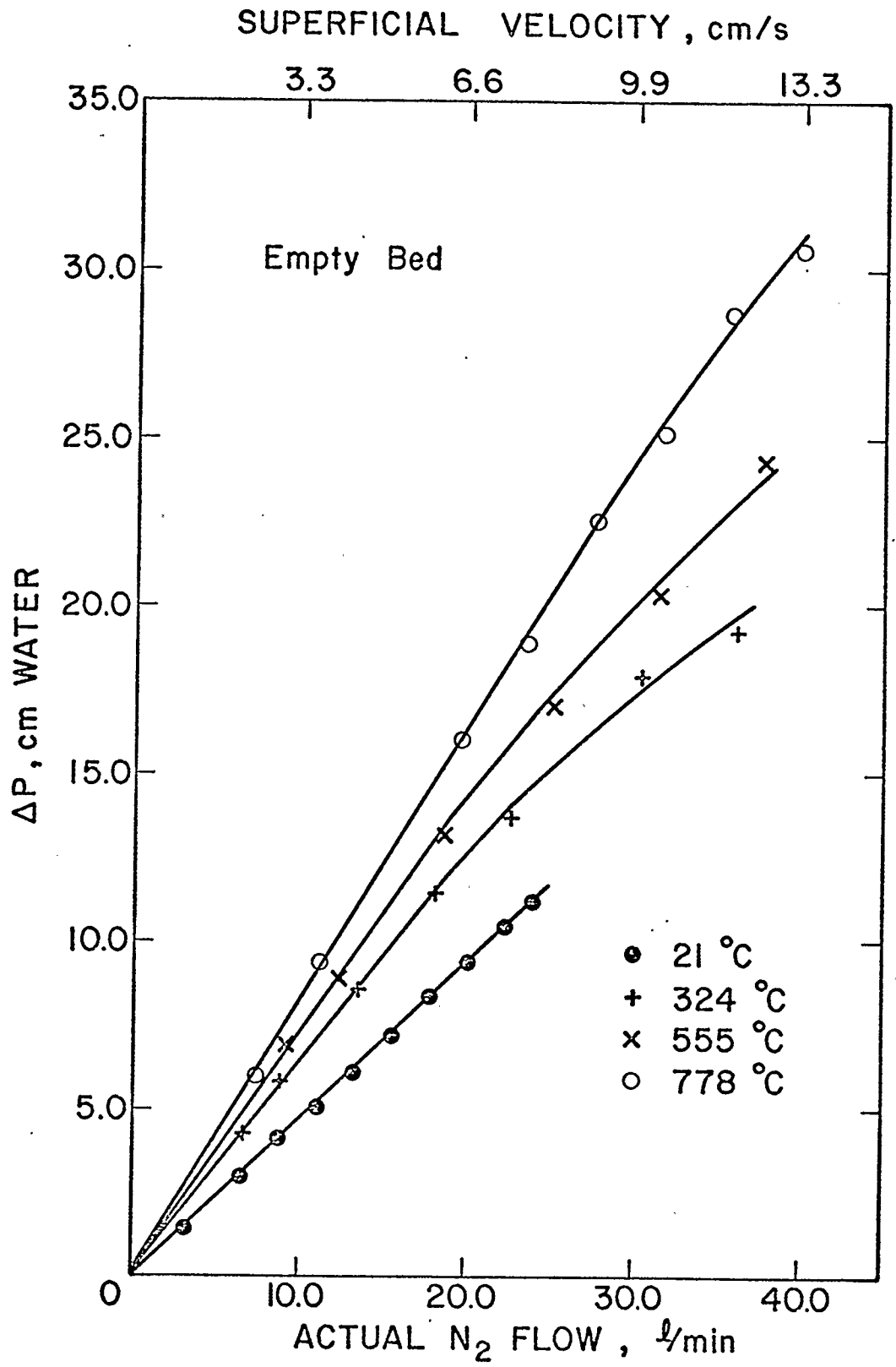


Figure 4.3 Pressure drop across the Bed-support.

Condition	Temp. (°C)	Slope (-ΔP/V) (cm H ₂ O s/lit)	Viscosity, μ x10 ² (g /cm s)	Slope/μ x10 ⁻² (cm H ₂ O s ² /lit)	Minimum Fluidization Velocity (cm/s)
No Solids	21	0.47	0.018	25.9	..
	324	0.63	0.026	24.4	..
	555	0.72	0.030	24.0	..
	778	0.82	0.034	24.0	..
bed of 125μm particles	21	0.56	0.018	31.1	1.49
	326	0.68	0.026	26.2	1.71
	555	0.76	0.030	25.3	1.82

Table 4.2 Characteristics of the Fluid-bed Reactor.

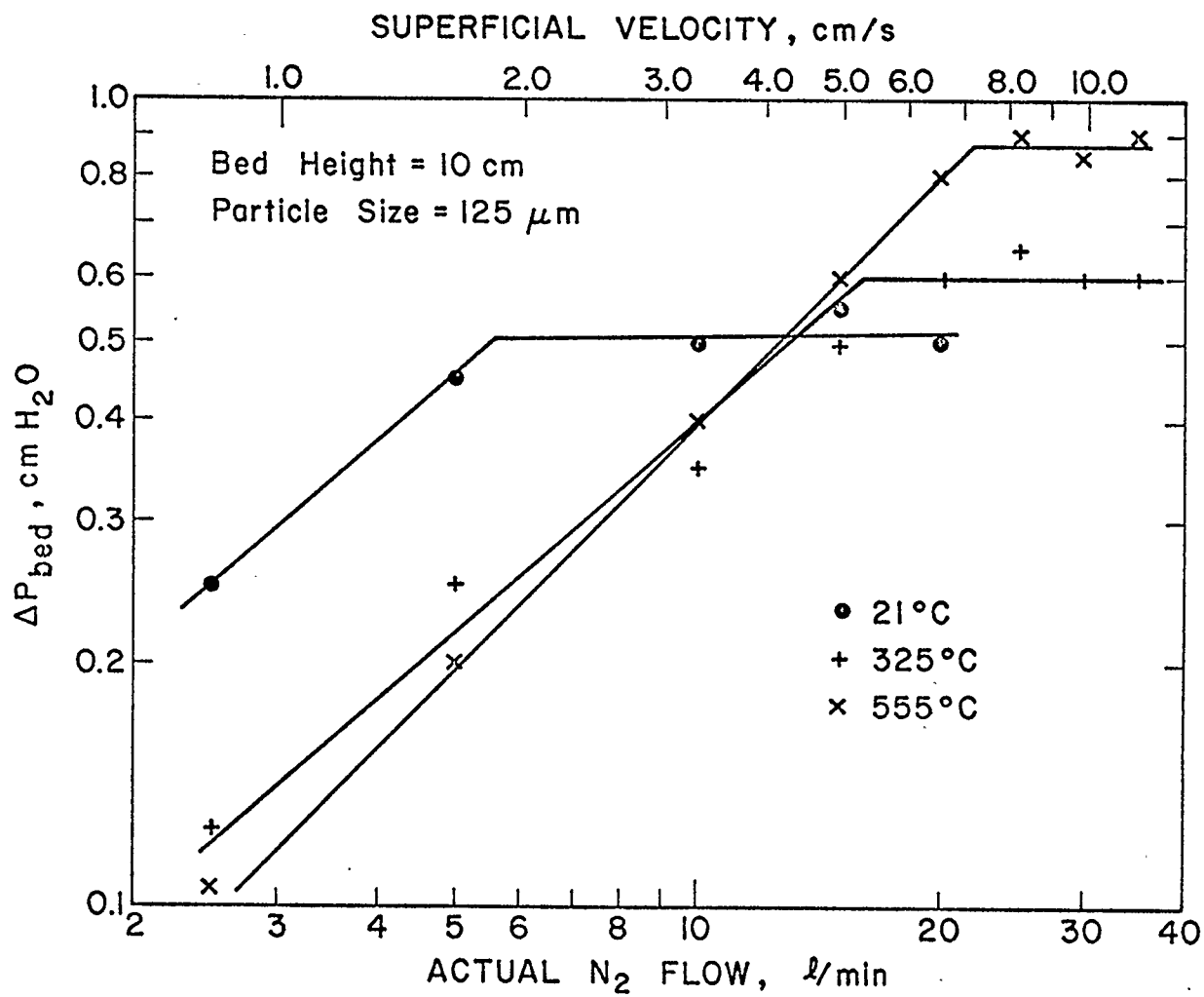


Figure 4.4 Pressure drop for Fluidized Bed.

increased. The bed support (porous frits) offered a much higher fraction of the total resistance to gas flow. The fraction of the resistance due to solids constitutes only 6-15% of the total. The minimum fluidization velocities are in the range 1.5 to 1.8 cm/s. The minimum fluidization velocity predicted by Wen and Yu correlation (59) is approximately 2.2 cm/s.

4.4 Procedure for Chlorination Experiments

The procedure adopted for the chlorination experiments is described briefly in this section.

4.4.1 Rotameter Calibration

The rotameters were calibrated with nitrogen and air using a wet test flow meter. It was found that the calibration curves provided by the manufacturer were within $\pm 3\%$ accuracy. The calibration was not done with CO and Cl₂ due to the hazardous nature of the gases and inability of the wet test meter to handle chlorine. Under the circumstances, a correction factor was employed to generate the curves for these gases. The correction factor is given as follows:

$$C_f = \left(\frac{\rho_1 T_1 P_2}{\rho_2 T_2 P_1} \right)^{0.5} \quad (4.1)$$

4.4.2 Calibration of Thermocouples

The Chromel-Alumel type K thermocouples were used for the temperature measurements. The thermocouples

were tested for three different temperatures against a precision mercury thermometer. The three reference temperatures were an ice bath, boiling water and a water bath at room temperature. The thermocouples were found to be within $\pm 0.5^{\circ}\text{C}$ of the reference values indicated by the thermometer.

The temperature drop that occurred across the thermocouple wells of the reactor was estimated. The measurements were done at $900\text{-}920^{\circ}\text{C}$ in a fluid-bed 10 cm deep of $164\ \mu\text{m}$ ash particles. A long thermocouple was inserted directly into the reactor and thus was exposed to the temperature of the bed. Another thermocouple was inserted into the lower most well of the reactor shown in Figure 4.2. Several temperature comparisons indicated that the readings through the well were within 1°C of the actual temperature. It can be stated, therefore, that the temperature measurements with the thermocouple wells contribute to a maximum error of 1°C . The temperature values reported throughout the study are those obtained through thermocouple wells, and are subject to an error of -1°C .

4.4.3 Preparations for Experimental Runs

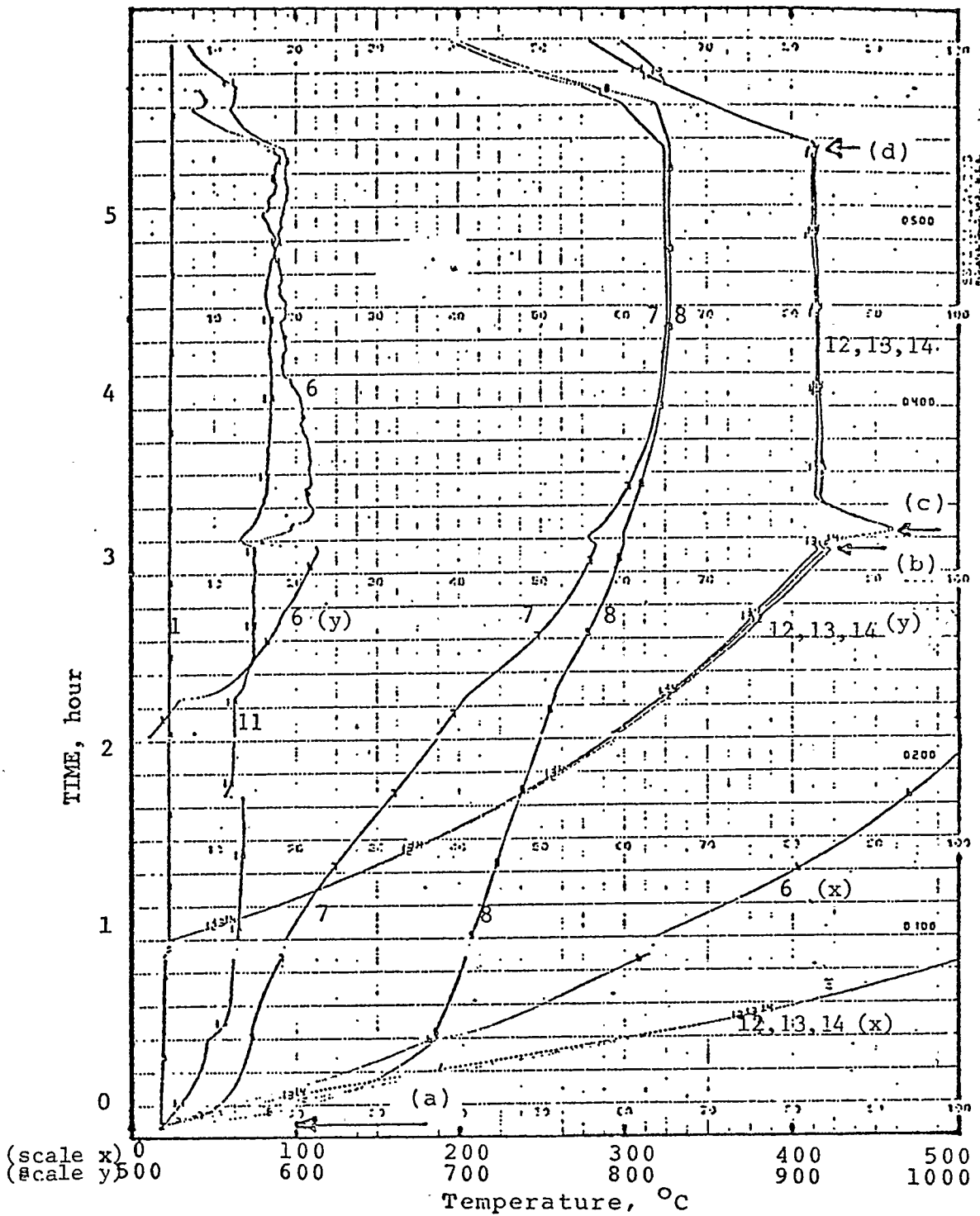
The quartz reactor was filled with a weighed amount of narrow-sized ash sample. The fines present in the ash sample were removed by passing nitrogen through the bed. It was found that the fraction of

finer was of the order of 1-2%, and the ash weight was adjusted for this loss. The assembly of the cyclone separator and the quartz tubing was completed. High vacuum grease was used to provide sealing of the glass connectors. Fresh solutions of caustic (30 litres of 125-150 g/l) and dilute hydrochloric acid (13 litres of 0.1-0.2 N) were placed in the respective tanks. The thermocouples were placed in the thermocouple wells provided at various locations. A helium leak detector (Varian 925-40 Porta-test Mass Spectrometer) was used to detect the system for any leakage.

4.4.4 Experimental Runs

The initial heating up of the reactor was carried out in an inert atmosphere of nitrogen. The flow of nitrogen was maintained at about 1.5-2.0 times the minimum fluidization velocity for the ash particles. The furnace and the chart recorder were switched on. Thus a complete record of the experimental run was obtained. A typical recording of temperature history for one complete run is given as Figure 4.5.

Once the furnace temperature reached the desired temperature in about 2 to 3 hours, the nitrogen flow was continued for an extra 15 minutes. This was necessary to allow the reactor to achieve uniform temperature. Following this, the flow of reacting gases (Cl_2 and CO) was commenced while the nitrogen flow was



LEGEND:

- 1. Exit gas 6. Cyclone inlet 7. Cyclone outlet
- 8. Quartz tubing 11. column inlet
- 12, 13 & 14. Reactor temperature
- (a) Furnace activated. (b) start of the run.
- (c) increase in temperature due to heat of reaction.
- (d) end of the run; furnace turned off.

Figure 4.5 Temperature History
 of a Typical Chlorination Experiment.

discontinued. The experimental run was timed as soon as the reacting gas entered the reactor. Various pressure gauge readings and the pressure drop across the reactor were monitored throughout the run.

Samples (150 ml) of the recirculating dilute HCl solution were withdrawn at regular time intervals. The temperature of the reactor was also recorded through a digital device at the time of each sampling.

The temperature of the reactor increased sharply at the start of each run. The increase in temperature was of the order of 20-35°C and occurred in about 3 to 5 minutes. The temperature returned to the maintained value in 10-15 minutes. The rise in temperature could indicate the initial rapid rate of chlorination reactions. The reactor temperature following the initial rise was maintained within $\pm 1^{\circ}\text{C}$.

The runs were terminated after a predetermined period of time. The reacting gases were discontinued and the flow of nitrogen was once again commenced. The furnace was switched off. The reactor assembly and the quartz tubes were allowed to cool for at least 4 hours before the set-up could be dismantled for cleaning. The samples of HCl solution and caustic, before and after the run, were also collected for atomic absorption analysis.

After the quartz sections had cooled sufficiently, the tubes were rinsed thoroughly with approximately 0.5 N HCl solution to dissolve the solids that had condensed over the inside. The volume of each rinsing was recorded and the samples were kept for the metals analysis. A sample of the mass in the reactor was retained for the determination of metals by atomic absorption technique to be discussed in Chapter 5.

4.5 Condensation of Metal Chlorides

In spite of electrical heating and thorough insulation of the quartz sections, partial condensation of metal chlorides occurred over the period of entire run. The solids condensed, however, could be recovered only after the termination of each run. Since the fraction of solids condensed was 6-30% of the total formed, it was necessary to make the adjustments.

The driving forces for the condensation of solids are the surface temperature of tubes and the concentration of metal chlorides in the gas stream. The surface temperature profile would be almost identical in all experimental runs due to the maintained uniformity in electrical heating rate, same insulation and constant room temperature. Thus the only parameter that would govern the condensation is the concentration of individual metal chlorides in the gas stream. It is, therefore, assumed that the fraction of a metal chloride

condensing, J, at any time is proportional to the total amount, L, in the flowing gas, i.e.

$$J = k L \quad (4.2)$$

Also the fraction of the chloride dissolved, E, is the difference of L and J,

$$E = (L - J) \quad (4.3)$$

By combining Equations (4.2) and (4.3), the following is obtained

$$L = E / (1 - k) \quad (4.4)$$

Since the fraction of solids condensed for any run is measured at the termination of each run, only one pair of J and L was obtainable from a run. The total number of chlorination runs was 25. Linear regressions performed with the results of all the runs showed a good fit for the data. In Table 4.3, the correlation coefficient for aluminum and iron chlorides is 0.95. The best fit regression lines for aluminum and iron chlorides are given in Figure 4.6, and for silicon and titanium in Figure 4.7. For the case of silicon, the scatter is significant indicating that this treatment does not work satisfactorily for SiCl_4 . It is also noticed that the condensed fractions are dependent on the boiling points of the metal chlorides (Table 4.3). The fraction is higher for the species

Species	No. of data points	Boiling Temp. °C	Correlation Parameters		Correlation Coefficient r	Level of Significance (%)
			a	b		
FeCl ₃	25	315.0	-62.3	0.325	0.95	>99.9
AlCl ₃	25	178.0	-18.3	0.275	0.95	>99.9
TiCl ₄	19	136.4	-10.3	0.273	0.86	>99.9
SiCl ₄	20	57.6	36.5	0.061	0.33	<90.0

Table 4.3 Correlation of Condensed to Total Metal Chlorides.
(J = a + bL)

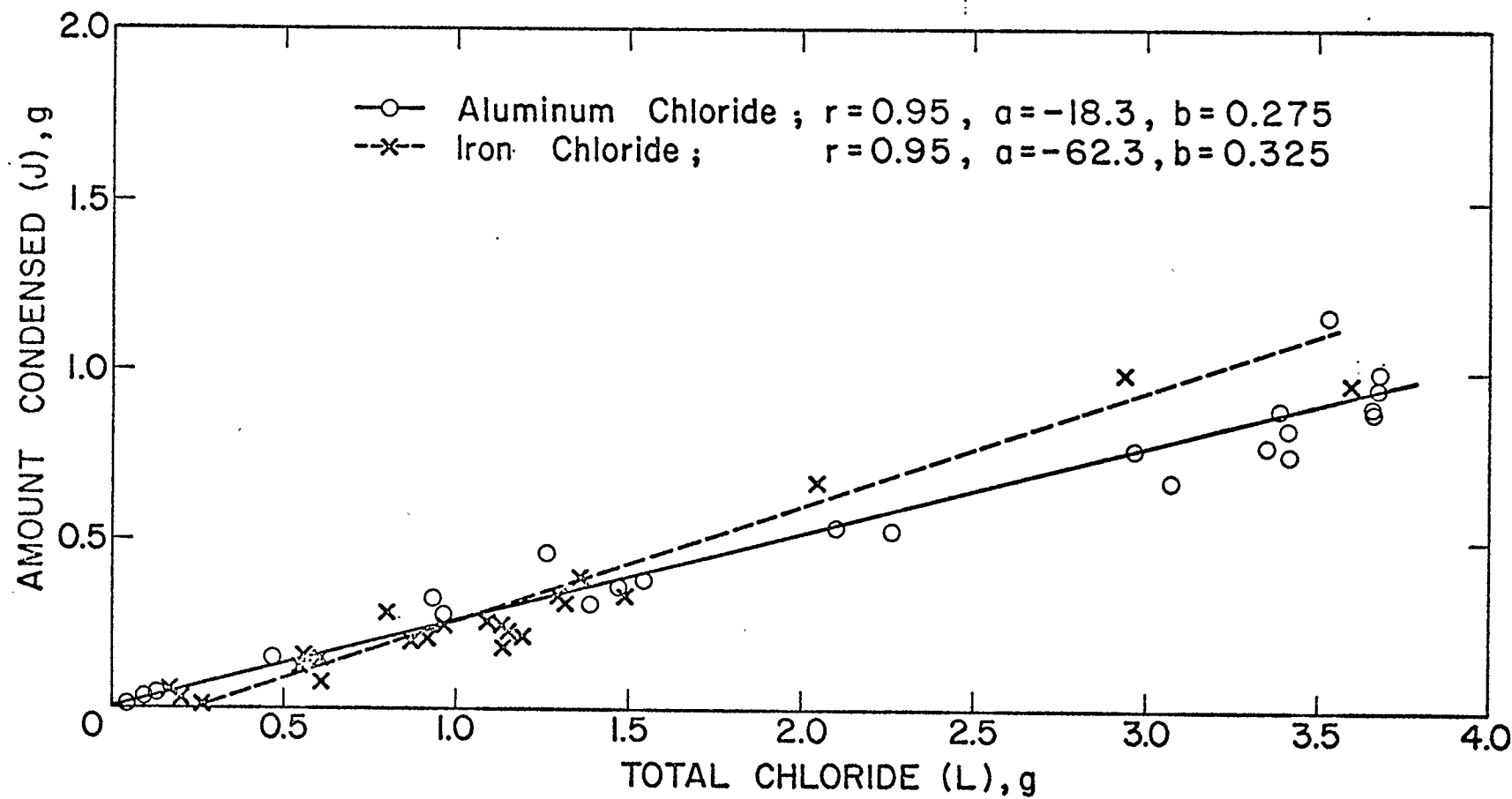


Figure 4.6 Condensation of Aluminum and Iron Chloride Vapours.

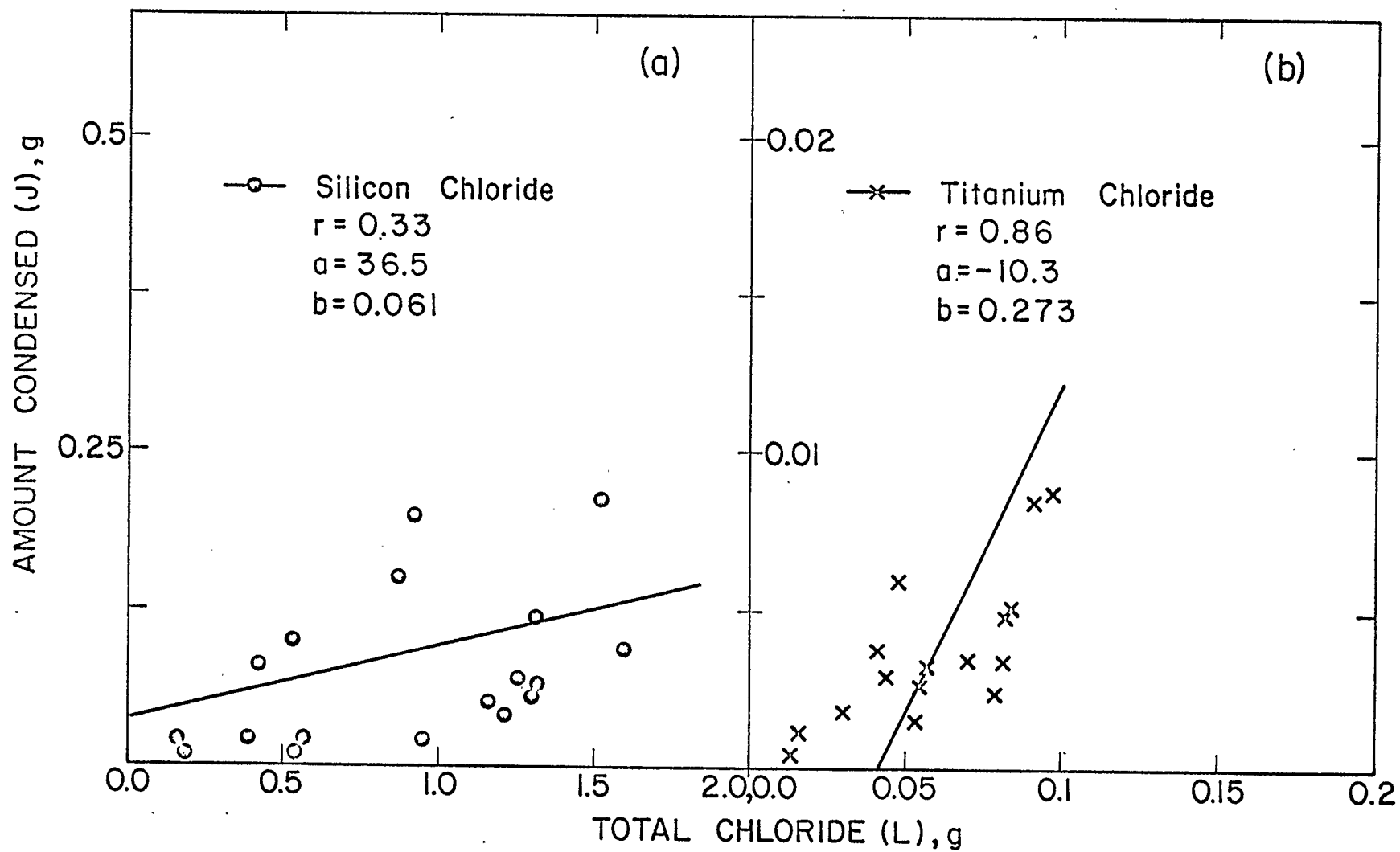


Figure 4.7 Condensation of Silicon and Titanium Chloride Vapours.

with a higher boiling point.

Due to the fact that several ash particle sizes were employed in the chlorination tests, the flow rates of reacting gases were different in all the runs. But the superficial velocities fall within a narrow range of 2.3 to 3.6 cm/s for most of the experiments. A variation in the flow rate also changes the residence time of the vapours in the glass tube. The amounts of condensed and total solids for all 25 runs along with the flow rates used are given in Table 4.4. Linear regressions were repeated once again for the fraction of each metal chloride with respect to the flow rate. The correlation of the fraction of metal chlorides and the gas flow rate is unsatisfactory (Table 4.5). The fraction of chlorides condensed is an inverse function of the gas flow rate in all cases. Increasing the flow rate lowers the fraction of chlorides condensed. The correlation coefficients (the $|r|$ values) are always less than 0.5.

From the foregoing, the procedure to correlate the condensation of metal chlorides is proved very reliable. The condensed fraction of metal chlorides, except SiCl_4 , is a function of the total amount present in the gas phase. The confidence limit for aluminum, iron and titanium are over 99.9% (Table 4.3). For silicon, the confidence limit is much less than 90%. The

Run No.	Total Gas Flow (l/m)	Al		Fe		Si		Ti	
		Cond. (mg)	Total (mg)						
1	16.5	1.3	53.0	1.6	260.0	--	--	--	--
2	15.0	57.0	140.0	55.0	160.0	--	--	--	--
3	10.7	38.0	130.0	45.0	200.0	--	--	--	--
4	10.2	4.0	59.0	3.2	82.0	--	--	--	--
5	14.4	330.0	930.0	280.0	1800.0	--	--	--	--
6	9.8	160.0	470.0	340.0	1300.0	21.0	160.0	3.8	41.0
7	7.3	460.0	1300.0	670.0	2000.0	7.2	180.0	45.0	140.0
8	7.3	1200.0	3500.0	1500.0	4100.0	12.0	540.0	48.0	200.0
9	7.0	1700.0	4650.0	1000.0	2900.0	310.0	1000.0	--	--
10	5.6	770.0	3000.0	970.0	3600.0	160.0	580.0	8.7	97.0
11	6.9	530.0	2300.0	250.0	110.0	200.0	920.0	2.8	44.0
12	8.1	880.0	3400.0	260.0	960.0	210.0	1500.0	0.4	13.4
13	7.8	280.0	980.0	160.0	550.0	100.0	530.0	1.1	15.0
14	6.9	540.0	2100.0	135.0	530.0	150.0	870.0	2.6	54.0
15	6.9	670.0	3100.0	210.0	920.0	21.0	950.0	3.2	56.0
16	8.1	900.0	3700.0	390.0	1400.0	66.0	1200.0	8.5	91.0
17	8.1	360.0	1500.0	350.0	1500.0	83.0	420.0	6.0	47.0
18	8.1	310.0	1400.0	93.0	600.0	19.0	390.0	1.7	29.0
19	8.1	830.0	3400.0	215.0	1200.0	120.0	1300.0	3.5	70.0
20	6.9	380.0	1500.0	150.0	600.0	22.0	560.0	19.0	75.0
21	6.9	750.0	3300.0	180.0	1100.0	37.0	1200.0	5.1	83.0
22	7.8	1000.0	3700.0	320.0	1300.0	63.0	1300.0	3.4	81.0
23	7.8	950.0	3700.0	200.0	870.0	55.0	1300.0	2.3	78.0
24	7.8	780.0	3400.0	230.0	1100.0	52.0	1200.0	1.5	53.0
25	7.8	890.0	3600.0	260.0	1100.0	93.0	1600.0	4.9	82.0

Table 4.4 Fraction of Metals Recovered by Condensation.

Species	No. of data points	Correlation Parameters		Correlation Coefficient r	Level of Significance (%)
		a	b		
FeCl ₃	25	0.35	-0.014	0.44	>95.0
AlCl ₃	25	0.29	-0.004	0.12	<90.0
TiCl ₄	19	0.22	-0.017	0.17	<90.0
SiCl ₄	20	0.31	-0.027	0.25	<90.0

Table 4.5 Correlation of Fraction Condensed with Flow Rate (Q).
($k = a + bQ$)

variation in flow rate had a less significant effect on the fraction condensed. The confidence limit for iron is over 95%, but it is much less than 90% for the other chlorides (Table 4.5).

4.6 Products of Chlorination

Each of the metals considered for the study can assume a variety of valencies and thus there is a possibility of each of them forming a number of chlorination compounds. For example, aluminum can react with chlorine to yield AlCl , AlCl_2 , AlCl_3 , Al_2Cl_2 and Al_2Cl_6 . Instead of identifying individual chlorinated forms for each metal, the results were based on the most probable chloride form.

A preliminary screening of the possible chlorinated forms can be aided by the results of the equilibrium calculations. In the presence of sufficient quantities of chlorine and the reducing agent it is shown that the more probable species of aluminum are AlCl_3 and Al_2Cl_6 . At temperatures below 800 K, Al_2Cl_6 decomposes to give AlCl_3 molecules. The stability of Al_2Cl_6 in the vicinity of 450 K which is the sublimation temperature for AlCl_3 , is only minimal. It can be inferred, therefore, that the product of chlorination of aluminum will be Al_2Cl_6 . However, the lower temperature in the condensation column would cause the dissociation of Al_2Cl_6 to give AlCl_3 . This is also

substantiated by the observation that the condensation of aluminum chloride was observed only in the cooler sections of the quartz tubing. The sections which were exposed to temperatures above 300°C did not have an appreciable deposition of aluminum chloride. It can be concluded that the most probable chlorinated species of aluminum is AlCl_3 for the present system. Nevertheless, since the aluminum to chlorine ratio in both AlCl_3 and Al_2Cl_6 is identical, the representation by either one of them would be acceptable for this study.

The situation for silicon and titanium is relatively simple. From the equilibrium calculations, the likely chlorides of silicon and titanium are SiCl_4 and TiCl_4 , respectively. The presence of SiCl_4 and TiCl_4 is also confirmed by the condensation of solids data shown in Figure 4.7. In both cases, the di- and tri-chlorides tend to have much higher boiling points (above 1000°C). In the event the lower chlorides were to form, the condensed fractions in Figure 4.7 would be much higher. Therefore, for silicon and titanium the most probable chlorinated forms are SiCl_4 and TiCl_4 , respectively.

The situation for the case of iron is very interesting. From the thermodynamic calculations it was found that at higher temperatures (> 1000 K) the dichloride form becomes more dominant than the

trichlorides. Whereas at lower temperature (< 800 K), FeCl_3 is the only probable form. Thus the likelihood of the formation of $(\text{FeCl}_2)_x$ is significant at the reaction temperatures, as the product gas mixture is cooled the trichloride will be obtained. The necessary chlorine amount in this transformation will perhaps come from the excess chlorine in the carrier gas. Once again, the preferential formation of FeCl_3 is confirmed by the condensation data shown in Figure 4.6. The condensation temperature for ferrous chloride is > 950 K, whereas that of FeCl_3 is < 600 K. If FeCl_2 were to be the probable species, the fraction of iron chloride condensed would be more than 31% and significantly higher than 26% for AlCl_3 with sublimation temperature 466 K.

From the foregoing analysis it is concluded that the most probable products of chlorination for the four metals studied are their highest chlorides.

CHAPTER 5

MATERIALS AND METHODS

5.1 Characteristics of Ash

A number of physical and chemical characteristics of ash samples were determined. In this section, the techniques and results obtained will be discussed briefly.

5.1.1 Particle Size Distribution

The particle size distribution of fly and bottom ash were obtained by sieve analysis. The sieving was continued for 30 minute periods and each determination was repeated for improved reliability. The sieving of particles of diameter smaller than approximately 75 μ m was poor and extremely slow. This is believed to be due to a build up of electrostatic charge which resulted in the agglomeration of the fines. In all there were 4 different samples of ash available from a power plant in Central Alberta; 2 each of fly and bottom ash. The samples of coal ash were obtained by sampling over a period of time. The sieve test results are plotted as differential analyses in Figure 5.1. The sieve analysis of the fluid coke is given in Figure 5.1(b).

The curves for fly ash indicate similar size distribution for the two samples. There is, however, a

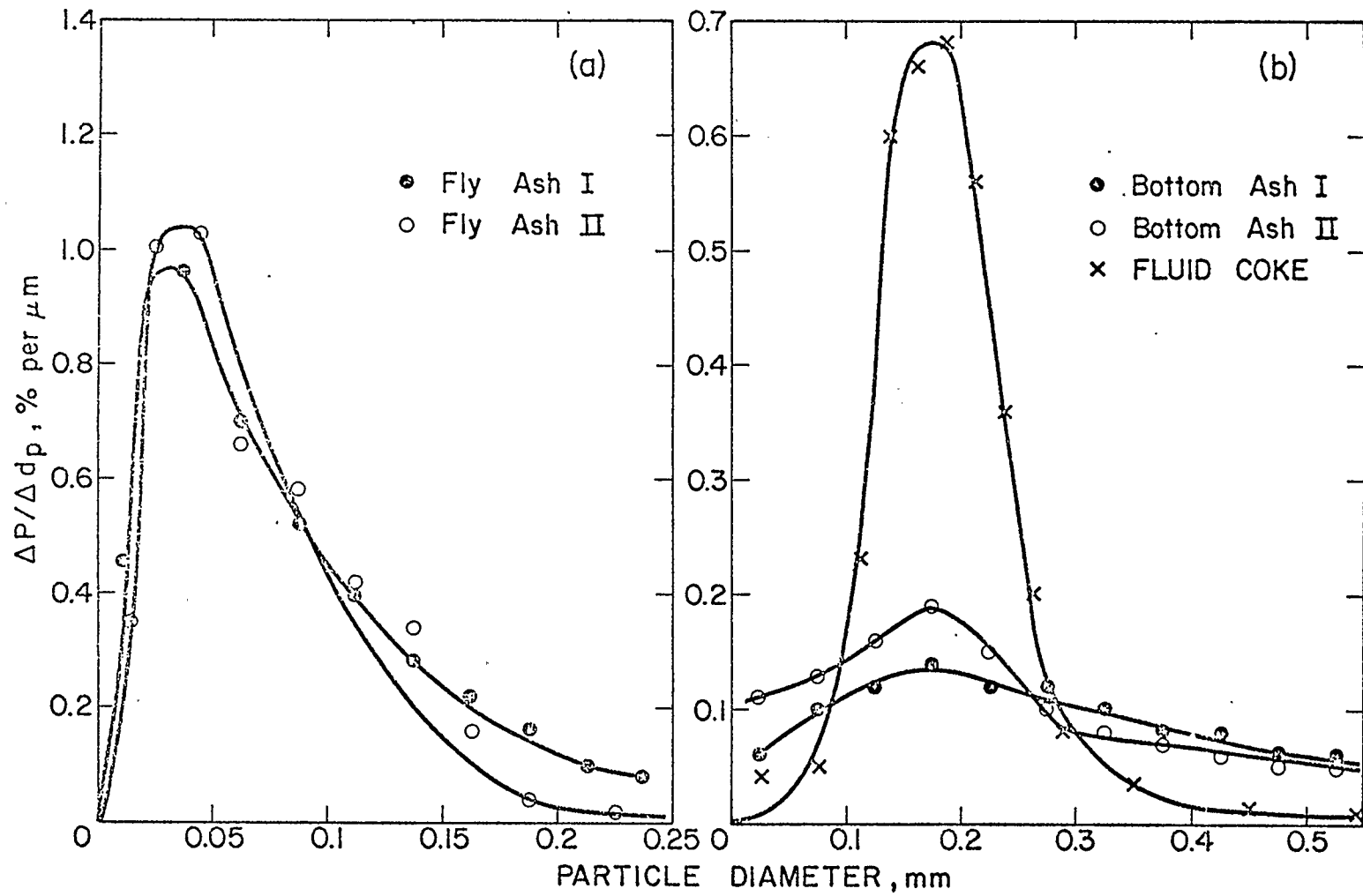


Figure 5.1 Particle Size Distribution of Ashes by Sieve Analysis.

larger fraction of particles with diameter $>100\mu\text{m}$ in batch I as compared to batch II. Both ash samples indicate sharp peaks around $25-50\mu\text{m}$. Bottom ash, in contrast, is much coarser in nature. Frequently, particles as large as 3 cm were found to be present in bottom ash. Bottom ash samples show more uniform particle size distribution, with very low peaks around $150-200\mu\text{m}$. Bottom ash sample II contained more fines than batch I. For fluid coke, a sharp peak is observed around $150-200\mu\text{m}$.

5.1.2 Density

The density of several size fractions was determined using a pycnometer procedure and distilled water as reference. Care was taken to remove air bubbles from the samples. The results are listed in Table 5.1. In general, the density of bottom ash fractions is lower than fly ash. Ash samples after the removal of the volatile fraction show an increase in the density.

5.1.3 Volatile Fraction

Ash samples contain 2-4% of the mass as a volatile fraction. This was removed by heating the sample at 650°C for 15 minutes. The fraction is higher in bottom ash, given in Table 5.1, due to a larger fraction of carbon particles present.

Ash	Tyler Size	Avg. Dia. (μm)	Density (g/cm^3)	Volatile (%)	Moisture (%)
Bottom	-20+50	505	2.01	3.2	...
	-50+60	274	1.94	4.6	...
	-60+80	210	1.97	4.0	...
	-80+100	163	1.99	3.4	0.11
	-100+140	125	1.99	2.6	...
	-140	<105	2.03	2.4	0.17
	-20+50*	505	2.30
	-80+100*	163	2.17
Fly	+80	>177	2.01	3.4	...
	-80+100	163	2.10	2.9	0.08
	-100+140	125	2.20	2.3	...
	-140+200	89	2.21	2.2	0.10
	-200	<75	2.24	2.2	...
	-100+140*	125	2.24
	-140+200*	89	2.26

* Samples after ashing at 650°C.

Table 5.1 Physical Properties of Ash Fractions.

5.1.4 Moisture Content

The moisture content, determined at 110°C , is found to be very small for the case of fly ash. Bottom ash needed considerable drying before the sieve tests could be performed. The moisture content for bottom ash, given in Table 5.1, is after this primary overnight drying.

5.2 Chemical Analysis of Ash

For the determination of metal concentration in ash samples, the following procedure was adopted:

- (a) 0.1 g ash + 0.5 g LiBO_3 were fused together in platinum crucible at 1000°C for upto 2-hour period.
- (b) the crucible was submerged in hot 50% HNO_3 for a period of 4 hours or more.
- (c) the diluted solution was finally adjusted to 100 ml for atomic absorption analyses.

The lithium metaborate fusion procedure is commonly used for the determination of metals in soil samples (56). Difficulty was experienced, however, in dissolving the fused mass completely in acidic medium. Several other dissolving reagents, such as aqua regia, 50% HCl etc., were also tried, but a small fraction of white flaky substance always remained undissolved. The analysis given in Table 5.2 represents the composition of the supernatant. The determination of silicon by this procedure appears erratic and is questionable

Ash type	Size (um)	Elements, % by wt.							
		Al	Fe	Ti	Na	K	Ca	Mg	Si*
Fly	125	16.0	1.3	0.4	1.2	0.7	0.8	0.1	27.4 (23.0)
	89	15.8	1.3	0.3	1.3	0.7	0.8	0.1	27.6 (21.9)
	75	15.5	2.2	0.5	1.5	0.5	0.9	0.2	26.9 (6.1)
	<75	12.6	2.9	0.6	2.0	0.8	1.5	0.3	28.0 (5.4)
Bottom	163	15.4	2.4	0.6	1.2	0.6	1.0	0.2	26.8 (16.7)
	125	15.1	2.5	0.5	1.4	0.6	1.2	0.2	26.9 (16.7)
	89	14.0	2.1	0.6	1.4	0.6	1.0	0.2	28.1 (14.0)
	<89	14.3	2.0	0.5	1.5	0.6	1.5	0.2	27.6 (4.8)

* obtained by difference; the actual analyses are shown in brackets.

Table 5.2 Metals in Coal Ash.

(actual analyses are also given). The silicon fraction as calculated from an element balance of ash, assuming 5% of the ash to be other fractions, is also indicated in Table 5.2. The concentration of calcium is also low, when compared with the analysis of a similar ash sample (18), given in Table 2.1.

5.3 Acid Leaching of Ash

The purpose of this study was to help understand the dissolution of metals in ash into 1 N HCl solution. The ash samples of two different sizes were selected to obtain the extent of metals dissolution at room temperature. The known quantities of the ash samples were placed in 6 flasks and measured amount of 1 N HCl solution was poured into each flask. The contents at room temperature were mixed with a magnetic stirrer. The contents were filtered at regular time intervals and the filtrates collected were analyzed by atomic absorption analysis. A very minor increase in the pH of the filtrates indicated that the strength of the solution remained constant. The results are expressed as the fraction of metals dissolved at the end of each time period. The metals that the filtrates were analyzed for are aluminum, iron, silicon and titanium.

The fractions of each metal dissolved for the two ash sizes are plotted against the logarithm of time in Figure 5.2 (a) and (b). The effect of particle size on

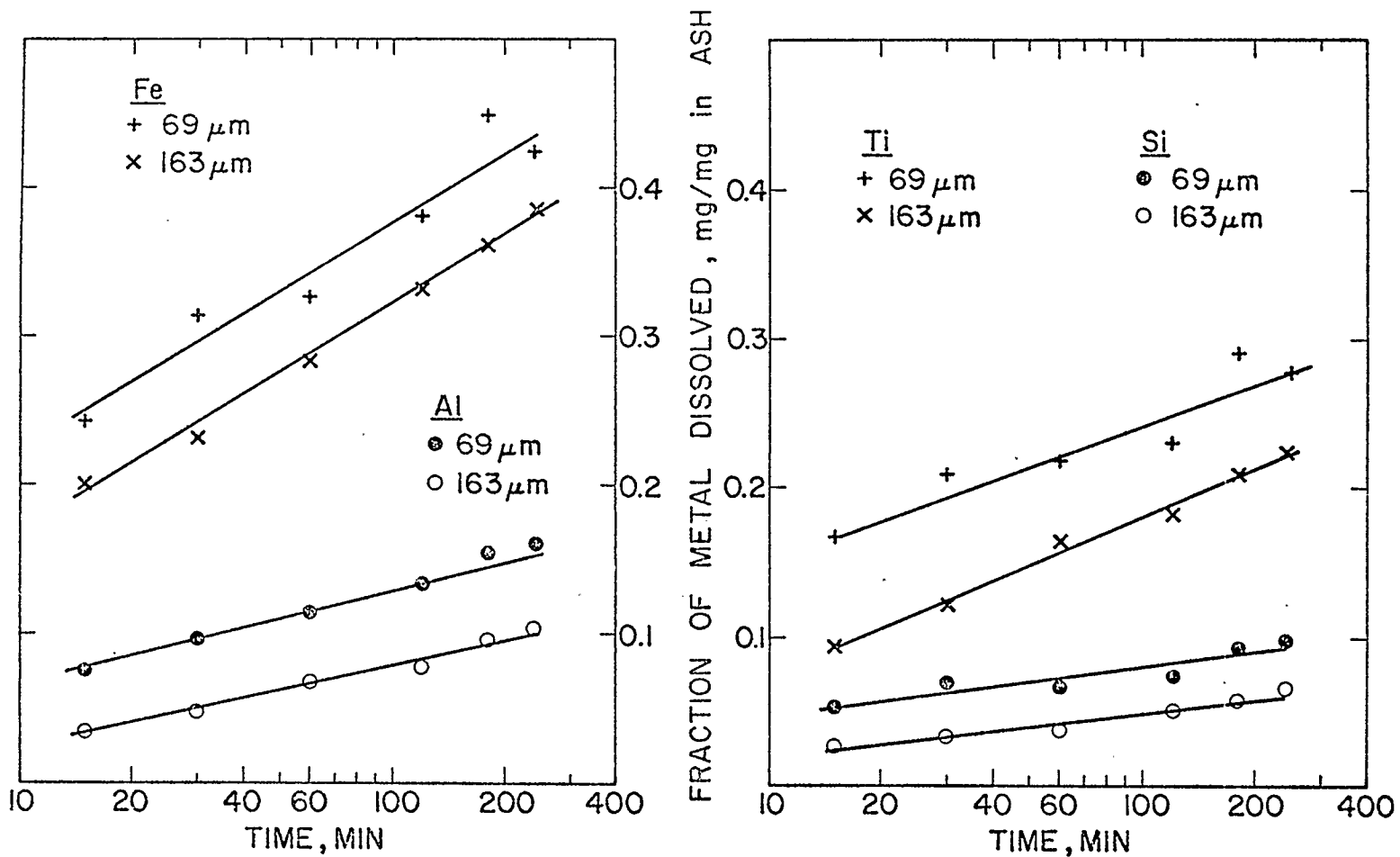


Figure 5.2 Dissolution of Metal Fractions in HCl solution.

the extent of leaching is clearly evident. Reducing the particle size results in the increase of fraction dissolved for all 4 cases. The time required for the same fractional dissolution in the c approximately doubled when the particle diameter is reduced by more than half. This indicates that the rate for iron is proportional to the mean particle diameter. Reducing the particle size by a factor of 2.4 increases the rate by 5 to 10 times for aluminum, silicon and titanium.

It can be concluded, therefore, that though the rate of dissolution of metals in ash is rather slow, the overall rate is definitely a function of particle size. The extent of such dissolution is greatest for iron and the slowest for silicon and aluminum.

5.4 Thermal Behaviour of Ash

The presence of a liquid phase was observed when ash samples were heated to beyond 800°C . The liquid fraction was sufficient to cause the caking of ash particles. This occurred in the temperature range $820-840^{\circ}\text{C}$ and was more prominent with particles smaller than $125\ \mu\text{m}$. The formation of liquid resulted in the failure of fluid-bed operation.

5.4.1 The Differential Thermal Analysis

In order to study the thermal changes that take place when ash is heated up, a differential thermal analysis (DTA) of the samples was performed. The tests were conducted on a DuPont 900 Differential Thermal Analyzer at the Research Council of Alberta Laboratories, Edmonton.

In DTA tests, energy changes are detected as the difference in temperature between two matched thermocouples. One thermocouple was placed below the platinum cup holding the sample while the other one remained in contact with a thermally inactive sample (Al_2O_3 in this study). The reference thermocouple was placed in an ice bath. As the sample showed energy transitions resulting in absorption or release of heat, the curve on the recorder showed an endotherm or an exotherm, respectively. Though the maximum temperature which the samples were raised to was around 1250°C , the furnace was capable of attaining temperatures to 1600°C .

The samples were heated in an inert atmosphere of helium at 1 atmosphere. The heating rate for all runs was maintained at 10 mv/min, which for Pt-Pt 13%Rh thermocouples gives an initial heating rate of approximately $45^\circ\text{C}/\text{min}$. Due to the non-linear nature of temperature-millivolt curve for this thermocouple, the heating rate drops as the temperature increases. The

DTA curves, for this reason, have a non-linear temperature axis.

Though only the heating curves were recorded in most cases, the thermogram traces obtained during the ambient cooling of samples were recorded in some cases as well. The comparison of heating and cooling curves can provide useful information. For instance, if there is no weight loss with thermal activity, such as melting, the two curves should be more or less identical. If, however, the process is accompanied with certain weight loss, such as decomposition of a constituent, the curves will not have similar profiles.

5.4.2 Thermograms of Ash Samples

The DTA thermograms for fly and bottom ash samples are given as Figures 5.3 and 5.4. There are apparently two regions of intense thermal activities. The temperature range of the first endothermic activity is 375-525°C. The second and more prominent activity takes place at approximately 1000°C. Since both of these endothermic dips are reproduced in the cooling curve (Figure 5.3(b)), it can be concluded that these correspond to certain phase transformations. The anticipated melting of compounds around 800-850°C is not apparent in the thermograms. Nevertheless, the endothermic dips are observed clearly in this temperature range for the two bottom ash samples. It is also

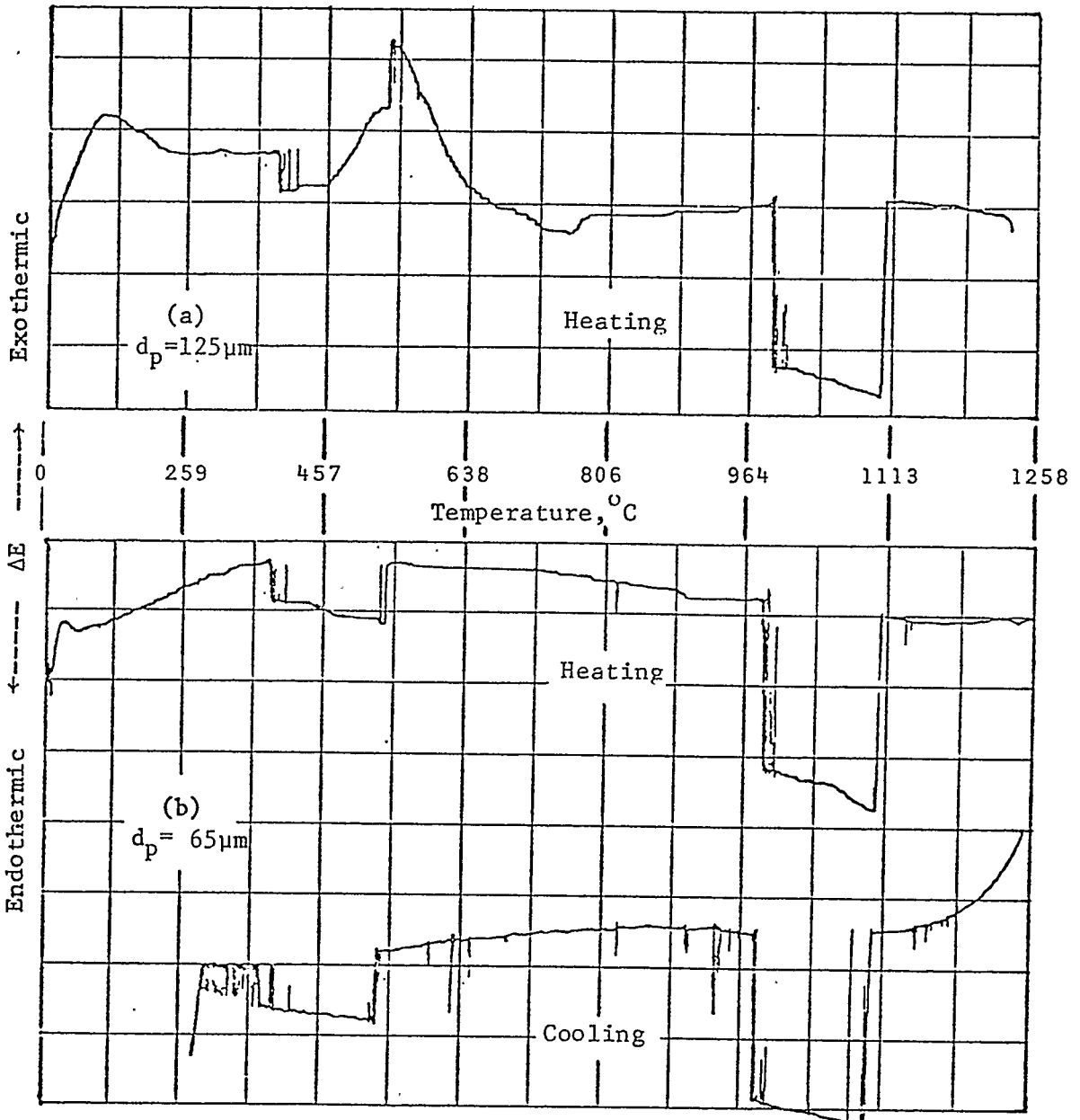


Figure 5.3 DTA Thermograms for Fly Ash Samples.

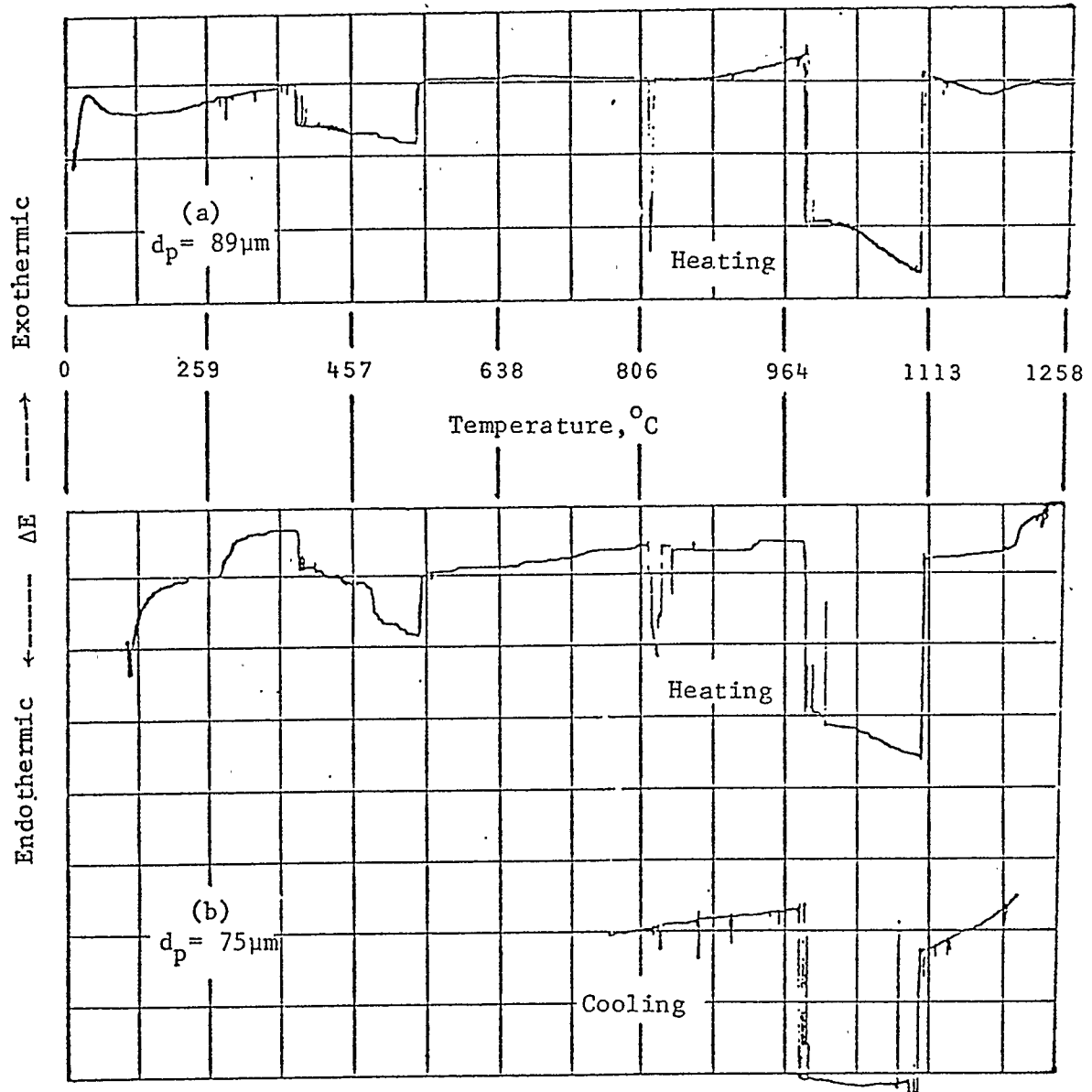


Figure 5.4 DTA Thermograms for Bottom Ash Samples.

interesting to notice a number of minor endothermal dips in the cooling trace for the finer ash particles. The fly ash sample ($d_p = 125\mu\text{m}$) was examined under atmospheric environment, and thus the exothermic peak in the vicinity of 500°C may be indicative of the combustion of carbonaceous matter in ash.

There is only a limited amount of information that can be obtained from the DTA tests for a complex mixture of constituents, such as ash. The presence of trough shaped endotherms could indicate the occurrence of a number of endotherms close to one another. An attempt to identify compounds that may be causing the observed thermal activities would be fruitless. The task of identifying the compounds is complicated due to the formation of eutectics within the species. The eutectics may possess much lower overall melting points. Further attempts in this direction were beyond the scope of the present work. A list of compounds which may be contributing to the observed thermal changes is compiled as Table 5.3.

5.5 Surface Characteristics

5.5.1 Microscopic Studies

A general understanding of the physical geometry of ash particles was obtained by examining the particles with a Carl Zeiss photomicroscope. A 35 mm camera was attached to the microscope for taking pictures. Ash particles under the microscope were found to be of

Substance	Phase Change	Temp., °C
$\text{Al}_2\text{O}_3 \cdot \text{Na}_2\text{O} \cdot 6\text{SiO}_2$	melting	1100
$\text{Al}_2\text{O}_3 \cdot \text{K}_2\text{O} \cdot 6\text{SiO}_2$	melting	1150
CaCl_2	melting	772
CaCl_2	boiling	>1600
CaCO_3	decomp.	825
CaSiO_3	trans.	1190
FeSO_4	decomp.	671
$\text{Fe}_2(\text{SO}_4)_3$	decomp.	480
KCl	melting	790
KCl	boiling	1500
K_2CO_3	melting	891
K_2SiO_3	melting	976
MgCl_2	melting	712
MgCl_2	boiling	1412
MgCO_3	decomp.	402
MgSO_4	melting	1127
NaCl	melting	800
NaCl	boiling	1413
Na_2CO_3	trans.	450
Na_2SiO_3	melting	1089
Na_4SiO_4	melting	1018
SiO_2 , Quartz	trans.	806

Table 5.3 Some Compounds Showing Phase Change in Temperature Range 400-1400°C.

varying physical characteristics. A majority of the particles were more or less round in shape. The tendency of particles to be more spherical increased when the smaller particle size (<75 μ m) was selected.

The spherical particles also demonstrated a striking variation in colour, varying from blueish green to red. This colour variation would suggest a significant nonhomogeneity in the chemical structure among the particles. The photographs of 3 different size ranges are given as Plates 5.1 to 5.3. The highly roughened surface of the coke particles from a fluid bed coking unit is apparent in Plate 5.4. While Plate 5.1 is prepared using a transmitted beam of light, all other photographs are with the reflected light. The particles of ash are highly lustrous with the presence of unburnt carbon fraction. The particles of <75 μ m range tend to be more round. A large proportion of fines in Plate 5.1 would substantiate a note, in Section 5.1.1, regarding the difficulty in sieving small ash sizes.

Ash particles that have undergone partial chlorination conclusively show a lack of the lustrous characteristics noted previously for the unreacted ash samples. The particles in Plates 5.5 and 5.6 appear to have changed dramatically in their physical appearance. The surface of black coke particles in Plate 5.6 is also noticed to have changed physically during the

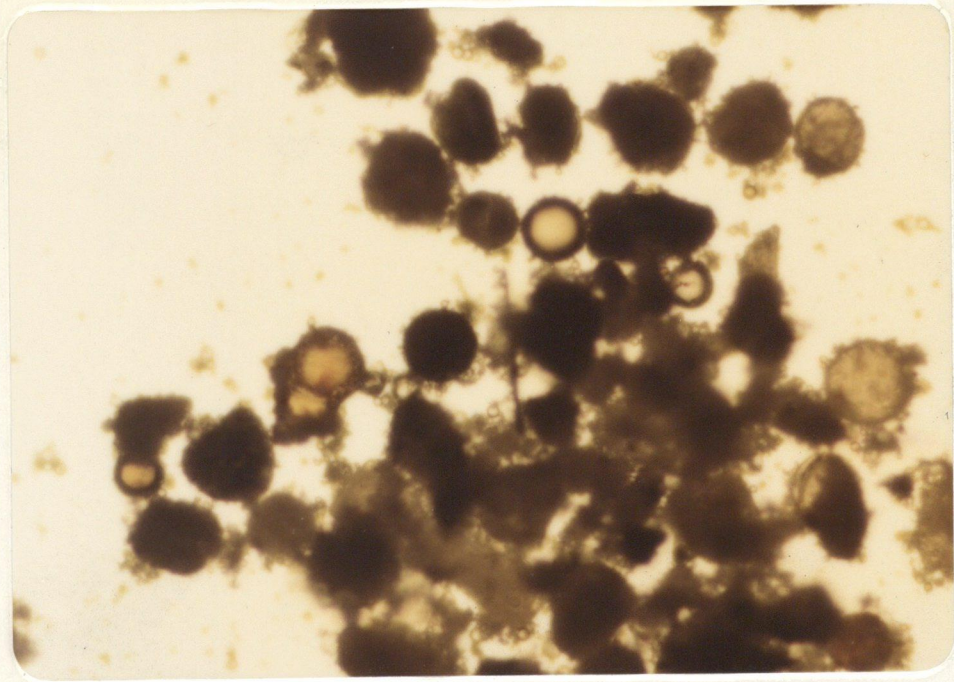


Plate 5.1 Fly Ash < 75 μm [X 160].

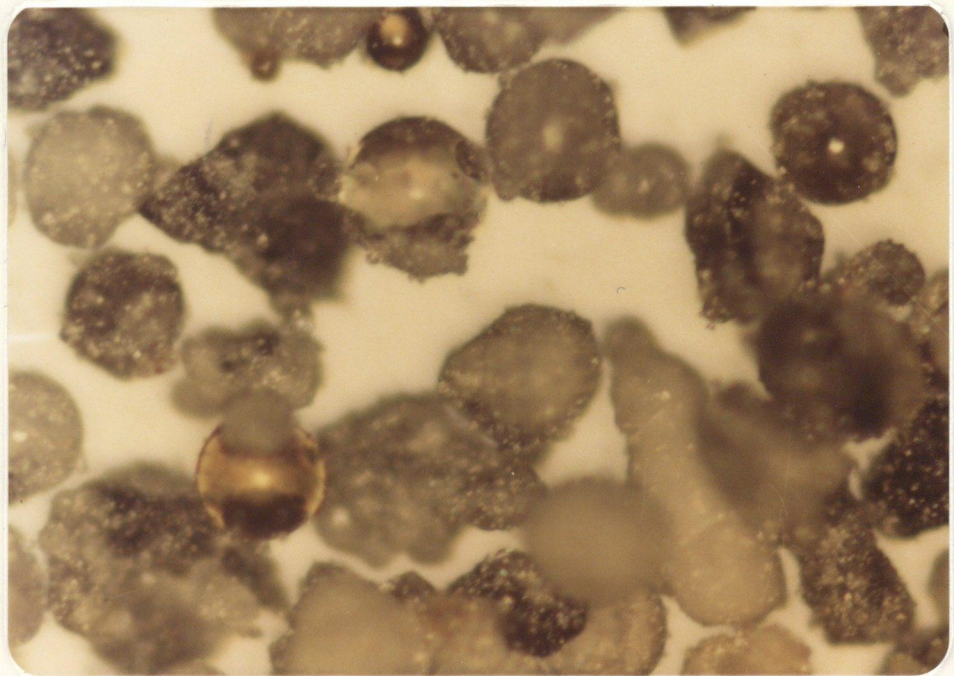


Plate 5.2 Fly Ash 89 μm [X 200].

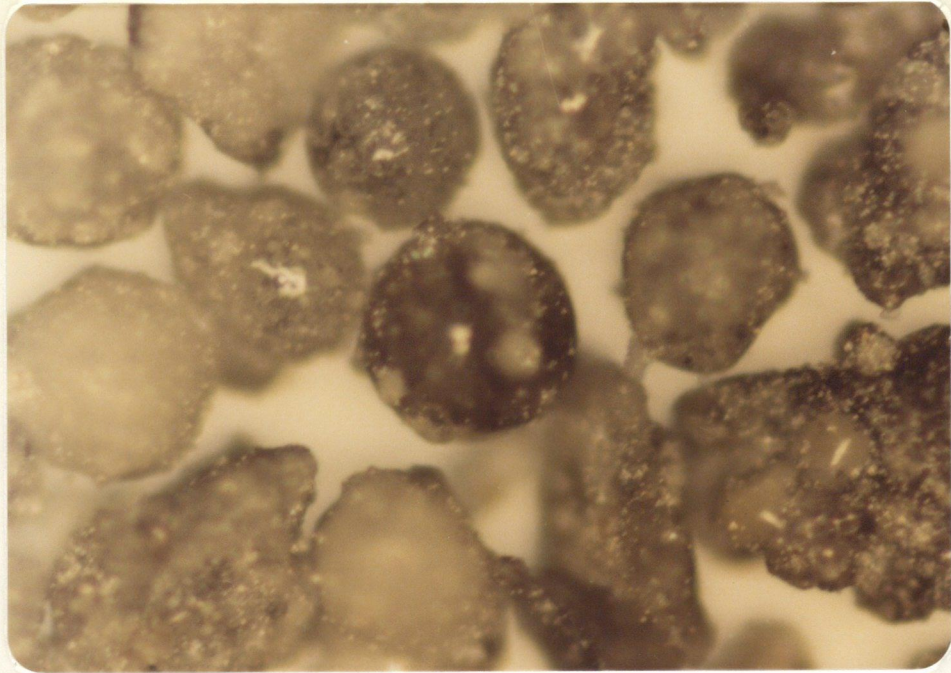


Plate 5.3 Fly Ash 125 μm [X 200].

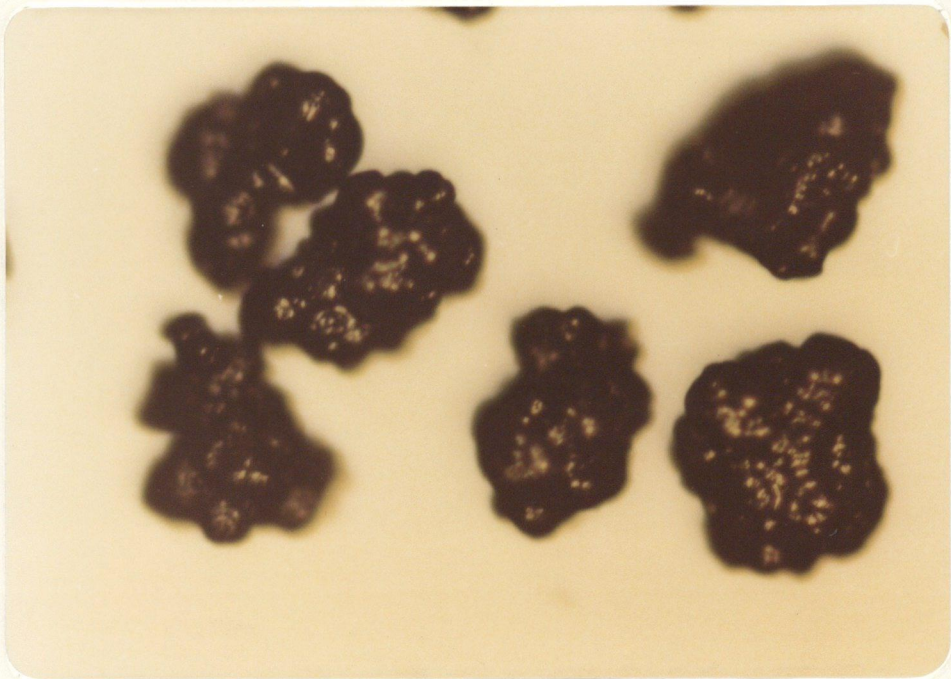


Plate 5.4 Fluid Coke 163 μm [X 200].

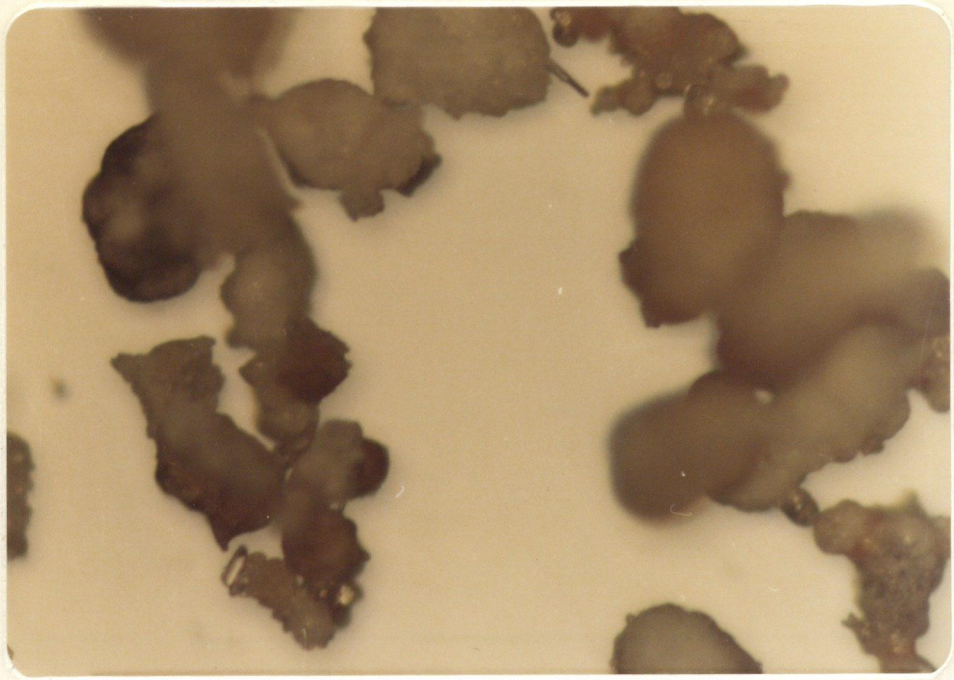


Plate 5.5 Spent Ash (# 10) [X 200].

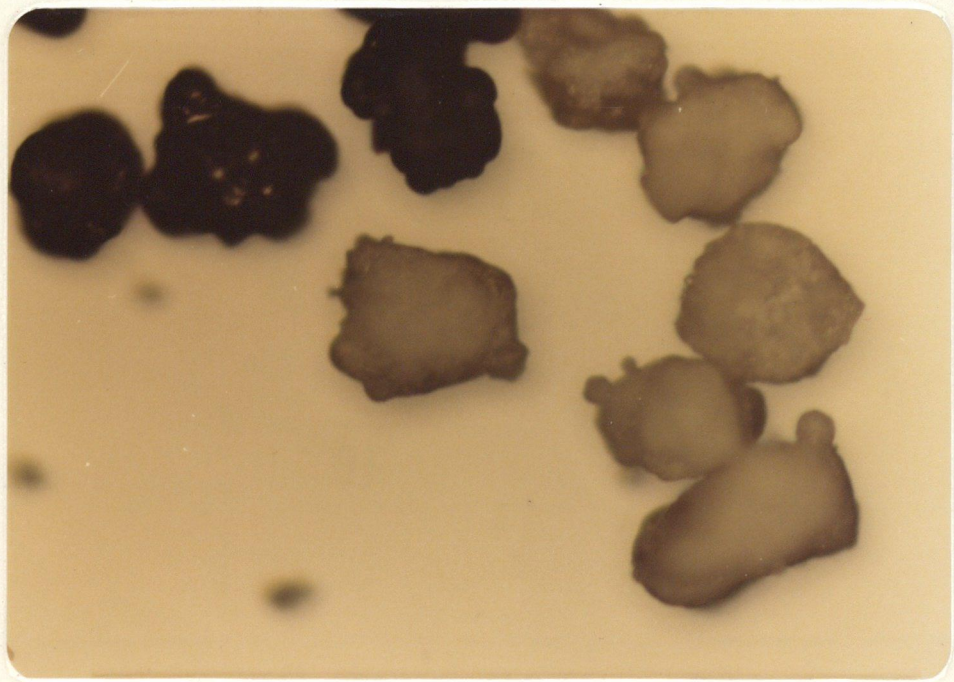


Plate 5.6 Spent Ash + Coke (# 21) [X 200].

chlorination process. The reacted ash particles in Plate 5.5 have a coating of certain brownish-red material, which is absent originally in the ash. This material has definitely resulted from the chlorination reactions.

5.5.2 Surface Area Determination

The measurement of particle surface area was performed on a Perkin-Elmer Sorptometer model 212D. Basically, the measurement technique required adsorption of nitrogen molecules onto the particle surface using helium as the carrier gas. The analysis of gas released during the desorption cycle provided an estimate of the amount of nitrogen adsorbed. The area occupied by a monolayer adsorption is a known quantity and it provides an estimate of the total surface area. The samples were degassed at 190-195°C for over an hour prior to the adsorption step. Several different size samples of fly and bottom ash were tested by this procedure and were repeated for improved reliability of the results. In addition, the surface area of partially chlorinated ash samples along with 3 fluid coke samples were estimated. The results are given in Table 5.4.

In order to appreciate the extent of intraparticle surface area that is available in each case, the measured values should be compared with the area

Sample No.	Material	Size mm	Specific Surface Area, m ² /g		Ratio of Measured to Calculated Areas	Area Lost During Chlorination m ² /g
			Measured	Spherical Calculated		
1	Fly Ash	163	3.5	0.018	200	-
2		125	3.7	0.022	170	-
3		89	1.4	0.031	46	-
4		65	1.0	0.041	23	-
5	Bottom Ash	125	7.2	0.024	300	-
6		89	4.4	0.033	130	-
7	Fluid Coke	163	13.5	0.025	530	-
8		125	14.1	0.033	430	-
9		89	15.8	0.047	340	-
10	Reacted Bottom Ash	125(# 8)	1.0	0.022	46	6.2
11		89(#10)	0.2	0.031	7	4.2
12	Reacted Fly Ash + Coke	89(#21)	1.6	0.033	50	9.9
13		89(#24)	2.4	0.033	72	9.7

Table 5.4 Specific Surface Area Measurements.

calculated assuming the particles to be perfectly spherical. These calculated values are also listed in Table 5.4. The measured values in all cases are at least an order of magnitude larger than the corresponding area for spherical particles. This indicates that the ash particles either have rough surface or are porous in nature. It is also noticeable that the magnitude of surface area decreases with the mean particle diameter. There can be two explanations for this observation. It is shown in Table 5.1 that the larger diameter ash fractions contain a greater fraction of volatile matter. The volatile fraction is contributed by the unburnt carbonaceous fraction remaining with the ash. But at the same time the volatile fraction for smaller size is around 2%. Thus the difference in volatile fractions in large and small particles can not completely account for the observed variation in surface area. The other explanation is that the smaller size fractions contain particles which are created by the condensation of various volatile constituents of ash (20). The condensation process would produce particles that are non-porous and spherical in shape. The surface area for such particles will be much smaller than the naturally occurring ash particles.

The surface area values for the fluid coke fractions are quite high. Also the surface area is a weak function of the particle diameter. Increasing the particle diameter slightly reduces the surface area. But the values are of the same order of magnitude, indicating that the porous or rough nature of the coke surface is more or less independent of the particle diameter.

The ash samples having undergone partial chlorination of metal constituents have a much reduced surface area. For example, the bottom ash sample with an initial surface area of $7.2 \text{ m}^2/\text{g}$ is found to have a much lower value of $1.0 \text{ m}^2/\text{g}$ after chlorination. The same is true for the case where fluid coke and ash were premixed in a ratio (3:1). The combined surface area of ash-coke mixture is reduced by a factor of 5 to 7 during chlorination.

5.5.3 Surface Loss During Chlorination

Surface area measurements of the previous section clearly demonstrate a significant loss of particle surface area during ash chlorination. The loss in area is primarily due to the presence of metal chlorides which exist as liquid at the temperature of reaction. The reaction temperature was high enough to liquefy these chlorides but not enough to cause their vapourization. Such chlorides are mainly of calcium, sodium, magnesium and potassium. The normal melting and boiling points

of these are given in Table 5.3. It can be seen in the table that the melting temperatures for all four chlorides are below 800°C whereas the boiling point for the case of CaCl_2 is greater than 1600°C .

A relatively simple procedure to demonstrate the presence of these chlorides employs the fact that the metal chlorides are water soluble. A comparison, therefore, can be made of the dissolved fractions in water for unreacted and partially reacted ash samples. Carefully weighed samples (approximately 10 g) of ash were dissolved in 100 ml of deionized water. The samples were heated at 80°C for over 45 minutes to ensure total dissolution of soluble components. The samples were filtered and filtrate was made up to 200 ml. The determination of metal fractions was done by atomic absorption technique. Analysis was done for 8 metals: Al, Si, Fe, Ti, Ca, Mg, Na and K. The solids after filtration were allowed to dry overnight at 110°C and weighed to obtain an estimate of the total weight loss. The filtrate was also analyzed for total chloride and sulfate contents. Chlorides were determined by titrating against a standard silver nitrate solution with potassium chromate as the indicator. Total sulfates were determined using a Bausch & Lomb Spectronic 710 spectrophotometer. The results are summarized in Table 5.5.

Sample No.	Contents		Weight Loss mg/g ash	Fraction Dissolved, mg/g ash						
				Ca	Na	K	Mg	Al	Cl ⁻	SO ₄ ⁻²
1	Fly Ash	163μm	7.8	3.2	0.06	--	--	0.15	0.34	0.26
2		125μm	10.6	3.4	0.06	--	--	0.22	0.69	0.16
3		89μm	7.6	5.7	0.10	--	--	0.12	0.63	0.28
4	Bottom Ash	125μm	9.1	0.5	0.08	--	--	0.04	0.39	0.06
5		89μm	8.0	0.5	0.14	0.02	--	0.14	0.41	0.16
6	Reacted	# 8	64.0	23.6	1.17	0.34	0.04	--	40.9	--
7	Bottom Ash	#10	70.5	9.9	0.95	0.08	0.10	--	17.8	--
8	Reacted	#21	71.5	23.8	0.19	--	0.10	0.19	39.0	--
9	Fly Ash	#20	41.0	13.2	0.71	0.26	0.09	0.53	24.8	--
10	+	#23	50.0	17.0	0.17	--	0.07	0.43	28.3	0.17
11	Coke	#24	59.5	22.0	0.37	0.12	0.11	1.10	40.1	--
12	Coke	125μm	3.2	--	0.04	--	--	--	0.14	--

Table 5.5 Water Soluble Constituents in Ash Samples.

A material balance of the ionic content for each filtrate is given in Table 5.6. For unreacted ash samples, the major water soluble cation is clearly calcium. The concentrations of silicon, iron and titanium were below the detection limit of 1 mg/l for all cases. The anions in terms of chloride and sulfate do not match the cations. The difference in the two signifies the presence of other undetected anions such as hydroxides, carbonates, bicarbonates, etc. No attempt was made to analyze or identify the remaining anions.

The samples of ash after partial chlorination have calcium and sodium concentrations that have greatly increased during chlorination. Potassium and magnesium fractions are also present in the reacted ash samples. The data for samples 8 to 11 are based on coke free ash content. A significant soluble aluminum content in these samples is probably due to aluminum chloride being dissolved in the rest of liquid chlorides.

The increase in the soluble metal fractions due to chlorination corresponds with a simultaneous increase in the total chlorides. The anions are essentially chlorides and account for over 90% of the total cations. This would indicate that there are about 10% of the anions which are other than the chlorides.

Sample No.	Contents	10 ³ Dissolved Ions x millimoles/g ash							10 ³ Measured Total. x millimoles/g ash	
		Ca ⁺²	Na ⁺	K ⁺	Mg ⁺²	Al ⁺³	Cl ⁻	SO ₄ ⁻²	Cations	Anions
1	Fly Ash	80	3	0	0	6	10	3	181	16
2		85	3	0	0	8	19	2	197	23
3		142	4	0	0	4	18	3	300	24
4	Bottom Ash	13	3	0	0	1	11	1	32	13
5		11	6	1	0	5	12	2	44	16
6	Reacted Bottom Ash	589	51	9	2	0	1152	0	1242	1152
7		247	41	2	4	0	501	0	545	501
8	Reacted Fly Ash + Coke	594	8	0	4	7	1099	0	1225	1099
9		329	31	7	4	20	699	0	764	699
10		424	7	0	3	16	797	2	909	801
11		549	16	3	5	41	1130	0	1250	1130
12	Coke	0	2	0	0	0	4	0	2	4

Table 5.6 Ionic Balance of Water Soluble Constituents in Ash.

It is evident from the solubility study that the partially chlorinated ash samples contain increased concentration of water soluble metal chlorides. The fact that these metal chlorides exist as liquid above 800°C makes it possible for them to provide a sort of surface coating to the ash particles. The accumulation of liquid over the surface of ash particles will explain the loss of surface area during chlorination.

5.6 Factorial Design of Experiments

A commonly used statistical tool for parameteric study of the process variables is factorial design of experiments. In factorial design, the effects of a number of variables are studied at selected levels. The details of the procedure and the necessary equations are summarized in Appendix II. The procedure is well documented in literature and is adopted from Gregory (55). The replication of experiments was not practised in order to limit the extent of experimentation. The 3-factor interaction term is neglected since most practical systems rarely show a three way interaction. The value corresponding to the 3-factor sum of squares is interpreted as the estimate of error variance. The procedure will be used in Chapter 8 for studying the effect of temperature, particle diameter and gas ratio on chlorination of ash.

CHAPTER 6

PRESENTATION OF RESULTS

CHLORINATION OF ASH WITH CARBON MONOXIDE

The equilibrium thermodynamic calculations, discussed in Chapter 3, indicated the effectiveness of carbon as well as carbon monoxide as reducing agents for the chlorination reactions. From the kinetic view-point the use of gaseous CO should facilitate the gas-solid reactions between chlorine, CO and metal fractions in the ash. In this chapter, the experimental results of the Cl_2 -CO reaction system will be discussed. The experimental data for all the runs are summarized as tables in Appendix III.

6.1 Exploratory Runs at Low Temperatures

A number of chlorination experiments were performed employing the gaseous carbon monoxide. The first of such runs was conducted at 430°C . The temperature for the successive runs was increased gradually in steps of 100 to 150°C .

The product yields are expressed in terms of fraction of each metal originally present in ash that is chlorinated during an experimental run. At low temperatures the yields and reaction rates were low. A

summary of the experimental conditions along with the yields obtained are given in Table 6.1. In addition to the effect of low temperatures, there are two other factors which may have contributed to the observed low conversions. The particle size range was 164 to 229 μm , and the reacting gas mixture contained 28% chlorine. The selection of larger particle size was intended mainly to reduce the carry-over of particles from the reactor.

6.2 Effect of Temperature

The results of the ash chlorination experiments are summarized in Table 6.1. The effect of temperature on the global rate of chlorination reactions is small. The increase in temperature from 430°C to above 950°C resulted in small increases in the rate of aluminum chlorination. The rate of reaction for iron, however, showed a more significant improvement with temperature. The results for silicon and titanium show no definite trends with the variation in temperature. The yields for these two metals were also found to be very low. Thus the temperature does not appear to be the controlling factor in determining the overall reaction rate.

Shown in Table 6.1, the temperature of operation for the run numbers 11 through 13 was maintained in the neighbourhood of 800-810°C. This lowering of the reaction temperature was necessitated due to the occurrence

Run No.	Ash Type	Mean Dia. μm	Avg. Temp. $^{\circ}\text{C}$	Gas Ratio $\text{Cl}_2:\text{CO}$	Duration of Run (min.)	Fraction Recovered, %			
						Al	Fe	Si	Ti
1	Fly	194	430	28:72	60	0.1	8.3	---	--
2	Fly	164	522	28:72	70	0.2	3.2	---	--
3	Fly	164	648	28:72	60	0.3	5.4	---	--
4	Fly	164	758	28:72	80	0.1	2.5	---	--
5	Fly	229	849	28:72	70	1.5	35.0	---	--
6	Bottom	212	902	28:72	110	0.9	29.6	0.2	3.0
7	Bottom	212	960	28:72	120	2.5	48.9	0.2	10.7
8	Bottom	125	975	28:72	175	11.0	74.0	1.0	25.4
9	Bottom	164	970	28:72	180	7.5	57.9	0.9	--
10	Bottom	89	924	50:50	49	4.5	66.8	0.5	7.8
11	Fly	89	808	50:50	180	8.0	48.4	2.2	8.2
12	Fly	125	802	50:50	180	6.5	22.8	1.7	1.0
13	Fly	89	811	67:33	90	3.5	23.7	1.1	2.8

Table 6.1 Summary of Chlorination Experiments with CO as the Reducing Agent.

of an intriguing phenomenon. When an ash sample was being preheated routinely in an inert atmosphere of nitrogen, the bed temperature ceased to increase. The cause for such observation is the creation of a liquid phase when the ash particles are heated to 820-845°C. The disruption of the fluidized state of the ash bed was found to be more pronounced with particles of size 89µm or smaller. The bed with 125µm or larger particles remained fluidized even at temperatures higher than 950°C. The study and discussion of the limitations imposed by this behaviour will be the subject of a later section.

6.3 Effect of Particle Diameter

The rate of metals chlorination is found to be a function of the particle diameter. Shown in Figure 6.1 are the curves for reaction yields with time corresponding to 4 different ash sizes. The curves for aluminum show a definite increase in the yields with reduction in mean particle diameter, d_p . All curves are for the same gas ratio and a narrow range of temperature. The yields based on a 30-minute reaction period indicate an approximate proportionality with the inverse of mean particle diameter. This may be interpreted as the dominance of film diffusion resistance on the overall kinetics in this temperature range.

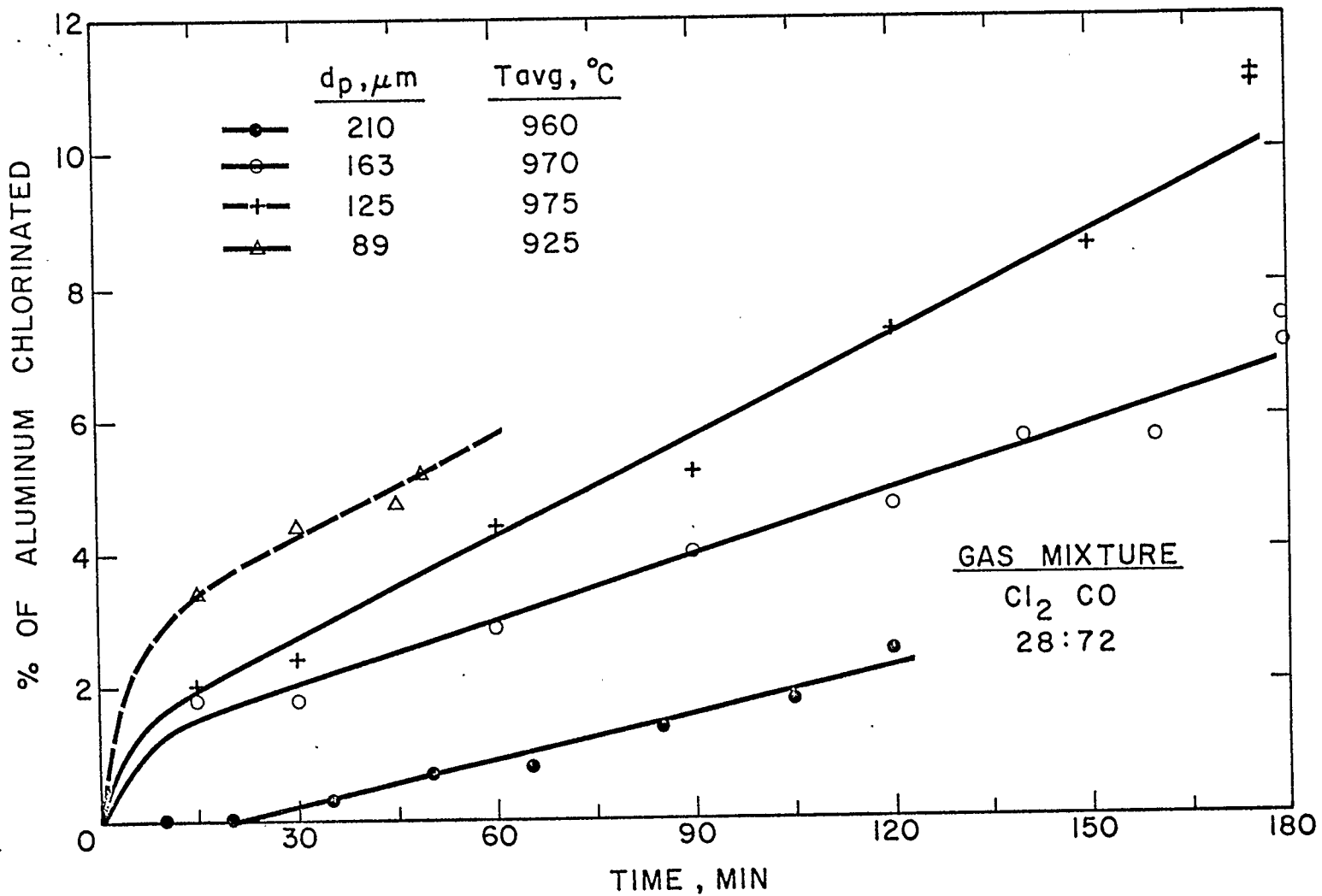


Figure 6.1 Effect of Particle Size on Chlorination of Aluminum.

yields for iron is shown in Figure 6.2. Though the effect is not as apparent as for the case of aluminum, the two larger particle sizes give slower rates. The trend in the yields obtained for silicon and titanium with respect to particle size is inconclusive.

The curves for both aluminum and iron indicate that the reactions proceed rapidly initially in each experimental run. After this initial 15-20 minute period, the reactions proceed at constant rates. This could suggest the presence of two different reaction controlling mechanisms. The high initial rates are in agreement with an observation that the reactor temperature rose sharply as soon as the reacting gases entered the reactor. Since the overall chlorination reactions are exothermic in nature (Table 3.1), the initial reactions generated heat which increased the reactor temperature.

6.4 Effect of Gas Composition

The equilibrium calculations predict an equimolar gas ratio for the reductive chlorination reactions. This is because for each atom of oxygen removed from metal oxides in ash, one molecule of Cl_2 would be needed for chlorination.

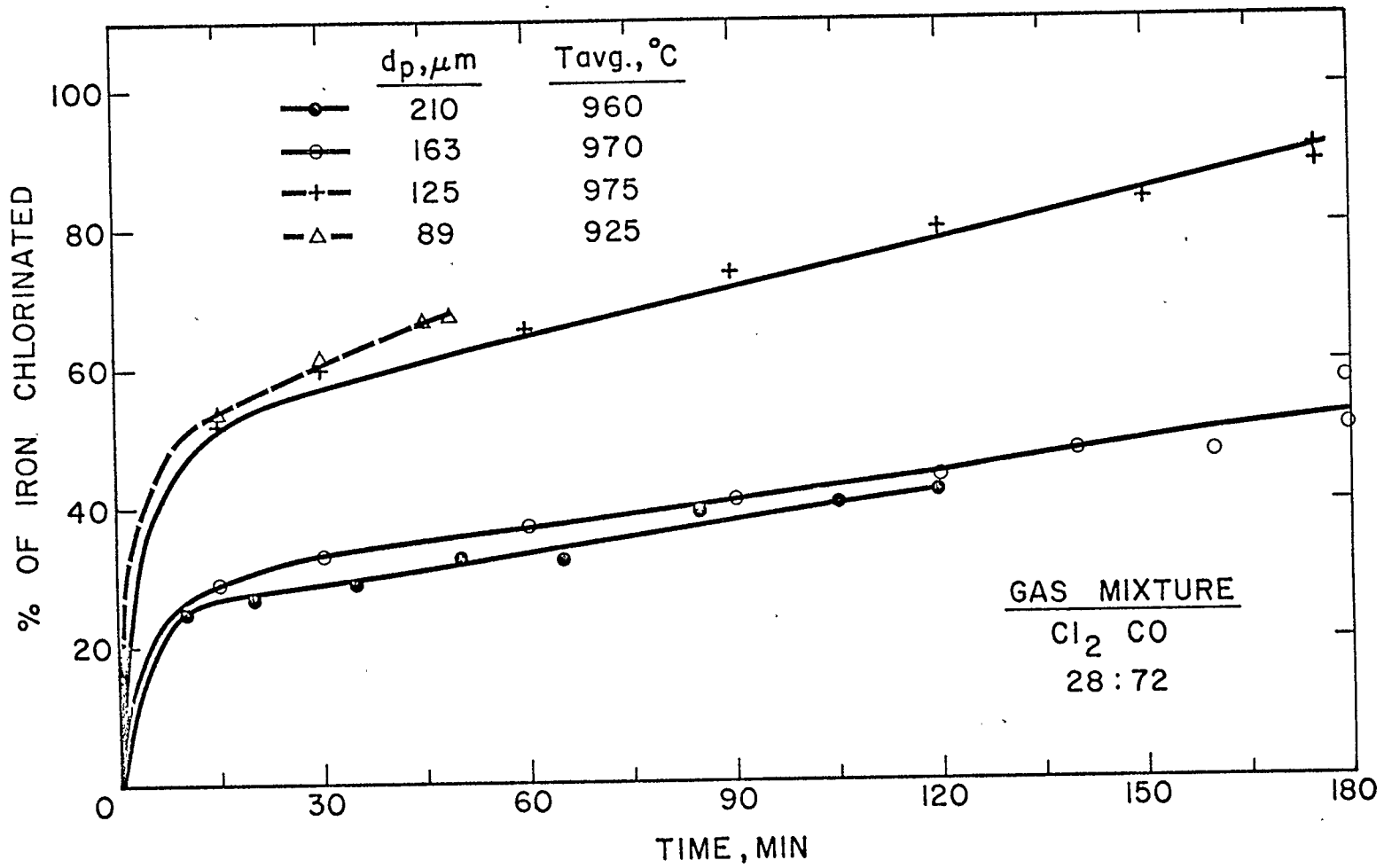


Figure 6.2 Effect of Particle Size on Chlorination of Iron.

The effect of gas composition is shown graphically in Figures 6.3 and 6.4 for aluminum and iron, respectively. The effect of changing gas ratio from (50:50) to (67:33) is small for both metals. It should be noted that these data are for the runs at lower temperature. The comparison for the higher temperature range is not possible due to the loss of bed fluidization at a higher temperature. It is shown in the figures that increasing the chlorine fraction to 67% actually lowers the rates for AlCl_3 and FeCl_3 . This is due to a reduced partial pressure of CO in the gas mixture when the chlorine fraction is increased.

6.5 Effect of Ash Type

While performing the experiments with CO as the reducing agent, samples of fly ash as well as bottom ash were tested. The overall reactions were generally slow in both cases. There does not appear to be any significant difference in the results with the two types of ashes. The effect, if there is any at all, could have been obscured due to the simultaneous variation of other parameters.

6.6 Reduction in Reaction Rate

Although the overall aluminum yields are noted to be low, the reaction proceeds at a faster rate initially. The reactions do not cease even after a 3-hour time period. This is indicated by the straight line

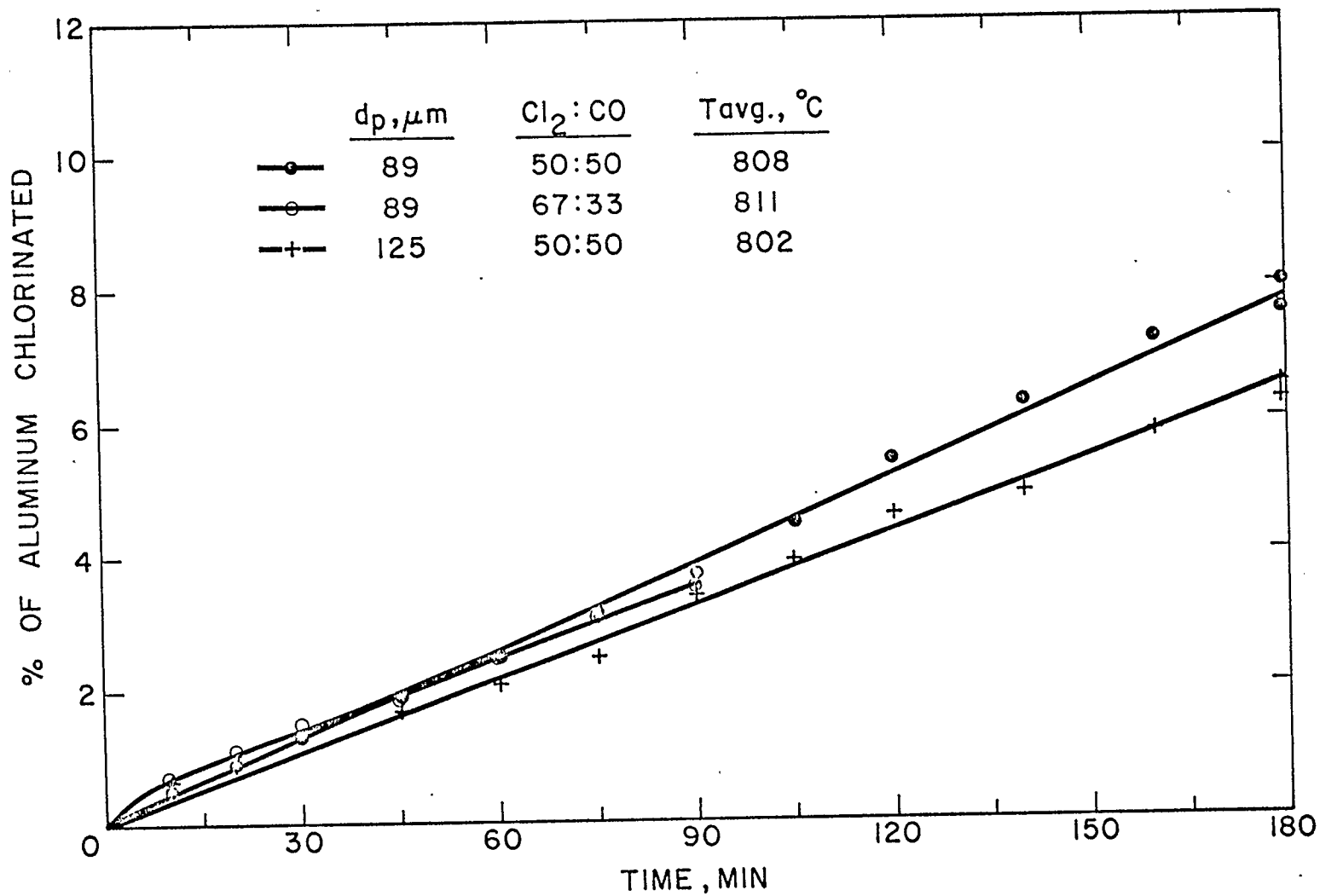


Figure 6.3 Effect of Gas Composition on Aluminum Chlorination.

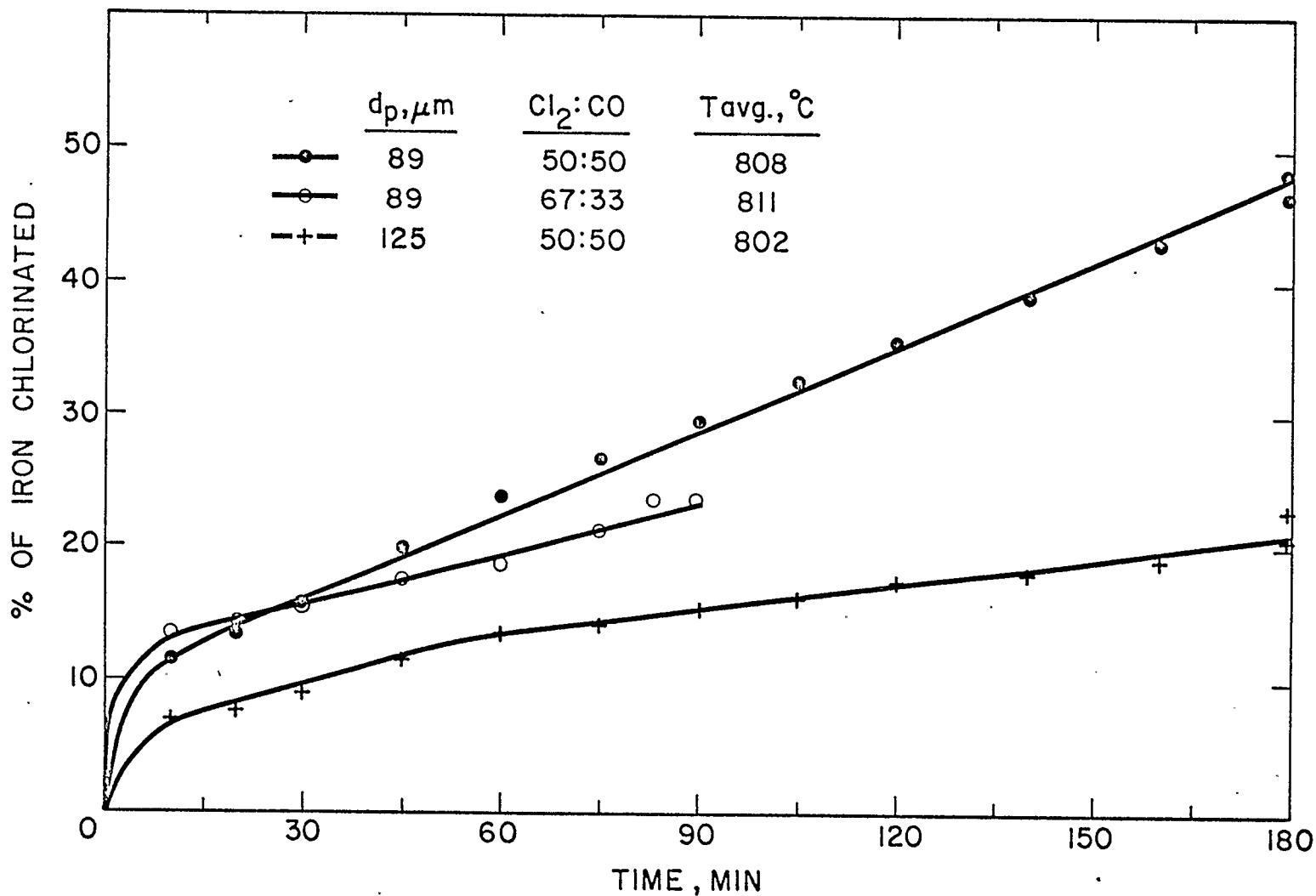


Figure 6.4 Effect of Gas Composition on Iron Chlorination.

portion of the yield curves. This would suggest that the reactions in the later period are influenced by a factor which is not present initially.

6.6.1 Chlorination of Alkali Metals

Coal ash contains small fractions of several minor and trace metals (Table 5.2), such as K, Na, Mg and Ca. The ease with which these constituents can be chlorinated is demonstrated by the equilibrium calculations in Chapter 3. The chlorides of these metals exist as liquids at the reaction temperatures considered in the study. The metal chlorides after chlorination would remain within the reactor, well mixed with the unreacted ash. Thus extra amounts of liquid could coat the ash particles. The presence of such liquid products could be detrimental to the reactions. The chlorination of such metal fractions is possible even without any reducing agent.

6.6.2 Generation of Liquid Melt

As pointed out earlier, the creation of a liquid phase was a serious problem. Though the use of CO did not contribute to this problem directly, the impact of the problem should be realized. When ash was heated to above 820°C, the appearance of liquid within the reactor caused complete disruption of the fluid state. This occurred prior to the passing of the reaction gases.

In one experiment, Run number 10, the experiment was continued despite the loss of bed fluidization. The continued flow of reacting gases resulted in serious slugging of the bed. The experiment had to be discontinued for the fear of an accident due to violent pressure fluctuations. Although the melt may not be enough to cause sticking of the particles, as observed with larger size particles, it will provide some sort of liquid coating on the ash particles. This would give rise to an added resistance to the overall gaseous diffusion. The net effect of the presence of liquid melt will be to slow down the reactions.

6.6.3 DTA Thermograms of Spent Ash

The samples of spent ash recovered after the conclusion of chlorination runs were examined by the DTA technique. The thermograms of ash from run numbers 8 and 10 are given as Figure 6.5. When compared with the thermograms for unreacted bottom ash (Figure 5.4), no significant difference is noticeable. Since the extent of chlorination in both cases was limited, the partial chlorination of ash did not alter the thermal behaviour of ash. The three minor endotherms in Figure 6.5(b) might be due to the chlorides of alkali metals.

6.6.4 Handling the Melt

The creation of liquid is associated with the heating of ash to beyond 820°C . It was anticipated

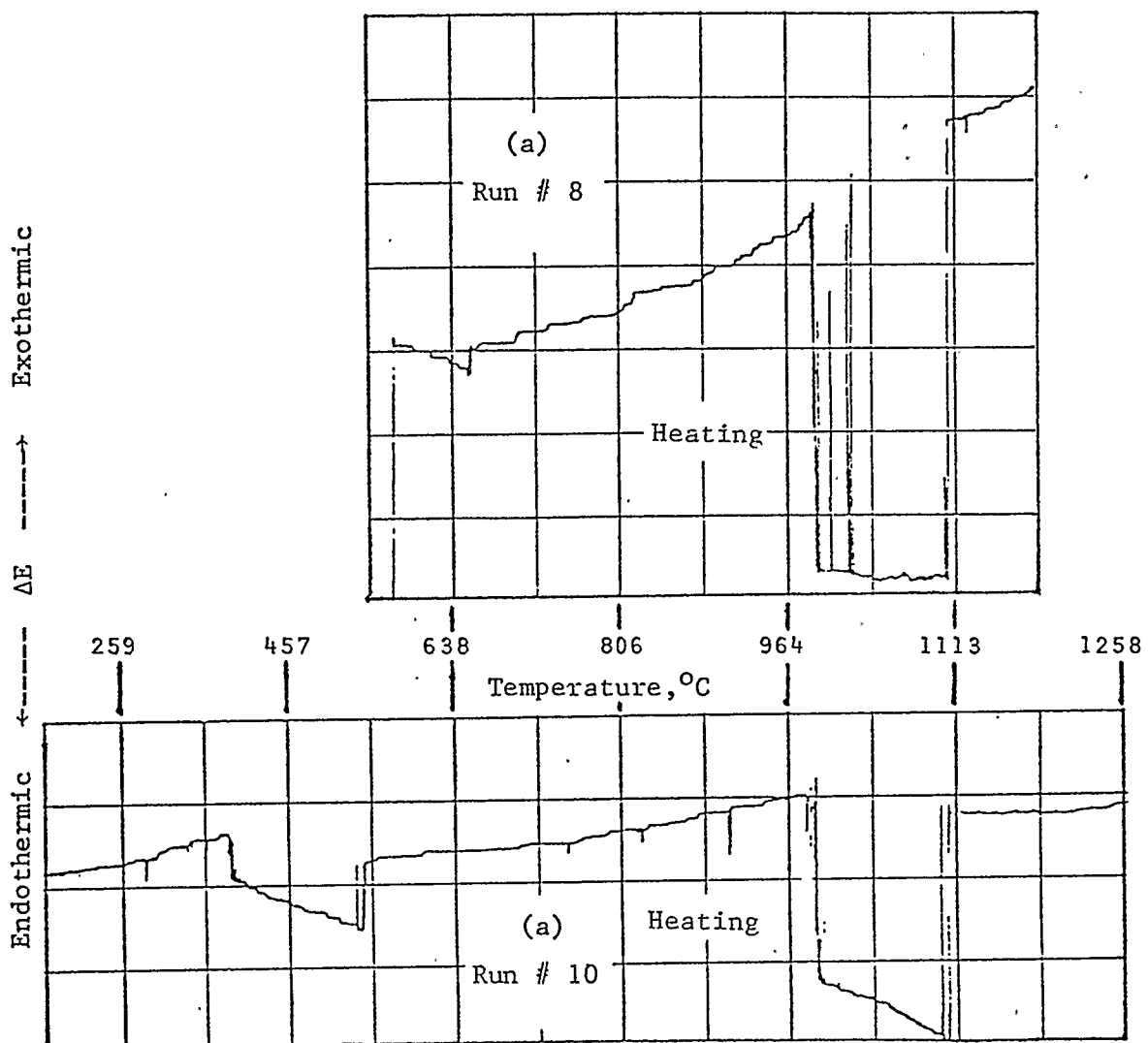


Figure 6.5 DTA Thermograms for Spent Ash Samples of Run Numbers 8 & 10.

that the addition of a non-melting material could be beneficial. The presence of this material, in particulate form, would reduce the overall concentration of the liquid phase. The particulate material should be non-reacting under the environment of chlorine and reducing agents. Therefore, it was decided to study the role of carbon in chlorinating the ash. Carbon particles premixed with coal ash were expected to serve not only as a reducing agent, but also to reduce the liquid fraction in the mixture.

6.7 Sources of Error

The amount of ash for each run was weighed carefully to 0.1 g. But the carryover of the fines into cyclone separator resulted in a loss of the reacting ash. A typical loss due to carryover for most of the experiments was within 1-2% for the run. This loss of the reacting mass is not considered for the purpose of estimating the conversion values. The results of component balance calculations, before and after the reaction, are summarized in Table 6.2. The analyses of ash samples after chlorination are also given in the table. The calculations for silicon are not included due to a lack of reliability in its analysis.

The error for aluminum is mostly within 5-7% showing that the balance is quite satisfactory. The errors for iron and titanium are generally quite large. Iron

Run No.	Ash Mass, gm	Spent Ash Analysis, %			Material Balance Error, %		
		Al	Fe	Ti	Al	Fe	Ti
1	250	15.0	2.2	0.3	-0.1	-19.0	--
2	385	13.9	1.7	0.0	7.1	12.0	--
3	280	14.6	2.0	0.3	2.3	- 5.5	--
4	250	13.9	1.5	0.0	7.2	22.5	--
5	390	13.6	0.8	0.0	7.9	25.0	--
6	345	14.1	1.8	0.4	5.0	-19.5	17.0
7	320	13.8	1.4	0.4	5.5	1.0	11.0
8	200	12.6	0.9	0.3	5.0	-19.0	15.0
9	390	13.1	1.2	0.4	5.1	-18.0	--
10	460	13.2	1.2	0.4	7.5	-27.0	12.0
11	200	14.1	1.4	0.4	-2.0	-18.5	12.0
12	270	14.0	1.3	0.3	0.1	12.0	10.0
13	250	--	--	--	--	--	--

Table 6.2 Estimates of Error by Material Balance Calculations.

and titanium fractions in ash are quite small (Table 5.2). Even a minor variation in their analysis becomes large once the percent values are calculated. The concentration of titanium in the absorbing solution of weak HCl was extremely small (below 10 mg/l). Thus the results for titanium are subject to a greater uncertainty.

A greater confidence in the absorbing solution samples was achieved by increasing the sampling frequency. This is the solution where most of the product chlorides are dissolved. Thus any scatter in the yield data may be attributed to a sampling error. The amount of condensed metal chlorides was accounted for by the approach described in Chapter 4. Necessary precautions were taken in dissolving the solids in the acidic medium to ensure their complete recovery. The filtration of such solutions did not show the presence of any ash particles. This confirmed the effectiveness of the cyclone separator. The solids condensed prior to the cyclone separator were recovered in deionized water. This avoided the possibility of an error that could be caused due to acid leaching of the metal fractions in ash (as discussed in Chapter 5).

6.8 Summary

The chlorination of metal constituents in coal ash was examined using the gaseous mixture of Cl_2 and CO . The results indicate the possibility of chlorinating aluminum and other metal fractions. The experiments with gaseous reactants are characterized by lower yields. The main reason for the lower conversions is the formation of a liquid phase at the reaction temperatures. The amount of liquid was sufficient to disrupt the fluidized state of the reactor, especially in the case of particles smaller than $89\mu\text{m}$. This occurred typically at $820\text{-}845^\circ\text{C}$ and prior to the start of chlorination reactions.

The reactions for the cases of aluminum and iron proceed rapidly at the start of the experiments. There was a considerable decline in the global rate of reaction following the initial period. The time dependence of the global reaction rate will be investigated in greater details in Chapter 8.

CHAPTER 7

PRESENTATION OF RESULTS

CHLORINATION OF ASH WITH CARBON AND CARBON MONOXIDE

After studying the chlorination of ash in the presence of carbon monoxide, a study of the chlorination of ash with carbon was undertaken. As mentioned previously in Chapter 6, the addition of carbon to ash served two purposes. This provided an additional reducing agent and the bulk of it acted to reduce the liquid fraction in the bed. A summary of the 12 experiments performed with fluid coke premixed with fly ash is given in Table 7.1. The experimental data and other details for each run are tabulated in Appendix III. The sieve analysis results are presented in Figure 5.1(b). Surface area measurements for coke samples are given in Table 5.4.

7.1 Carbon to Ash Ratio

The ratio in which coke should be premixed with ash was determined. One important criterion was to achieve the fluidized state of the reacting bed when the temperature was raised to above 820°C . The ratio of (1:1) failed to maintain the fluidized state at 825°C , indicating that the fraction of coke in the bed

Run No.	Mean Dia. μm	Avg. Temp. $^{\circ}\text{C}$	Gas Ratio $\text{Cl}_2:\text{CO}$	Carbon to Ash Ratio	Duration of Run (min.)	Fraction Recovered, %			
						Al	Fe	Si	Ti
14	125	808	1:1	3:1	180	13.1	41.1	3.2	13.5
15	89	911	1:1	4:1	180	28.8	98.5	5.1	27.8
16	125	951	1:1	3:1	160	22.9	99.0	4.6	22.9
17	125	951	1:0	3:1	175	9.2	99.0	1.5	11.8
18	125	952	1:1	9:1	150	21.7	100.0	3.5	17.9
19	125	912	1:1	3:1	150	21.4	91.2	4.8	17.5
20	89	920	2:1	3:1	35	10.8	50.9	2.3	27.9
21	89	951	1:1	3:1	150	23.5	96.9	5.1	30.8
22	89	947	2:1	3:1	130	26.4	100.0	5.3	29.9
23	125	913	2:1	3:1	130	23.0	66.8	5.2	19.4
24	89	912	2:1	3:1	130	23.6	98.0	4.7	19.6
25	125	951	2:1	3:1	130	23.2	83.7	5.8	20.4

Table 7.1 Summary of Chlorination Experiments with Carbon and CO as Reducing Agents.

was insufficient. The ratio in the following trial was increased to (2:1). Upon heating, the bed collapsed at 845°C this time, indicating the need to increase the ratio still further. The ratio was increased to a value of (3:1). With this ratio, the bed remained fluidized without any signs of the liquid disrupting the operation while the temperature was raised to above 900°C. The ratio (3:1) was used as the minimum ratio for further studies.

Due to a significant difference in the densities of fluid coke and fly ash fractions, the selection of particles of similar sizes could result in segregation of the two in the bed. The ash particles have a higher density and may accumulate at the bottom of the bed. This could result in improper contacting of the solids. To offset this, the coke particles were intentionally selected to be larger than the ash particles for all the experiments. For the two ash sizes, 89 and 125 μm , the corresponding coke sizes were 125 and 163 μm , respectively.

7.2 Role of Each Reducing Agent

It will be of importance to estimate the individual effect of the two reducing agents, carbon and carbon monoxide, on the chlorination of metal fractions. The comparison of yields for 4 experimental runs is shown in Figure 7.1.

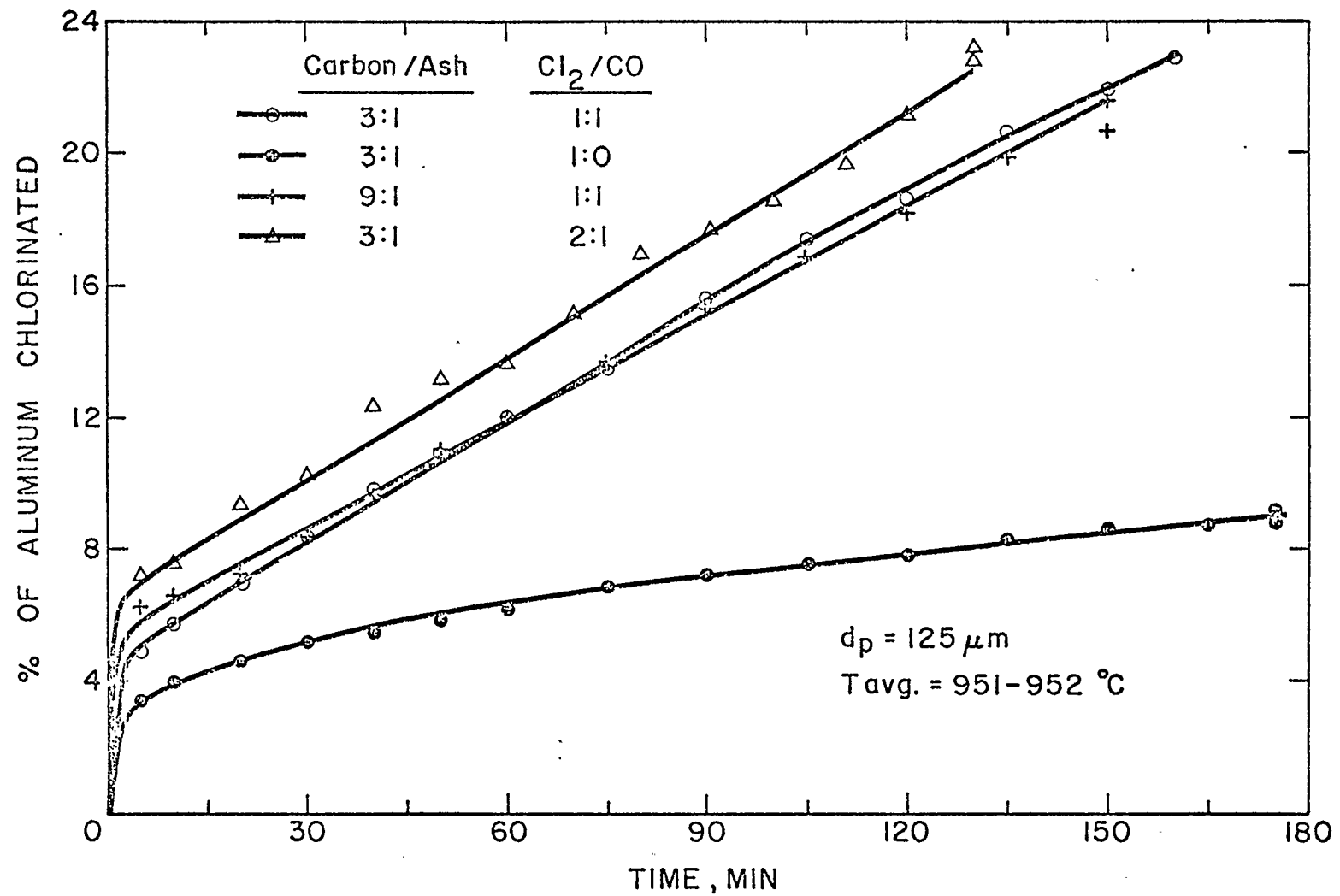


Figure 7.1 Effect of Reducing Agents Ratio on Chlorination of Aluminum.

In order to study the reaction yields with carbon alone as the reducing agent, the gaseous mixture for one experiment contained equimolar fractions of chlorine and nitrogen. The partial pressure of CO was replaced with the inert nitrogen. By doing this, the fraction of chlorine is maintained uniform with other runs. It is apparent from the results that partial chlorination of aluminum occurs at a slower pace. About one-half of the conversion obtained in 175 minutes is achieved during the initial 15 minutes. This is indicative of a much rapid initial reaction.

The result of the run with nitrogen in place of CO provides an interesting comparison. Under identical conditions, the presence of CO along with coke more than doubles the yield obtained with having coke alone. It is evident, therefore, that the chlorination of aluminum is caused by both reducing agents. It should be noted that the yield with coke alone is of the same order of magnitude when only CO is used (given in Figure 6.1).

The above discussion leads to the conclusion that both carbon and carbon monoxide play important roles in obtaining the chlorination of aluminum. The yields are conclusively lower when either one of the two reducing agents was absent.

In order to determine the effect of carbon to ash ratio in the bed, an experiment was performed with a substantially larger fraction of coke in the bed. The initial coke-ash mixture contained 90% coke by weight. The comparison of the results from this run with the 75% coke experiment shows no significant variation in the two. The initial rate for the 90% coke case is marginally faster than that for 75% coke. But the yields at the termination of the run are more or less the same. This would suggest that increasing the carbon fraction beyond the required minimum does not affect the chlorination of aluminum.

An experiment with the gas mixture containing 2 parts of chlorine to 1 part of CO gave improved results. It would appear that this improvement is due to the increase in chlorine fraction. Further discussion of this aspect will be given in a later section. The improvement in aluminum yield is, however, due to an increase in the partial pressure of chlorine.

The comparison of results for the chlorination of iron gives somewhat similar conclusions. Shown in Figure 7.2, the addition of carbon to ash definitely improves the reaction yields for the iron fraction. And once again, the addition of CO improves the results compared to the one with only carbon. A similar comparison for silicon and titanium shows that the yields

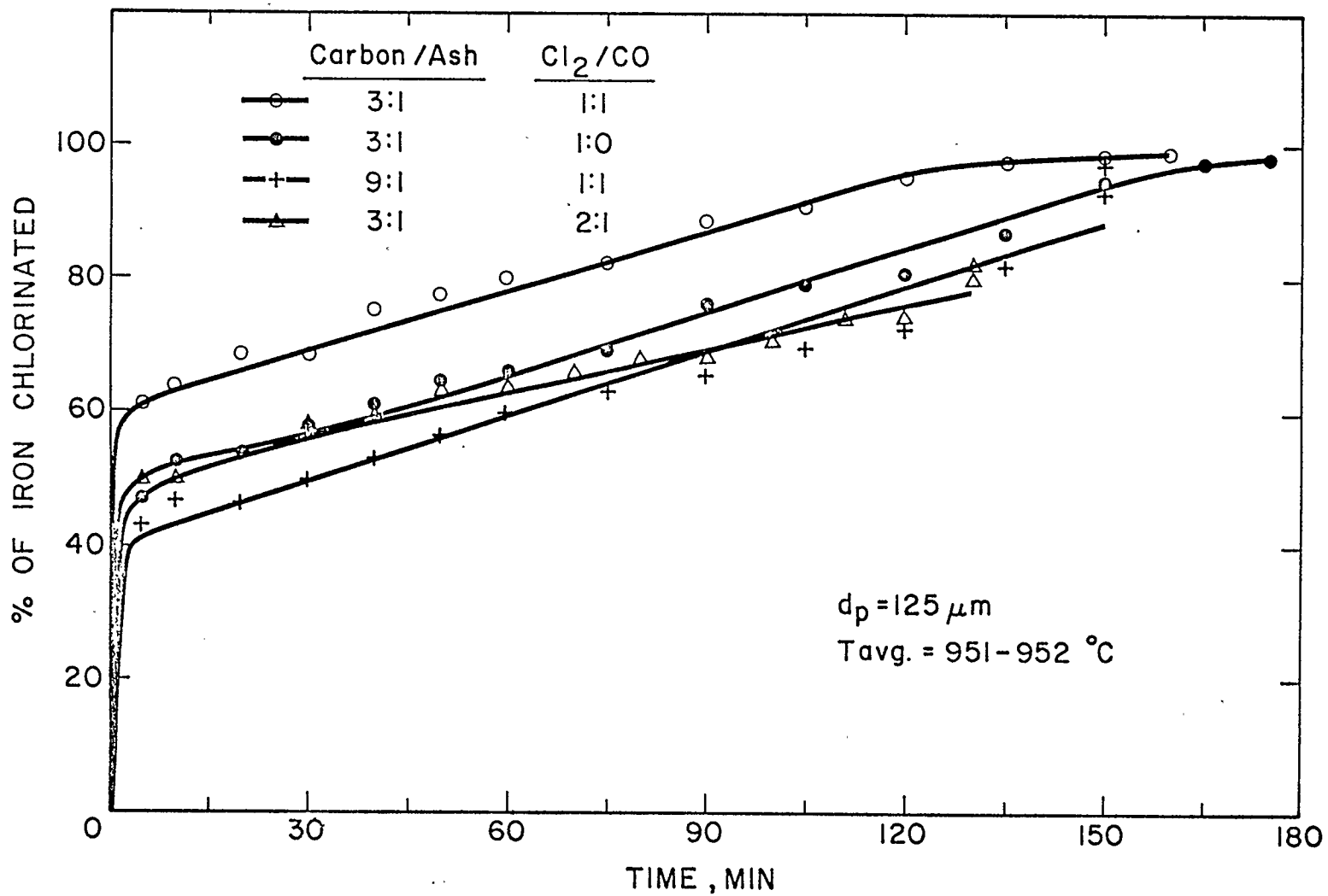


Figure 7.2 Effect of Reducing Agents Ratio on Chlorination of Iron.

are lower when carbon is the only reducing agent (Table 7.1). Increasing the carbon to ash ratio is not beneficial in improving the final conversion of these two metals.

7.3 Effect of Temperature

The lowest temperature employed to study the chlorination reactions with carbon was 808°C. At this temperature, the extent of aluminum chlorination with carbon and CO is greater than for the case where only CO is available. By comparing the results of run 12 (Table 6.1) and run 14 (Table 7.1), it can be deduced that the presence of carbon facilitates the chlorination of all 4 metal species. The final yields of the chlorides of aluminum, silicon and iron are approximately doubled when carbon was added.

The effect of temperature on the chlorination of aluminum is shown in Figure 7.3. The increase in reaction yield is significant when the temperature is raised from 808°C to 912°C. But a further increase in temperature by 39°C does not result in additional gains. Even the improvement in reaction rate is smaller than two-fold when the temperature is increased from 808°C to 912°C. Once again, the liquid formation was observed within this temperature range. Thus there is a possibility that the observed gain is due to a change in the characteristics of the ash bed and is not

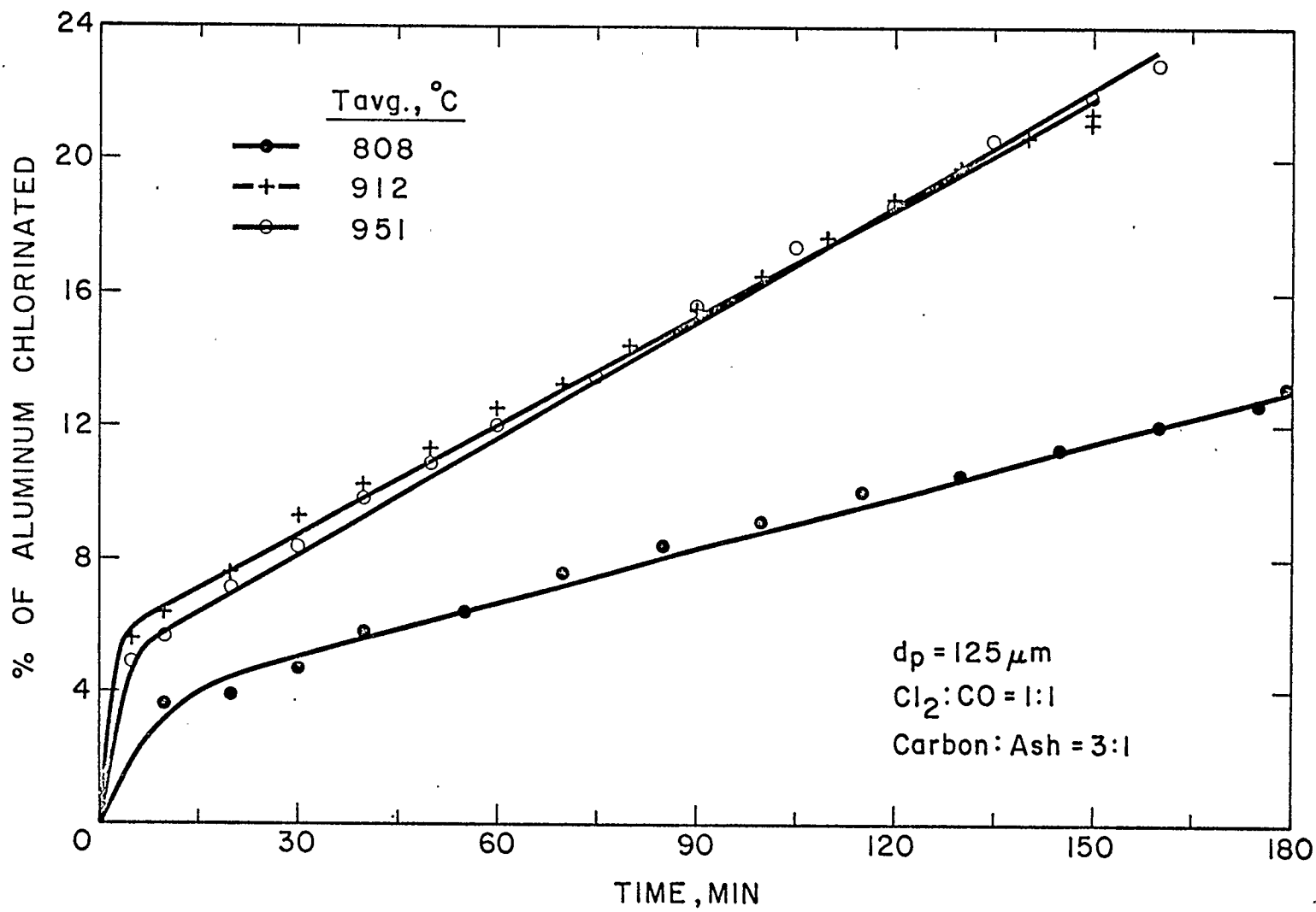


Figure 7.3 Effect of Temperature on Chlorination of Aluminum.

related directly with increase in temperature. If this is true, it would appear that the global reaction rate does not depend on the chemical kinetic step. This is substantiated by the results described in Chapter 6, where CO was the only reducing agent.

The effect of temperature on the chlorination of iron, silicon and titanium is shown in Figures 7.4 and 7.5. The chlorination of iron is clearly a function of the reaction temperature. At 951°C, nearly complete chlorination of iron is obtained in 2-hours. In general, the yields of iron with CO and carbon are considerably higher than the case where only CO is available. The conversions of silicon and titanium are also low at 808°C. But at temperatures above 900°C, there is a small increase in the yield. As in the case of aluminum, the temperature increase from 912°C to 951°C does not affect the chlorination of titanium significantly.

The increase in temperature from 808°C to above 900°C resulted in a general increase in the extent of chlorination for all 4 metals. However, increasing the temperature further to 951°C did not yield comparable results.

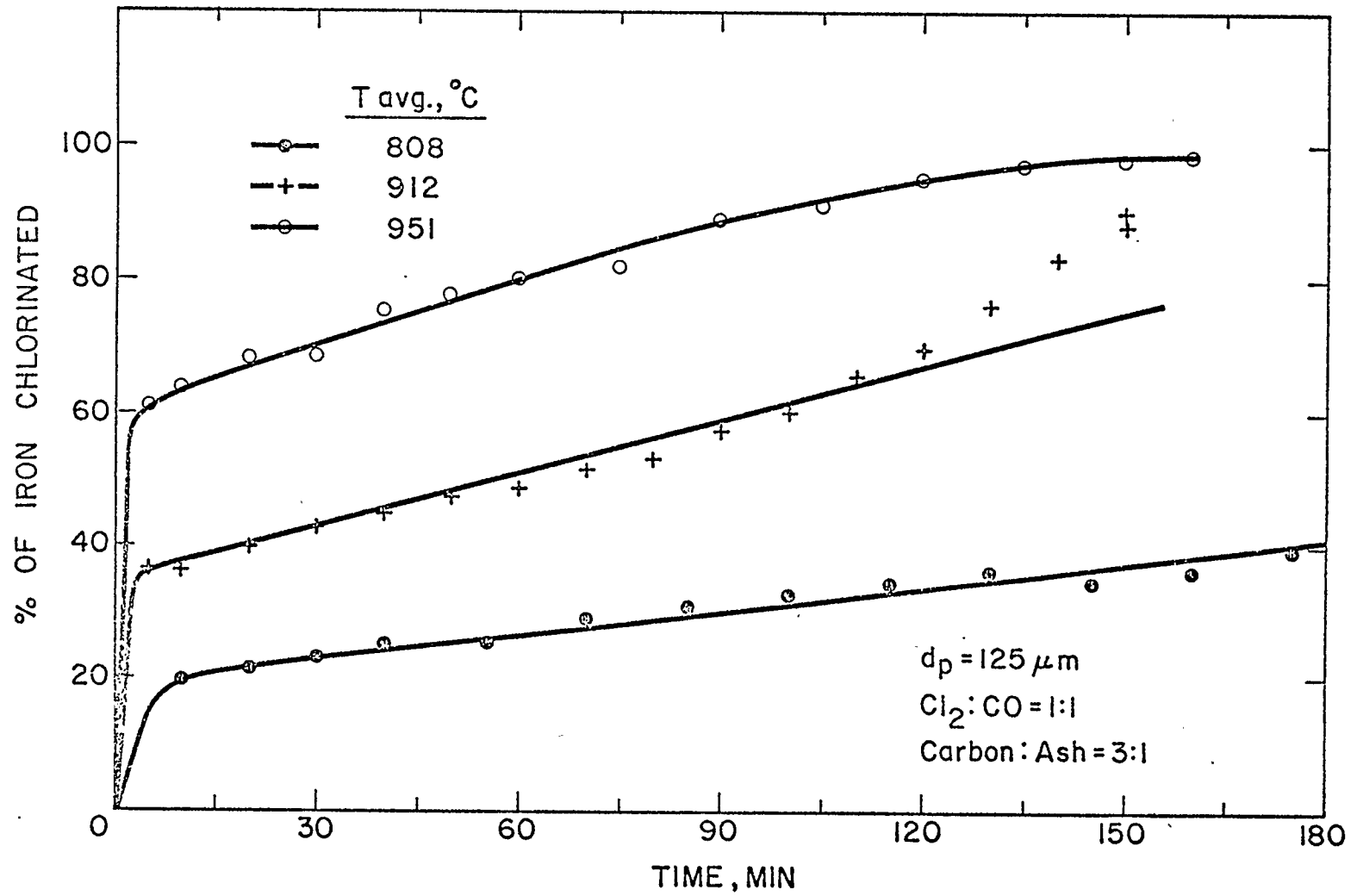


Figure 7.4 Effect of Temperature on Chlorination of Iron.

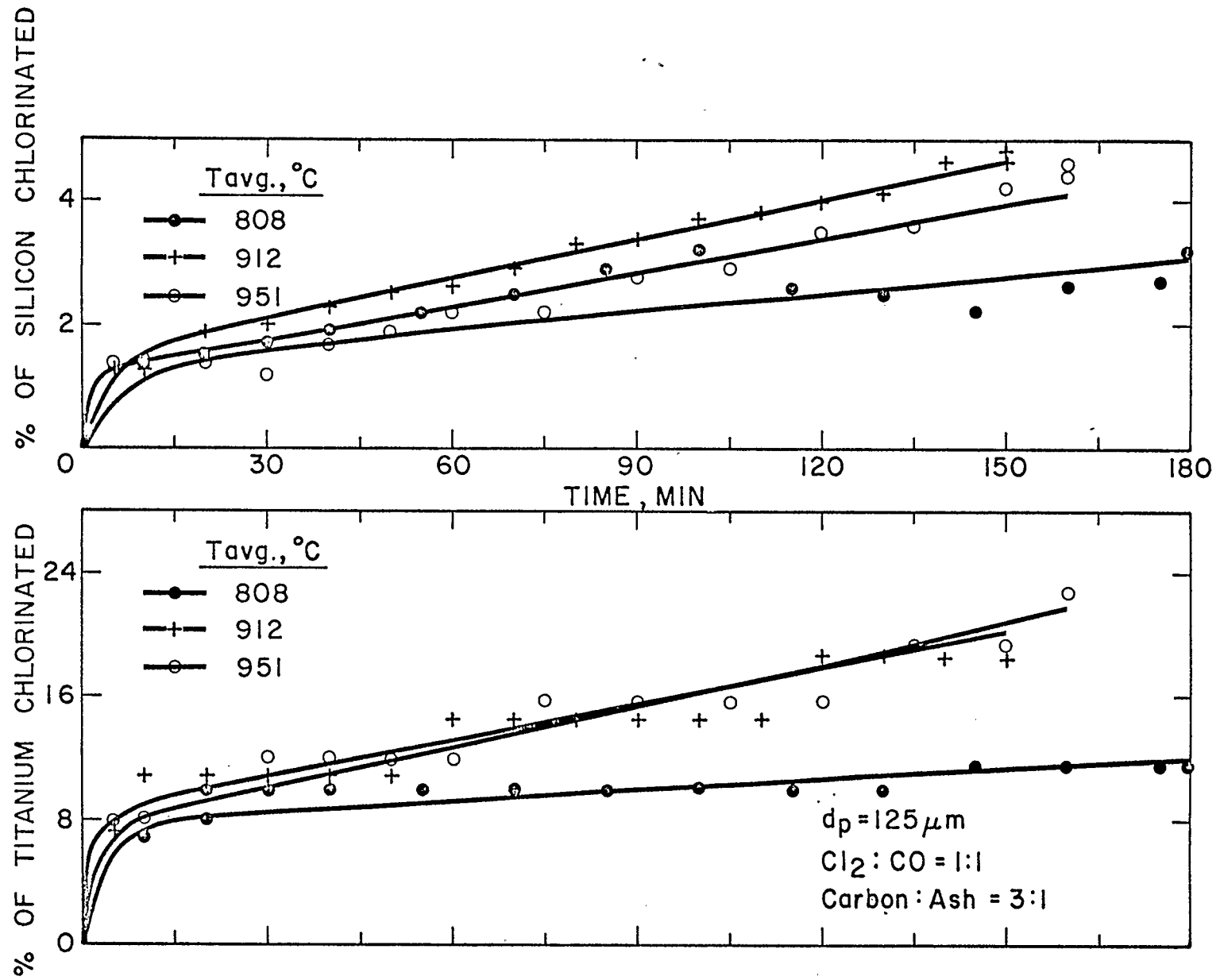


Figure 7.5 Effect of Temperature on Chlorination of Silicon & Titanium.

7.4 Effect of Particle Size

In the previous chapter, the ash particle size was shown to have significant effect on the chlorination of all four metals. A reduction in the particle diameter resulted in increasing the extent of metal fractions chlorinated with CO as the reducing agent. The effect of ash particle diameter on increasing the yield of aluminum as AlCl_3 is clearly seen in Figures 7.6 and 7.7. The comparison is shown for 4 sets of temperatures and gas ratios. In all the cases, it is observed that the yields are improved by reducing the particle size from 125 μm to 89 μm .

A comparison of the yield curves shown in Figures 7.6 and 7.7 gives an interesting observation. The slopes of lines in each pair are almost identical for all the cases. In spite of this, the smaller size particles give higher conversion than the larger particles. Therefore, the fraction of aluminum reacted initially is responsible for causing the yields to differ. In other words, the variation in particle size has an effect on the chlorination of aluminum during the initial period of the reaction. After this initial period the rate of reaction remains independent of the particle size.

The effect of particle size on the chlorination of iron, silicon and titanium is not reflected clearly in

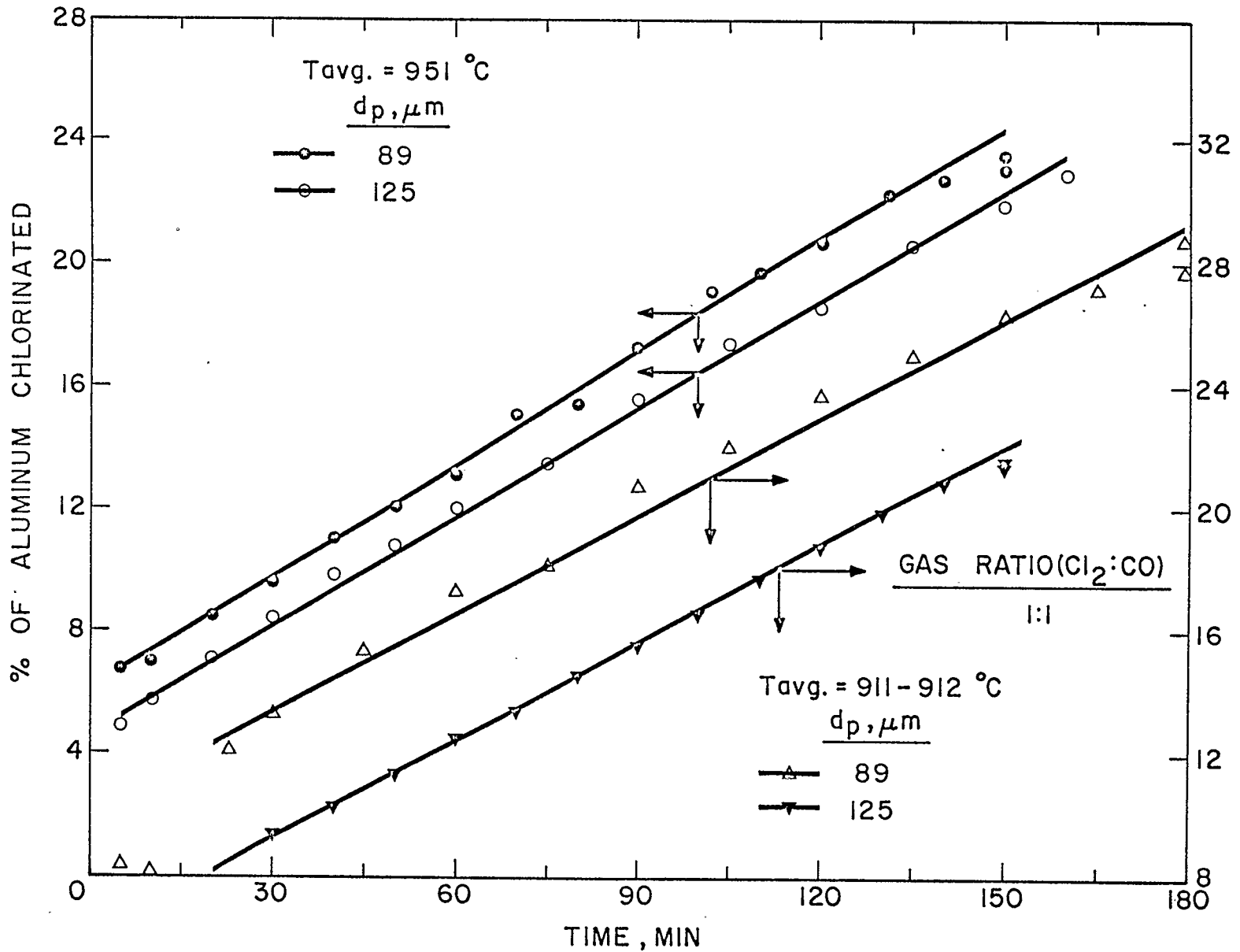


Figure 7.6 Effect of Particle Size on Aluminum Yield.
 (for Equimolar Gas Ratio of CO and Chlorine)

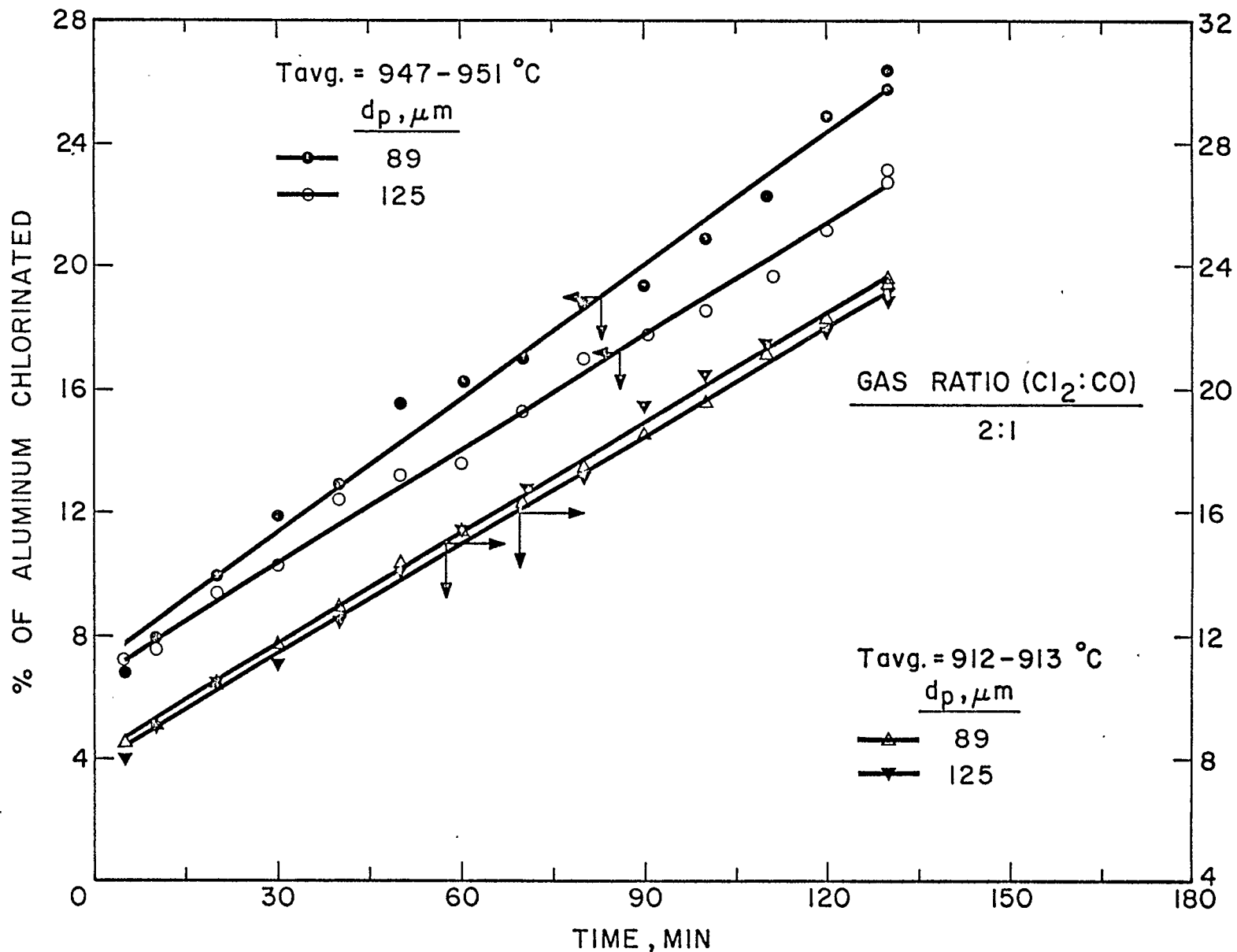


Figure 7.7 Effect of Particle Size on Aluminum Yield. (for Chlorine Rich Gas).

the results given in Table 7.1. For some of the runs, the yields are improved with the reduction in particle size, but it can not be generalized. In the case of iron, the chlorination is almost complete in a 2-hour reaction time when smaller particle size is employed. For the larger particles, however, complete chlorination is not achieved in all cases. The results for silicon also indicate that the extent of chlorination is generally higher with the smaller particles.

7.5 Effect of Gas Composition

Two different ratios of chlorine and carbon monoxide in the feed were selected for this study. The ratios are (1:1) and (2:1) of chlorine and CO respectively. The aggregate effect of varying the gas composition for aluminum is shown in Figure 7.8. While preparing the figure, the effects of other parameters, such as temperature and particle size, were not taken into consideration. It is interesting to note that higher yields of aluminum chloride are obtained when the fraction of chlorine is increased from 50% to 67%. A similar behaviour is demonstrated for the case of silicon in Figure 7.9. It is evident that a higher chlorine fraction resulted in enhanced yield of silicon chloride. The effect of gas composition for iron and titanium is not detected in the results.

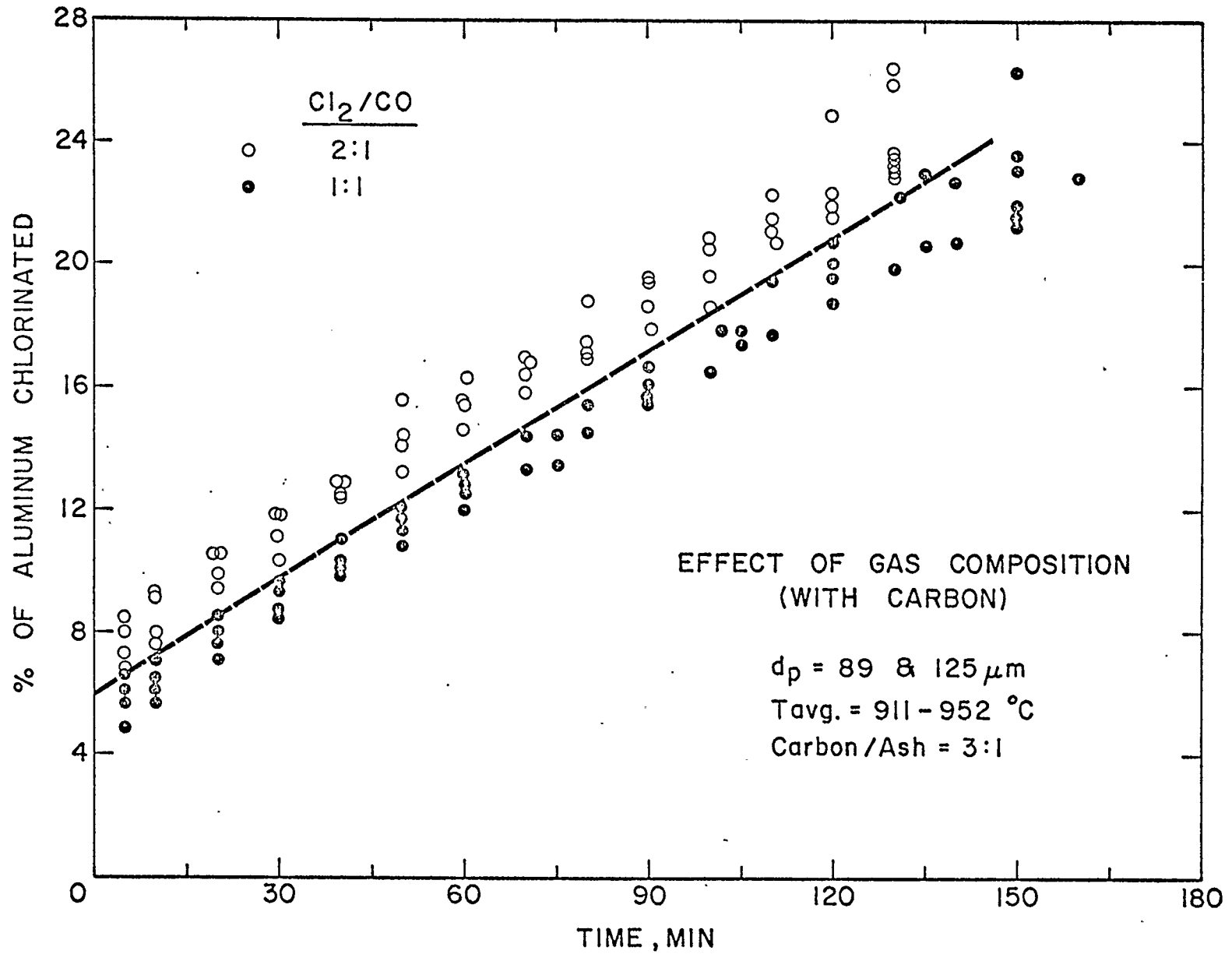


Figure 7.8 Aggregate Effect of Gas Composition on Aluminum Yield.

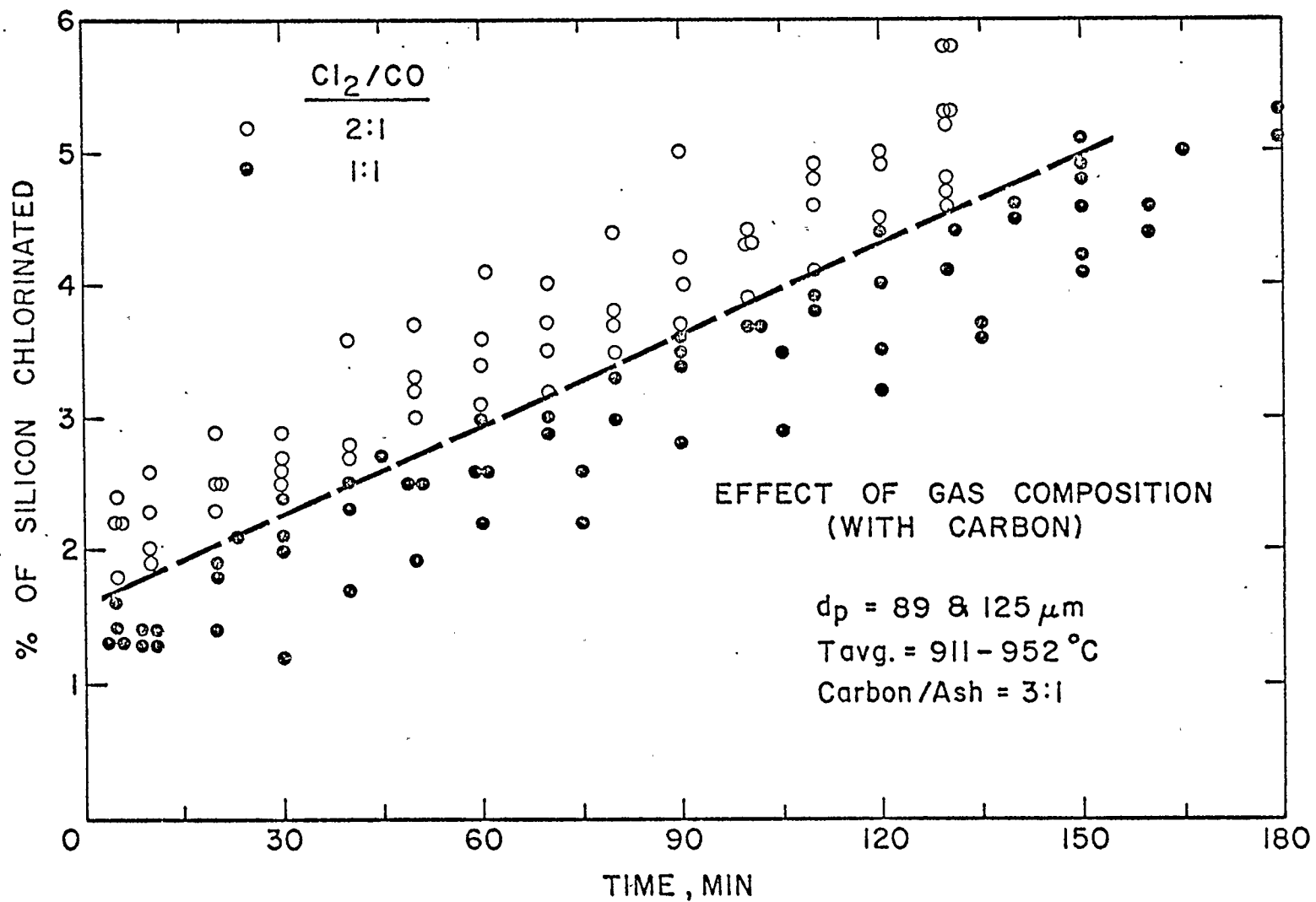


Figure 7.9 Aggregate Effect of Gas Composition on Silicon Yield.

The partial pressures of Cl_2 and CO are different in the selected gas ratios. Since the total pressure in both cases was near the atmospheric pressure, increasing the partial pressure of one would correspondingly reduce the partial pressure of the other. If the partial pressure of chlorine is increased from 50% to 67%, this would reduce the partial pressure of CO from 50% to 33%. In Figures 7.1 and 7.2, it was shown that the absence of CO in the feed gas caused a drastic reduction in the yields for aluminum and iron. Similarly, the chlorination of silicon and titanium was also affected severely (compare Runs 16 and 17 in Table 7.1). This indicates that the presence of CO in the gas mixture improves the extent of chlorination for all four metals. On the other hand, an increase in chlorine partial pressure alone resulted in an improvement of the yields.

The effect of gas ratio presented in Figures 7.8 and 7.9 is obtained with increasing chlorine and reducing carbon monoxide fractions. Since these two changes have opposite effects on the overall yield, it is the net effect that is seen in the figures. For the cases of aluminum and silicon, increasing the chlorine fraction offered advantage over an equimolar ratio.

7.6 DTA Thermograms of Spent Ash-Coke Mixtures

Two of the samples of spent ash-coke mixtures were examined by the DTA technique. The thermograms for samples of Runs 16 and 25 are given as Figure 7.10. These thermograms should be compared with Figure 5.3 for unreacted fly ash. The comparison reveals a third endothermic activity at slightly above 806°C . The presence of the chlorides of alkali metals may be responsible for this activity.

7.7 Sources of Error

The results of component balance calculations are summarized in Table 7.2. The error in material balance for the case of aluminum is consistent and mostly negative. Once again, the weight loss due to carry over of particles was not taken into consideration. Due to the increased conversion of all constituents, a larger reduction in the weight of ash would have occurred than for the case of CO (Chapter 6). However, these two errors have opposite effects on the balance calculations. The balance for the case of iron is much improved. Possible errors due to other sources will be similar in nature to the ones indicated in Chapter 6.

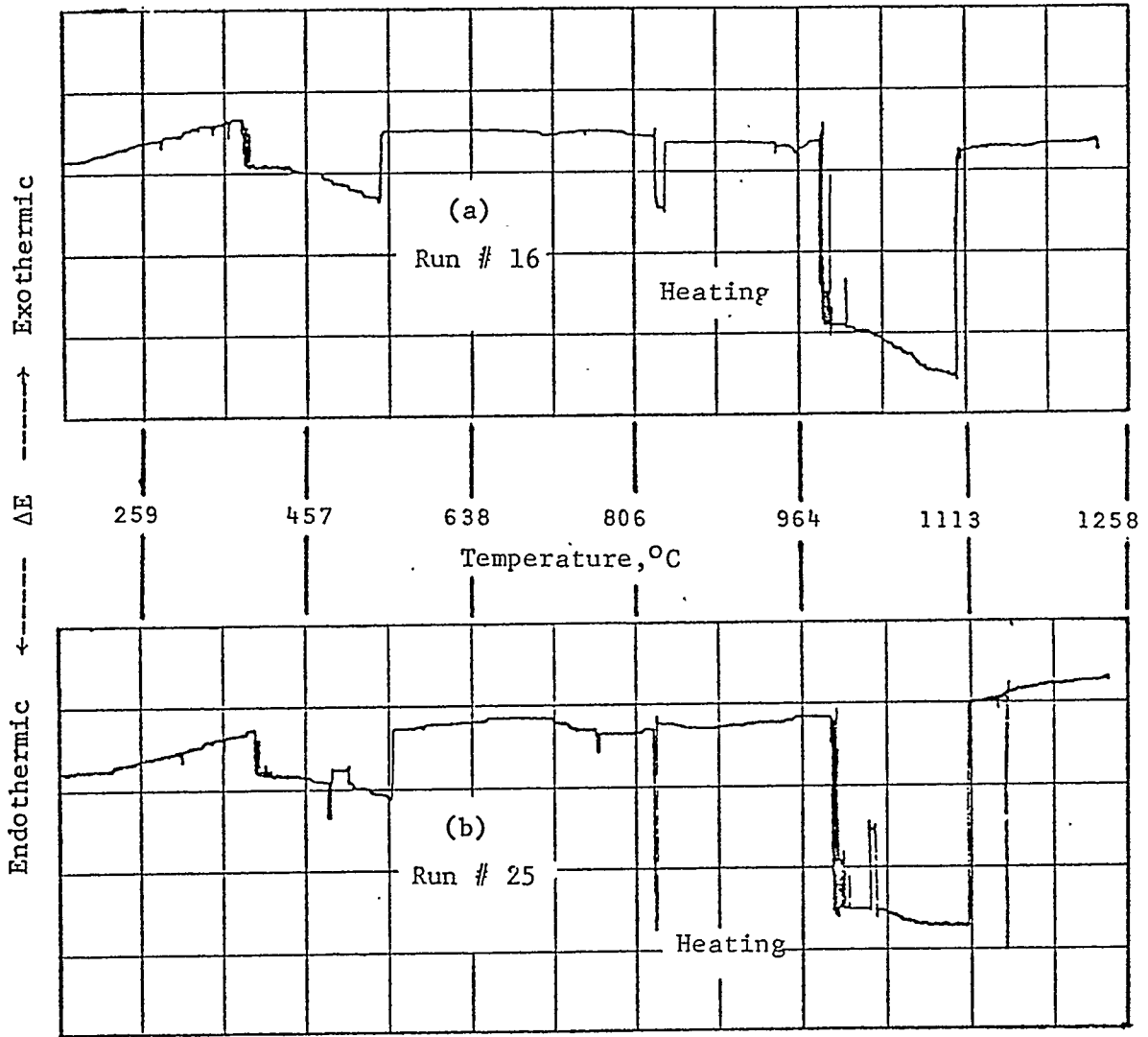


Figure 7.10 DTA Thermograms for Spent Ash-Coke Mixtures of Run Numbers 16 & 25.

Run No.	Ash Mass, gm	% Carbon		Reacted Mixture Analysis, %			Material Balance Error, %		
		Feed	Final	Al	Fe	Ti	Al	Fe	Ti
14	100	75.0	77.8	3.3	0.2	0.05	-6.2	- 7.7	30.0
15	75	80.0	82.4	2.0	0.0	0.05	-1.3	1.5	-20.0
16	100	75.0	76.6	2.8	0.0	0.10	1.9	0.0	-30.0
17	100	75.0	72.8	3.8	0.0	0.10	3.1	0.0	- 5.0
18	40	90.0	91.6	1.1	0.0	0.05	-3.8	0.0	-67.5
19	100	75.0	75.6	3.2	0.1	0.10	-3.1	-23.1	-20.0
20	100	75.0	78.0	3.2	0.2	0.05	-2.5	-21.0	- 3.3
21	100	75.0	79.4	2.4	0.1	0.05	2.5	-33.8	-10.0
22	100	75.0	79.2	2.6	0.0	0.05	-5.7	0.0	-10.0
23	100	75.0	76.7	3.2	0.1	0.05	-8.8	0.0	25.0
24	100	75.0	84.0	2.0	0.0	0.05	-2.5	0.0	-23.3
25	100	75.0	77.2	3.0	0.1	0.10	-5.6	-15.0	-20.0

Table 7.2 Estimates of Error by Material Balance Calculations.

CHAPTER 8

DISCUSSION OF RESULTS

The results of chlorination experiments with carbon and carbon monoxide, in general, indicate an overall improvement that is achieved with the addition of fluid coke to the reaction mixture. The extent of conversion in terms of aluminum recovered in 130 to 150 minute period is below 30% of the total available in all cases. The cause for the low yields will be discussed later in this chapter. It is essential, at this stage, to study the important reaction parameters in a systematic manner.

8.1 Factorial Design of Experiments

The factorial design of experiments technique was briefly described in Chapter 5 and the procedure is summarized in Appendix II. The technique was employed to study the effect of 3 reaction parameters on the chlorination of ash.

8.1.1 Selection of Process Variables

Varying the carbon to ash ratio from (3:1) to (9:1) showed no appreciable effect on the yield for aluminum (Figure 7.1). On the other hand, a ratio smaller than (3:1) was found unsatisfactory in main-

taining the bed fluidized. Thus the coke to ash ratio was disregarded as an important variable for this study. The reaction temperature and the ash particle size were two important and obvious process variables. The chlorination study with carbon monoxide indicated the significance of these two parameters in affecting the chlorination reactions. The variation in the feed gas composition, i.e. the CO/Cl_2 ratio, had an important bearing on the overall reaction rates. Therefore, the gas ratio provided the third important variable to be studied. Thus the three variables selected for the statistical analysis were the reaction temperature, ash particle size, and the feed gas ratio. An arrangement of these variables for the factorial design experiments is given as Table 8.1. Also indicated in the table are the levels selected for each of the three variables.

8.2 Analysis of Variance Tables

The experimental data of the yields for all four metals were plotted, and the fractions recovered at 3 different time periods were obtained. By studying the metal yields at different time periods, the time dependent effects are identified. The sum of squares calculations were performed according to the procedure outlined in Appendix II. The results of these calculations are given in Table 8.2. The entries in error column in the table are actually the 3-factor interac-

	GR ₁ (1:1)		GR ₂ (2:1)	
	d _{p1} (125 μm)	d _{p2} (89 μm)	d _{p1} (125 μm)	d _{p2} (89 μm)
T ₁ (911°C)	T ₁ ^{d_{p1}} GR ₁	T ₁ ^{d_{p2}} GR ₁	T ₁ ^{d_{p1}} GR ₂	T ₁ ^{d_{p2}} GR ₂
T ₂ (951°C)	T ₂ ^{d_{p1}} GR ₁	T ₂ ^{d_{p2}} GR ₁	T ₂ ^{d_{p1}} GR ₂	T ₂ ^{d_{p2}} GR ₂

Table 8.1 Arrangement for (2 X 2 X 2) Three Factor Complete Factorial Experiment.

		Main Effect			2-Factor Interaction			Error
		T	d _p	GR	Txd _p	TxGR	d _p xGR	Txd _p xGR
Degree of Freedom		1	1	1	1	1	1	1
Species	Time, min							
Al	10	2.53	3.25	3.25	0.10	0.15	2.10	0.14
	60	2.42	8.00	4.50	0.18	1.28	1.62	0.81
	120	0.04	11.52	10.13	0.00	1.62	0.84	1.44
Fe	10	28.16	37.88	46.12	295.21	3.35	19.20	86.65
	60	92.50	89.80	178.63	417.60	4.49	13.51	140.42
	120	81.31	3.05	59.98	404.64	20.77	141.91	48.01
Si	10	0.00	0.02	0.98	0.00	0.12	0.00	0.02
	60	0.02	0.05	1.45	0.04	0.12	0.00	0.02
	120	0.08	0.41	2.21	0.32	0.08	0.00	0.08

Table 8.2 Sums of Squares for Aluminum, Iron and Silicon.

tion sums of squares. Since the existence of a 3-factor interaction for most practical systems is rather rare (55), the estimated mean square value is interpreted as the variation due to experimental error. The calculations were repeated for the case of aluminum, iron and silicon.

The sums of squares given in Table 8.2 are tested for the significance. The results in terms of F-values are given in Tables 8.3 and 8.4. Table 8.3 is prepared directly from the values given in Table 8.2. Since each sum of square in Table 8.2 has only one degree of freedom, the significance test is for F_1^1 . Having one degree of freedom for the error term reduces the sensitivity of the test. It is seen in Table 8.2 that at least one of the three 2-factor sum of squares is small in comparison to the other two. If it is assumed that these 2-factor interaction terms are non-existent, their sums of squares can be pooled with the original error estimate (55). This procedure thus provides an additional degree of freedom to the error term. Consequently, the sensitivity of the significance test is greatly improved.

Following the above procedure, the error sums of squares were recalculated with one of the 2-factor interaction term pooled with it. The new values were then used to estimate new ratios of sums of squares,

Species	Time, min	Main Effect			2-Factor Interaction		
		T	d _p	GR	Txd _p	TxGR	d _p xGR
Al	10	18.02#	23.14#	23.14#	1.44	2.16	29.92#
	60	2.99	9.88	5.56	0.22	1.58	2.00
	120	0.03	7.99	7.02	0.00	1.12	0.58
Fe	10	0.33	0.45	0.54	3.49	0.04	0.23
	60	0.66	0.64	1.27	2.97	0.03	0.10
	120	1.69	0.06	1.25	8.43	0.43	2.96
Si	10	0.00	1.00	48.95*	0.25	6.24	0.25
	60	1.00	2.25	72.13*	2.24	6.24	0.01
	120	1.00	5.06	27.53#	3.99	1.00	0.06

* - significant for $\alpha=0.10$; # - significant for $\alpha=0.15$

Table 8.3 Significance Test with F-distribution Points.

Species	Time, min	Main Effect			2-Factor Interaction		
		T	d _p	GR	Txd _p	TxGR	d _p xGR
Al	10	20.94&	26.90&	26.88&	---	1.26	17.38*
	60	4.88	16.16*	9.08*	---	2.58	3.28
	120	0.06	15.94*	14.02*	---	2.24	1.16
Fe	10	0.64	0.86	1.04	6.70	---	0.44
	60	1.28	1.24	2.46	5.76	---	0.18
	120	2.36	0.08	1.74	11.76*	---	4.12
Si	10	0.00	1.60	78.38#	0.40	10.00*	---
	60	2.02	4.52	145.04#	4.50	13.54*	---
	120	1.88	9.52*	51.86#	7.52	1.88	---

* - significant for $\alpha=0.10$; & - for $\alpha=0.05$; # - for $\alpha=0.025$

Table 8.4 Significance Test with one 2-factor Effect Pooled with the Error Estimate.

and the significance tests were repeated. The new F-distribution estimates are given in Table 8.4. A comparison of Tables 8.3 and 8.4 will show the obvious benefit of the error pooling procedure. In Table 8.3, for instance, merely a few effects fell within the 90% confidence limit. By pooling of errors, the effects with even 97.5% confidence limits are identifiable.

The analysis of variance procedure only points out if the effect of a factor is significant in the two levels. It does not determine the direction of the effect. If a change is found to be significant from the statistical calculations, this could be either beneficial or detrimental to the yields. In order to identify the direction of a change, a simple procedure is suggested. It will be applied to study the direction of a change for the main effects only. The yield data for each factor are added to give two sums, one for each level. The ratio of two sums will simply determine whether the effect on the yield is positive or negative. In changing from level 1 to level 2, if the effect is positive then the ratio of sums will be less than 1.0. Conversely, for a negative effect the ratio will assume a value that is more than 1.0. The yield values with respect to time and the calculated ratios of the sums are given in Table 8.5. The effect of each of the three factors will be indivi-

Run No.	Code			Yields of Metals with Time, % of Total								
				Al			Fe			Si		
	T	D	GR	10 min.	60 min.	120 min.	10 min.	60 min.	120 min.	10 min.	60 min.	120 min.
19	1	1	1	6.6	12.4	18.7	37.0	49.0	70.7	1.5	2.7	4.1
23	1	1	2	9.0	14.9	21.9	45.8	52.5	60.5	2.0	3.2	4.8
15	1	2	1	9.5	16.5	22.9	57.1	71.2	82.2	1.6	2.3	3.1
24	1	2	2	9.1	15.4	22.4	41.3	45.8	75.0	2.0	3.0	4.1
16	2	1	1	5.8	11.7	18.8	63.4	80.6	95.0	1.3	2.3	3.5
25	2	1	2	8.0	14.0	21.4	51.2	63.4	77.4	2.1	3.5	5.0
21	2	2	1	7.5	13.4	20.7	40.8	50.2	64.2	1.3	2.4	3.7
22	2	2	2	8.4	15.7	24.4	40.8	51.5	77.3	2.4	3.4	4.7
$(\sum T_1 / \sum T_2)$				1.15	1.08	1.01	0.92	0.89	0.92	1.00	0.97	0.95
$(\sum D_1 / \sum D_2)$				0.85	0.87	0.89	1.10	1.12	1.02	0.95	1.05	1.12
$(\sum G_1 / \sum G_2)$				0.85	0.90	0.90	1.11	1.18	1.08	0.67	0.74	0.77

Table 8.5 Direction of Main Effect for Each Factor.

dually discussed in the following sub-sections.

8.3 Analysis of Temperature Variation

The effect of varying the reaction temperature from 911°C to 951°C is not significant on the yields (or, the reaction rate) for any of the three metals. The chlorination of aluminum during the first 10 minute is affected by temperature to some extent. Table 8.5 indicates that the increase in temperature actually reduces the yield in this initial period. However, the yields at the end of 2-hour period are essentially the same for both temperatures. Since the initial drop in the aluminum yield is shown to be within 95% confidence limit, the effect is conclusive. From the results of thermodynamic calculations of Chapter 3 (Figure 3.7), the stability of aluminum oxide is enhanced only when the temperature is above 1300 K. Hence the temperature 951°C is still below the region where the reverse reaction becomes significant. Moreover, the yields at both temperatures eventually become identical at the end of 2-hour period. This means that the reaction at 951°C is slow only initially, but is more rapid during the later stage. Hence a likelihood of significant reverse chlorination reaction can be safely discounted.

The effect of temperature on chlorination of iron and silicon is inconclusive from the data. Referring to Table 8.5, it is seen that increasing the

temperature may have beneficial effect on the chlorination rates for these two metals. But the effect is insignificant from a statistical view point. The above discussion suggests that the chemical kinetics is not the controlling step in the temperature range 911-951°C. Nevertheless, it was shown in Chapter 7 that increasing the temperature from 810°C to above 900°C resulted in an approximately 2-fold improvement in the aluminum yield (Figure 7.3).

8.4 Analysis of Particle Diameter

The effect of particle diameter on the chlorination of aluminum is statistically significant. The F-ratios in Table 8.4 show that the effect is within 90% confidence limit. The effect is even more definite for the initial reaction period where the F-value is 95%. It is indicated in Table 8.5 (and also Figures 7.6 and 7.7) that reducing particle size improves the chlorination of aluminum. At first this observation appears to be very reasonable, because reducing the particle diameter generally results in increased surface area. However, the surface area measurements given in Table 5.4 show that there is actually a reduction in surface area for ash samples when the particle diameter is smaller. The surface area of 125 μm diameter ash particles is 4 times the area for 89 μm size. For the reaction to be dependent on the surface area,

the observed yields should have been lower for smaller particle size. Yet the yield increased for the smaller diameter particles. And the available surface area has an opposite effect. Therefore, the surface reaction step does not control the overall chlorination reaction in the case of aluminum.

The inverse relationship between particle diameter and reaction rate suggests that the overall reaction process could be pore diffusion controlled (60). In spite of the reduced surface area of the smaller ash particles, the overall rate of reaction is about 15% higher in the first 10 minutes of the reaction. The magnitude of surface area indicates that fly ash particles cannot be labeled as truly porous. However, the dependence of aluminum chlorination on particle diameter, and not the actual surface, dictates that the reaction is influenced by pore diffusion resistance. A previous study on the chlorination of alumina with Cl_2/CO also revealed the dominance of the pore diffusion step (26).

The effect of particle diameter on the chlorination of iron fraction in ash is shown in Table 8.4 to be statistically insignificant. The main effect ratios in Table 8.5 show that the reaction rate may be slightly higher for larger ash particles. The larger ash particles also possess greater surface area. The

effect of particle diameter is minimal for the case of silicon as well. The effect for silicon chloride after 2-hour reaction period is within 90% confidence limit. This effect, as seen in Table 8.5, is similar to that for iron, i.e. higher yields are obtained with larger diameter ash particles. Thus in both these cases the reaction is apparently favoured by increased particle surface area.

It is concluded, therefore, that the particle diameter and surface area have an inverse relationship with the yield of aluminum. The effect of particle size (or the surface area) is much smaller in magnitude for the cases of iron and silicon. Overall yields of these two metals are somewhat improved when the particle size is bigger (with larger reaction surface).

8.5 Analysis of Cl_2/CO Gas Ratio

The effect of increasing chlorine partial pressure in the reacting gas mixture is significant for aluminum and silicon (Table 8.4). In changing from level 1 to level 2, the chlorine fraction in gas is increased from 50 to 67% whereas the CO fraction is reduced from 50 to 33%. The direction of change is shown to be positive for both cases (Table 8.5). The confidence limit for the case of aluminum is at least 90% and is even higher for silicon. Once again, the effect is more certain during the initial 10 minutes of the

reactions.

The effect of increasing the chlorine fraction should be viewed as a combination of two separate changes. Increasing the partial pressure of chlorine results in a simultaneous reduction for CO due to the constant total pressure. In the previous chapter, the contribution of CO in facilitating the chlorination of metals was demonstrated. The yield of aluminum chloride was found to be about halved when CO was replaced with nitrogen in one of the experiments (Figure 7.1). It would be anticipated, therefore, that lowering the partial pressure of CO from 50% to 33% may be detrimental to the reaction. On the other hand, increasing the partial pressure of chlorine may facilitate the reaction. The two changes would have opposite effects on the overall process. It is the resultant of the two effects that is identified in this study. The effect of gas ratio is not significant for the case of iron.

8.6 Two-Factor Interactions

The significance test values of Table 8.4 indicate that 2-factor interactions are generally not important. The effects that are found to be significant fall only within a confidence limit of 90%. Since no definite trends are observed, it will be assumed that the effects are actually due to random fluctuations.

Except for the case of iron, all other 2-factor interactions correlate with the main effects. For example, the only 2-factor interaction for aluminum can be related to the main effects of particle diameter and gas ratio. In case of iron, none of the main effects are shown to be significant. The error term for iron is rather high (Table 8.2), possibly due to random fluctuations. The concentration of iron in the ash is much smaller than of aluminum or silicon. Any error in the measurements would be greatly magnified while the percent recoveries are calculated.

It is, therefore, concluded that 2-factor interaction terms are practically insignificant. The presence of any seemingly significant effect is attributed to random fluctuation in the experiments.

8.7 Time Dependence of Reaction Rate

Previous discussion of the ash chlorination experiments indicates that the reaction rates vary significantly with time. The reaction yields for all 4 metals are reasonably high during the initial 10-15 minutes. The reactions after this initial period of time are retarded drastically. The thermodynamic calculations of Chapter 3 predict that chlorination of all important metals should proceed to completion. Hence, the yields should not be constrained by the consideration of reaction equilibrium.

In order to appreciate the extent to which the reaction rates are affected, the yield data described previously are presented in differential form. This procedure gives the global rates of reaction for the entire run. Comparison of the reaction rate data averaged over 5 minute time intervals is shown in Figures 8.1 and 8.2.

8.8 Significance of Chemical Kinetics Step

In Figure 8.1, the global reaction rates are given for 3 different temperatures. When the temperature is increased from 808°C to above 900°C an improvement in the reaction rate is observed. The difference between 912 and 951°C is not so significant. However, the difference in the initial and final rates is of an order of magnitude in all cases. At temperatures above 900°C, the reaction rate after about 30 minutes shows almost no decline in its magnitude.

Similar characteristics are again apparent when the reaction rates are compared for two particle sizes (Figure 8.2). A careful examination of the yield data for all other experiments confirms that the decline in reaction rate is present in all cases. The global reaction rates for the initial 10 minutes are compared with the rates during the later period. The numerical values are presented in Table 8.6. The reaction rates initially are about 5 to 8 times faster than for the

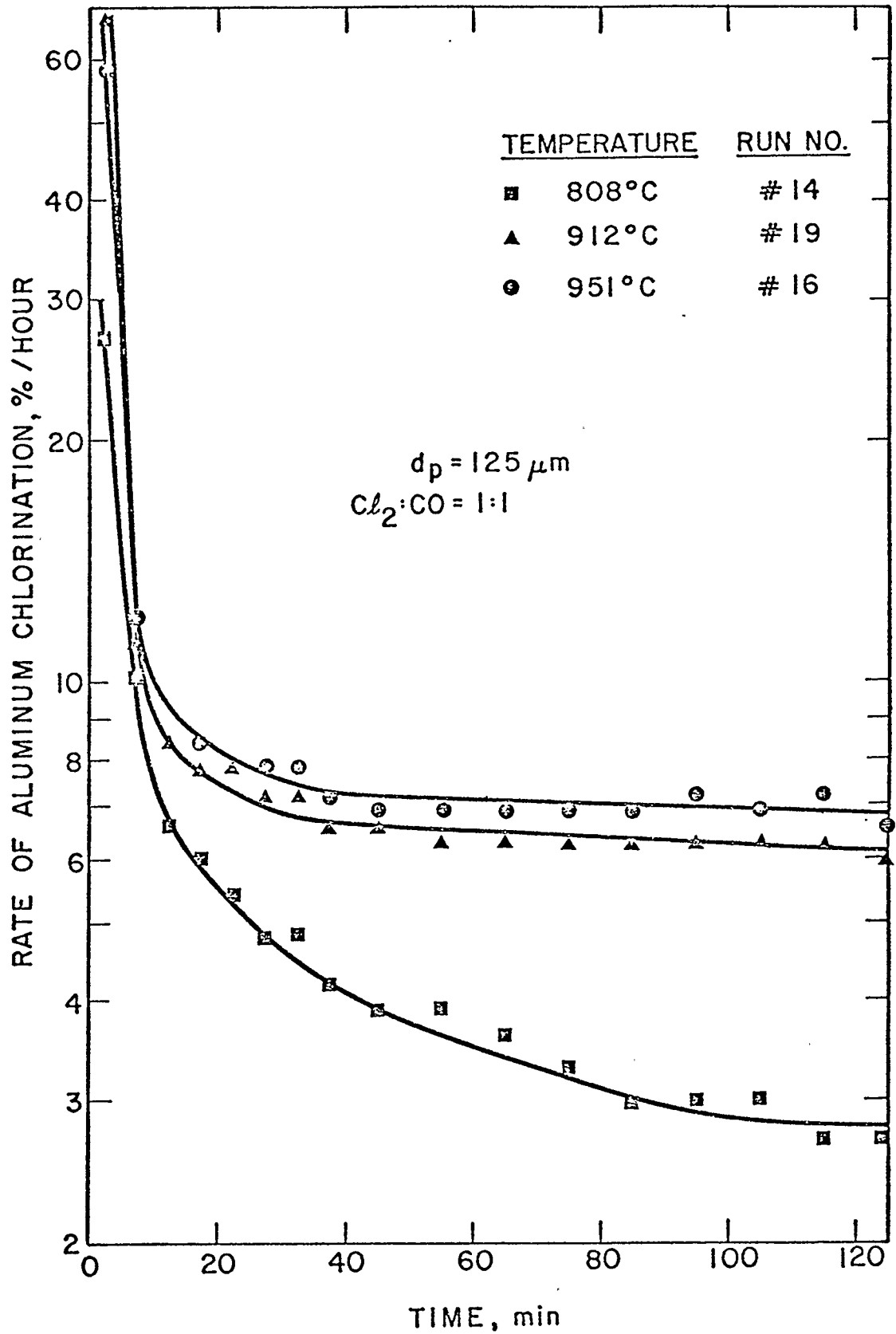


Figure 8.1 Time Dependence of Reaction Rate for Aluminum Chlorination.

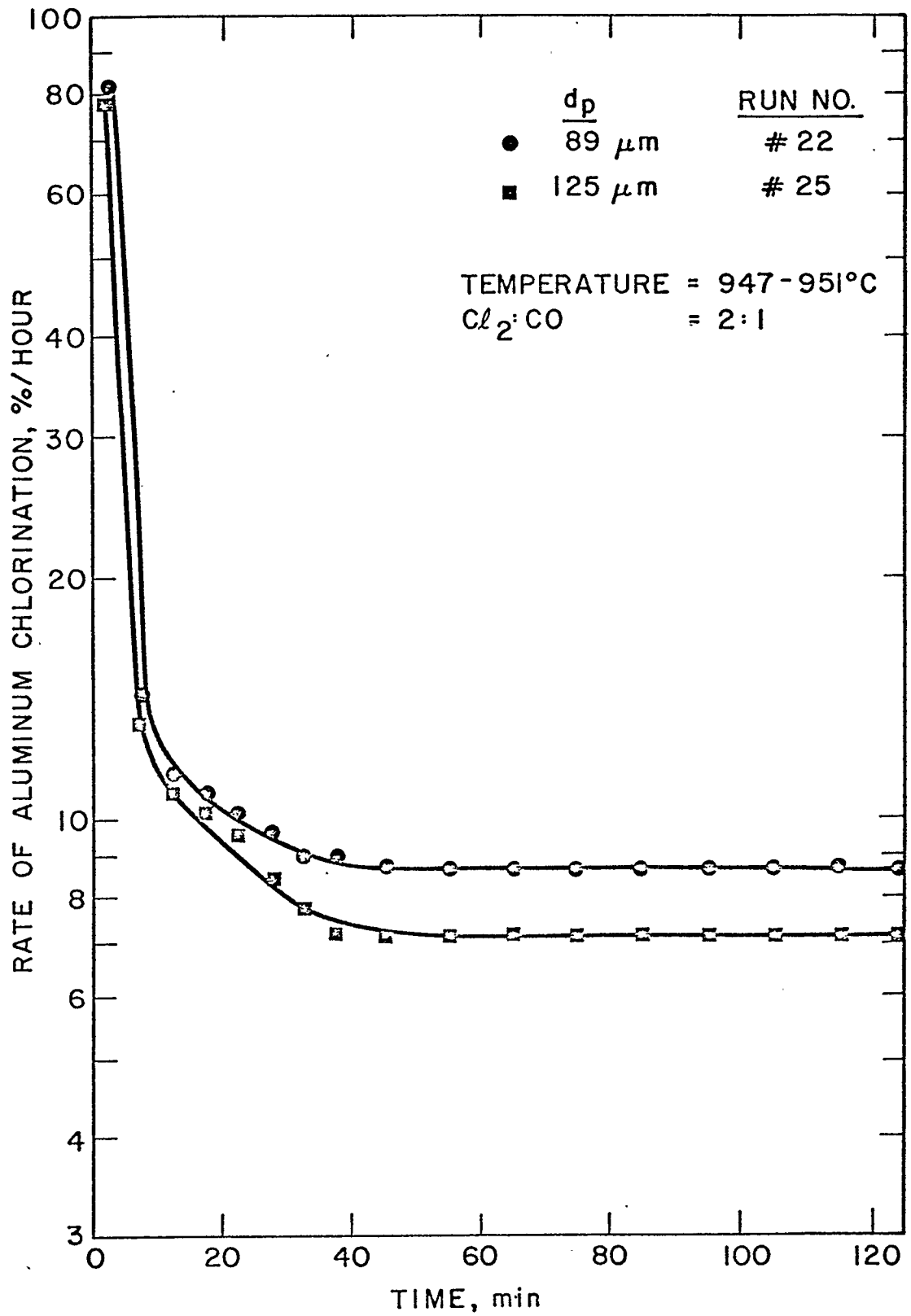


Figure 8.2 Variation in the Rate of Chlorination for two Particle Sizes.

Run No.	Global Reaction Rate, g/kg/min		Ratio of the Global Reaction Rates
	Initial 10 minutes	Straight line portion	
15	8.1	1.2	6.8
16	5.7	1.1	5.2
19	6.5	1.1	5.9
21	7.3	1.2	6.1
22	8.5	1.5	5.7
23	9.1	1.2	7.6
24	9.3	1.2	7.8
25	7.6	1.3	5.8

Table 8.6 Global Reaction Rate for Aluminum.
(Initial and Straight Line Sections)

later period. A graphical comparison in Figure 8.3 reveals a similar behaviour for the cases of iron, silicon and titanium.

A behaviour of this kind is not explained by assuming any apparent order of reaction kinetics. The initial portion of the curves may satisfy an extremely high order of reaction model, but a constant rate of reaction for the later stage will suggest a zero order reaction. Thus an explanation in terms of reaction kinetics is not satisfactory and was discarded.

8.9 Reaction of Compounds with Varying Structures

Another attempt to explain the strong dependence of reaction rate with time stems from the fact that coal ash is a heterogeneous mixture of numerous chemical compounds. The existence of several chemical structures in coal ash is demonstrated in the studies done by several researchers (12,13,14). The topic has been discussed previously in Chapter 2. Aluminum in coal ash, for instance, is shown to exist as alumina, aluminates, alumino-silicates, etc. It may be postulated, therefore, that each of these forms may be reacting independently at varying rates. The global rate of reaction, as found experimentally, would be a composite of the individual rates. The fast reacting constituents would be chlorinated initially leaving other species to react at a slower pace. Thus the

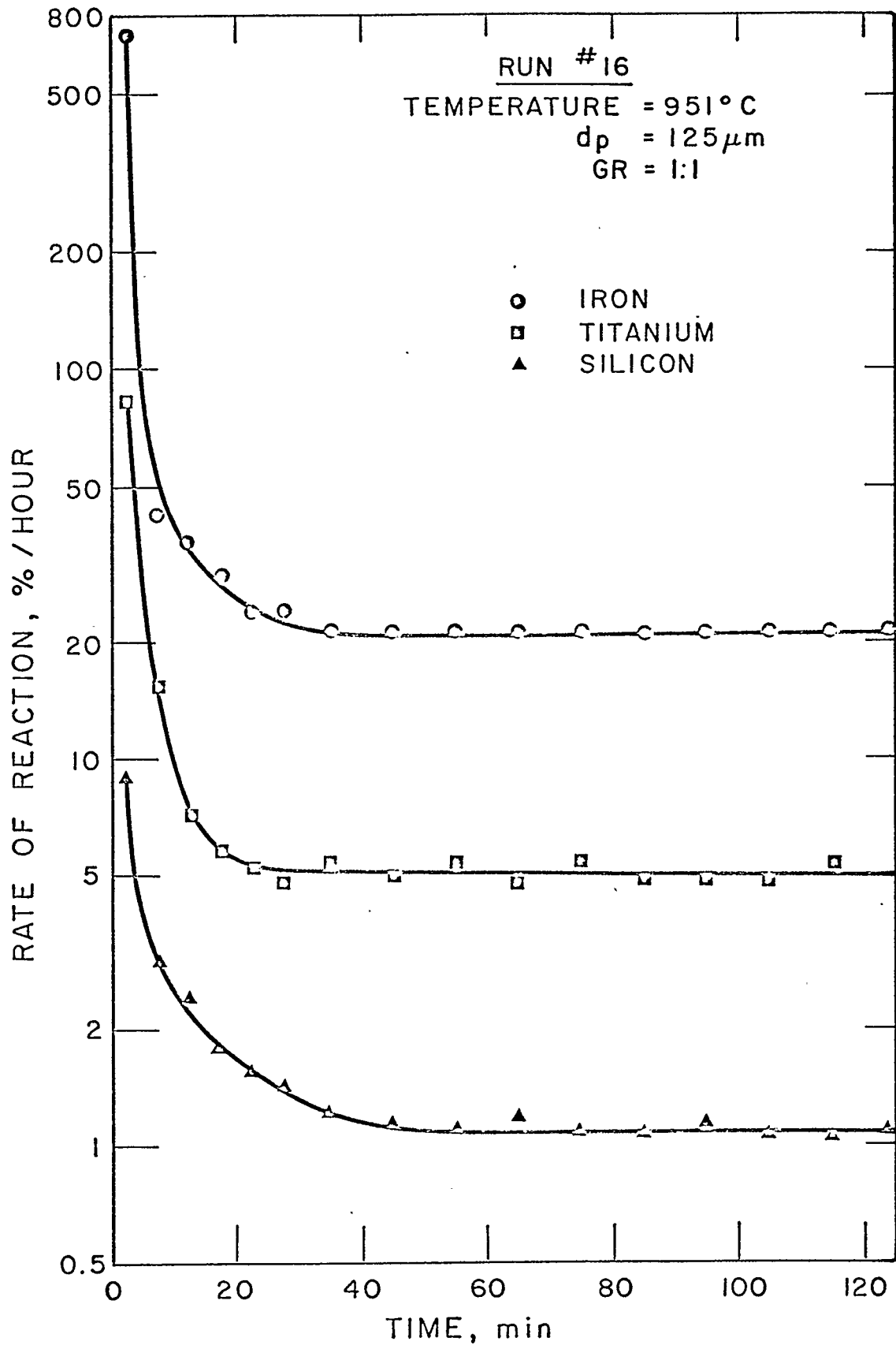


Figure 8.3 Time Dependence of Reaction Rate for Iron, Silicon and Titanium.

observed initial high rate of reaction could be due to the faster reacting compounds.

The yield curves for other metal constituents are given in Figures 7.2, 7.4, 7.5 and 7.9. It should be noted that the decline in global reaction rates occurs at about the same time and simultaneously for all metal constituents (Figures 8.1, 8.2 and 8.3). It could be argued that silicon, titanium and iron constituents in ash might also be present in several chemical forms. And that the rates drop due to the exhaustion of the faster reacting constituents. But there is a noticeable similarity in the yield curves for all the four metals studied. The decline in the reaction rate and the beginning of straight line portion of the curve occur at almost the same instant. Following the decline, chlorination of all metals proceeds with constant rates. Moreover, the reactions are retarded for all metals at the same instant irrespective of the variation in reaction temperature, particle size, or gas ratio. Thus the noted similarities in the yield curves are due to some other phenomenon. The rate of chlorination might be influenced by a variation in the chemical structure. But an identical and simultaneous decline for all four metals may not be explained in terms of such a variation.

8.10 Simultaneous Chlorination of Other Metals

A constant rate of reaction, shown in Figures 8.1 and 8.2, following the initial decline in the rate suggests that the reaction is mass transfer controlled. Thus far in the discussion, the chlorination of only four metals in ash has been considered. The analyses of ash, given in Tables 2.1 and 5.2, indicate that there are small but significant concentrations of calcium, sodium, potassium and magnesium also present. These metals belong to the first and second group in the periodic table of elements.

Thermodynamic calculations of Chapter 3 showed that chlorination of these metals takes place preferentially over silicon, aluminum and titanium. In other words, during the initial period of the reaction, the first and second group metals will be chlorinated rapidly.

8.10.1 Existence of Molten Chlorides in Bed

The melting and boiling point data of Table 5.3 reveals that the chlorides of these metals are liquid above 800°C . The boiling points fall in the range 1412°C for MgCl_2 to $>1600^{\circ}\text{C}$ for CaCl_2 . Thus the temperature range $808-950^{\circ}\text{C}$ is high enough to cause the melting of these chlorides, but not enough to allow them to vapourize. Once the formation of these chlorides is complete, these will remain as part of the

ash-coke mixture in the reactor.

The chlorides of all eight metals are soluble in water. A comparison of the water soluble fractions of all eight metals in unreacted and partially reacted ash samples was given in Tables 5.5 and 5.6. From the data it is evident that the soluble fraction of the first and second group metals increases after chlorination. In Table 5.6, the soluble forms after chlorination were shown to be mostly chlorides.

8.10.2 Reduction in Particle Surface Area

Specific surface area values of Table 5.4 revealed that there is a significant reduction in the surface area of ash after chlorination. The molten chlorides formed by chlorination of the first and second group of metals would be deposited on ash and coke particles. The presence of the liquid would partially flood the available ash surface. When the ash-coke mixture was cooled at the termination of experiment, the molten salts would have solidified. With the solidified salts covering the rough ash and coke surfaces, the specific surface area of the mixture would be reduced. A loss of the particle surface area during chlorination was confirmed by the surface area measurements (Table 5.4).

8.10.3 Gaseous Diffusion through Molten Salts

The presence of molten salts in the reaction mixture introduces an additional resistance to the overall reaction. As discussed previously, the molten salts would coat the particle surface providing a thin liquid film. The reacting gases, chlorine and carbon monoxide, will be required to diffuse through the film to reach the reaction surface. In addition, the reaction products will have to diffuse to the outer surface of the liquid film. It can be appreciated, therefore, that the reaction mechanism will involve these two additional mass transfer resistances.

8.10.4 Rate of Diffusion Estimation

An attempt is made to estimate the magnitude of gaseous diffusion through a film of molten salts. The data on physical properties, such as density and viscosity, of pure salts is available in the literature (63). However, the properties for a mixture of CaCl_2 , NaCl , KCl and MgCl_2 are not available. The solubility of chlorine in molten chlorides seems to involve an interaction between the gas and the melt (61). The gas liquid diffusivity data for Cl_2 is almost completely lacking for the chlorides of interest. Thus an effort to estimate the rate of gaseous diffusion is restricted due to a lack of the data.

The calculation procedure for a simplified case of NaCl-Cl₂ system is given in Appendix IV. The diffusivity of chlorine in NaCl at 950°C is calculated by Wilke-Chang correlation (62). Viscosity and density of molten NaCl are estimated using the polynomials given by Janz et al (63). The solubility of chlorine in NaCl is estimated by employing Henry's constant (64). The calculated solubility is of the order of 0.9×10^{-4} mol Cl₂/cm³, which is quite small. The rate of diffusion is finally estimated by using a model described in Figure 8.4. The model assumes a spherical particle coated uniformly with a thin film of liquid and is submerged in the diffusing gas. The calculations are done for the case where sphere diameter is 125 μm and the gas is 50% chlorine. The calculations are repeated for 3 different film thicknesses, 0.1 μm, 1 μm and 5 μm. The corresponding rates of diffusion are 2.1×10^{-9} , 2.1×10^{-10} and 4.5×10^{-12} mol/h, respectively.

8.10.5 Experimental Chlorine Consumption Rate

The actual rate of chlorine consumption by Al, Fe, Si and Ti fractions are estimated for Run#16. From the calculations of Table IV.1, the rate of chlorine consumption is 0.0954 mol/h for 100 gram of ash. While this rate is for the actual particle surface area, the flux calculations are for one spherical particle. The

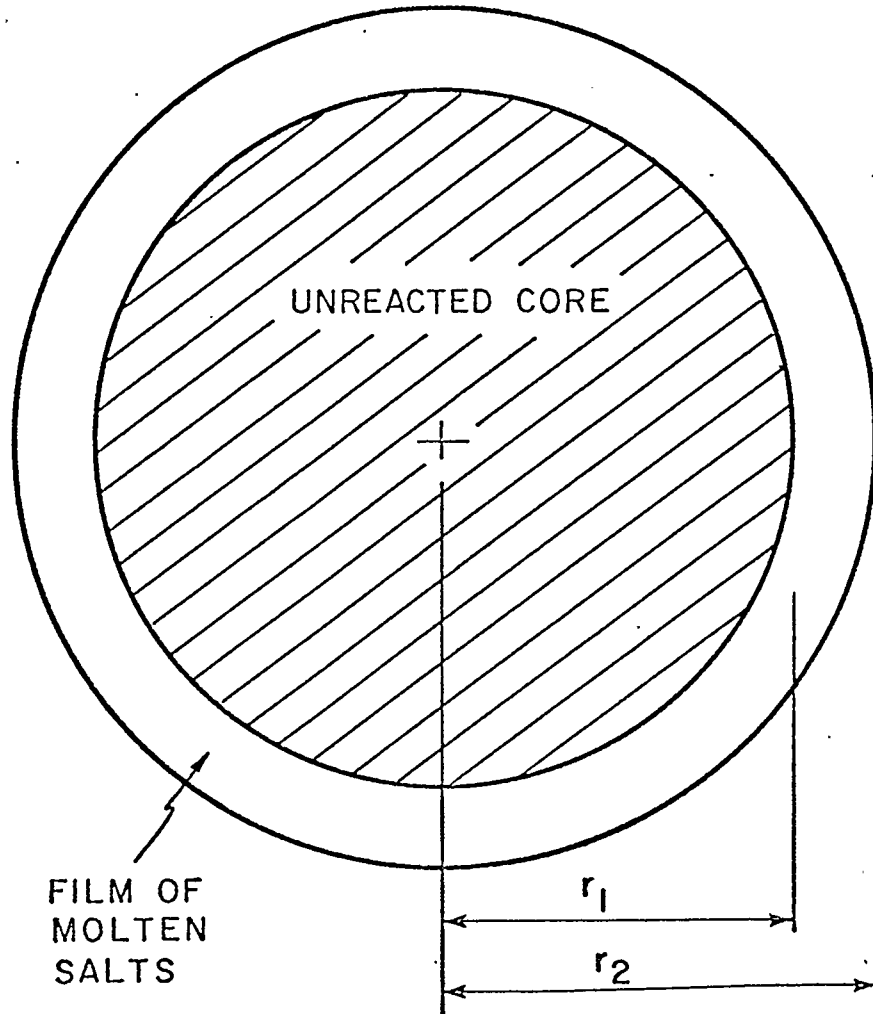


Figure 8.4 Diffusion through Molten Salt Film.

surface area measurements given in Table 5.4 indicate that actual surface area for 125 μm particle is 170 times the area of a sphere of the same diameter. If it is assumed that the flux is proportional to available surface, the corrected flux will be approximately 170 times the value calculated before.

8.10.6 Validity of the Model

A comparison of the two rates after the corrections indicates that in order for the two rates to match, the film thickness should be of the order of 1 to 5 μm . The mass of NaCl melt corresponding to this range of film thickness is estimated to be between 5.6 and 28.0 g for 100 g of ash. The predicted mass of NaCl film should be compared to the total corresponding to complete chlorination of the fractions originally present in ash. Based on the analyses of ash given in Tables 2.1 and 5.2, the mass of liquid chlorides is somewhere between 6 and 12 g for each 100 g ash. There is an excellent agreement between the two estimates. In spite of the several assumptions and simplifications made in the model, the agreement in the results is very remarkable. The gas-liquid diffusivity was calculated by using a simple generalized correlation. The properties of molten NaCl were assumed to represent those of the mixture. In addition, the counter diffusion of vapour metal chlorides was neglected. It was assumed

that the diffusion of chlorides such as AlCl_3 is relatively faster than that for chlorine, and does not control the overall rate of reaction.

It is, therefore, postulated that the observed decline in the rate of chlorination reactions is due to the creation of a liquid phase. The liquid phase is comprised of several molten metal chlorides. The metals which form the high boiling point chlorides belong to the first and second groups of the periodic table of elements. These metals occur naturally in coal ash. The rapid chlorination of these metal fractions results in the formation of liquid phase. The presence of liquid chlorides provides a thin film over the ash surface; this introduces a large resistance to gaseous diffusion. The ultimate effect of this liquid film is to slow down the overall rate of reaction.

8.11 Comparison of Results with Published Data

Though a number of studies have been made in the past to study the chlorination of pure metal oxides (Chapter 2), the results of such studies are of little significance to ash chlorination. First, only a small fraction of metals in ash is present as simple metal oxides. Secondly, as demonstrated previously in this chapter, the presence of a number of other metals affects the chlorination reactions for aluminum, silicon, etc. The effect of alkali and alkali earth metals

present in ash is shown to hinder the chlorination of aluminum in particular. Hence, very little will be gained if the comparison is made with the results of pure metal oxide. However, the results will be compared with two studies that are reported in literature on simultaneous chlorination with a mixture of metal oxides.

8.11.1 Chlorination of Georgia Clay

Ujhidy et al (38) studied the chlorination of Georgia clay using a fluidized bed reactor. As mentioned in Chapter 2, their study showed very slow reaction for aluminum at temperatures above 800°C. The conversion of aluminum was only 25% at the end of 2-hour with Cl₂-CO mixture. Addition of carbon increased the conversion to 40%. The corresponding conversions from the present study are about 10% and 25%. It should be understood that two completely different types of materials are being compared. The analysis of Georgia clay indicated smaller amounts of metals other than Al, Si and Fe, whereas the fraction is much higher in coal ash. The aluminum fraction in the clay is relatively higher than in ash. Thus the two materials are chemically very different.

A point of agreement in the results of the two studies is that the addition of carbon to the solids in reactor enhances the metals recovery. However,

ujhidy et al (38) mentioned the testing of alkali and alkali earth metals as catalysts, but found no improvement in the yield by doing so. The reaction temperature of above 800°C is higher than the melting points for the chlorides of these metals. Hence, the chlorides would remain as liquid in the reactor. As demonstrated in the present study, the presence of liquid chlorides in the reactor is actually detrimental to the main chlorination reactions. It is not clear as to how NaCl could act as a catalyst in chlorination reactions. The reasoning that led them to such an approach is highly questionable.

8.11.2 Chlorination of Ash in Packed Bed

The chlorination of fly ash is studied by Burnet et al(7,40) using a packed bed system. In their experimental apparatus, the conversions for aluminum, silicon and iron were measured only at the end of each run. Thus the conversion data with time, as obtained in this study, could not be collected. The reactions were studied with carbon alone as the reducing agent. The use of CO along with carbon was not explored. From their experiments with the non-magnetic fraction of fly ash, the final conversion of aluminum was found to be much higher than achieved in the present study. Also each of their experiments was terminated as soon as chlorine was detected in the outlet gas. Thus the

duration of their experiments varied with the conversion.

The yields for aluminum were as high as almost 100% at 950°C. However, the average rate of reaction was independent of temperature. The value for this average rate of reaction is between 30 and 50% on an hourly basis. A comparison of the global reaction rates for the first hour will indicate that the rates from the present study are less than half of their rates.

Since only the average rates are available, the rapid decline in reaction as found in this study can not be inferred from their experiments. The total fraction of other metals as oxides in their ash sample is 8.4%. It is comparable to the similar fraction in this study. Any effect due to the chlorination of other metals is not mentioned in their study. However, the possibility of gas phase diffusion to be controlling the overall reaction rate is suggested (7). This seems plausible for their packed bed reactor system.

From the above discussion, it is evident that the results of Burnet et al (7,40) are seriously restricted in their applicability. It is believed that their rate data involved extrapolation to some extent. An extrapolation of the conversion data for the ash chlorina-

tion reactions can lead to erroneous results. If the rate data at 910°C (shown in Figure 8.1) for the first 5 minutes are subjected to a linear extrapolation, the duration for complete conversion of aluminum would be about one hour. In contrast, the actual yield data reveals that approximately 25% of aluminum reacted in a 2-hour period. The fact that the presence of molten chlorides tremendously lowers the rate of reaction cautions against any extrapolation of the data.

8.12 Summary

The effects of three important parameters are studied by a factorial design of experiments. The analysis of variance indicates that the ash particle diameter and higher chlorine fraction in the gas mixture have statistically significant effects in improving the yield for aluminum. Temperature in the range $910\text{-}950^{\circ}\text{C}$ does not have any significant effect.

The chlorination reactions are strongly time dependent. It is likely that the chlorination of aluminum in the initial 10 minute period is pore diffusion controlled. While the reactions proceed rapidly in the beginning, the decline in the rate is dramatic following the first 10 minutes in each case. The main cause for this decline is identified as the creation of a liquid phase in the reactor. The chlorides of alkali and alkali earth metals are the main contributors to

the liquid melt. It is proposed that the molten salts provide a thin film of liquid over the particle surface area. The diffusion of chlorine, for example, is shown to be extremely slow in molten salts. Thus the overall reaction rate is controlled by liquid film diffusion resistance. It is concluded that the low rate of gaseous diffusion is the reason for decline in the reaction rate. As long as the molten chlorides are present in the reactor, the overall chlorination of metals in ash will be slow.

CHAPTER 9

CONCLUSIONS AND RECOMMENDATIONS

9.1 Conclusions

The following conclusions are reached from this study on the chlorination of metals in coal ash.

- (1) Coal ash has the potential to become an important mineral source for a variety of metals. The recovery of aluminum from ash is of particular interest. The chlorination route for recovering metals from coal ash offers several advantages over other suggested wet techniques.
- (2) Thermodynamic equilibrium calculations have demonstrated the feasibility of metals chlorination over a wide range of temperature. While chlorine alone can convert most of the metal oxides into their chlorides, the extraction of aluminum and silicon demands the presence of a reducing agent such as carbon. Selective chlorination of aluminum in coal ash is not possible. It was shown that a judicious recycle of silicon chloride can suppress any further chlorination of silicon from ash.
- (3) Difficulties were encountered in maintaining the fluidized state of the reactor bed above 820°C.

When smaller size ash fraction was heated to about this temperature, the bed fluidization was disrupted due to the agglomeration of ash particles. It is concluded that this is caused by the presence of certain low melting constituents in ash.

- (4) The extent of aluminum chlorination is low when carbon monoxide is the only reducing agent. Simultaneous chlorination of iron, silicon and titanium fractions was also evident. The rate of reaction was higher at the beginning, but it decreased with time.
- (5) Fluid coke of petroleum origin was mixed with the ash to avoid caking of the bed upon heating. It was found that a (3:1) ratio of coke to ash resulted in achieving the fluidized state of the bed over 900°C. Addition of coke also helped increase the extent of chlorination for all four metals. Increasing the coke fraction in the reactor bed, however, did not affect the chlorination reactions.
- (6) Effects of three important parameters on the overall yields are studied using a statistical technique. It is found that a variation in reaction temperature above 900°C does not affect the reactions appreciably. Increasing the tempera-

ture from 800°C to over 900°C, however, gives a 2-fold increase in the fraction of aluminum chlorinated. The effect of reducing particle diameter or increasing the fraction of chlorine in reacting gas is statistically significant for the case of aluminum.

- (7) Though the chlorination reactions proceed rapidly at the initial stage, a considerable decline in the rate is observed after a first 5-15 minute period. The reaction rates, after this initial period, remain virtually constant with time. It is shown conclusively that the decline is due to the formation of a liquid phase. The liquid phase results from the simultaneous chlorination of alkali and alkali earth metal fractions present in ash. The chlorination of such metals occurs preferentially and during the initial few minutes of the reaction. The chlorides of alkali and earth metals are essentially liquid above 800°C.
- (8) The presence of such chlorides on the surface of reacted ash mass is shown by a number of techniques. With the help of a simple mathematical model it is shown that the decline in the reaction rates is due to the mass transfer resistance. Since gaseous diffusivity through molten chlorides is extremely slow, even a film

thickness of 1 μm to 5 μm may cause a drastic reduction in the rate of gaseous diffusion.

9.2 Recommendations for Future Research

- (1) Further attempts are necessary to achieve higher conversions of aluminum. Since the reaction yields are reduced by the presence of molten salts, the primary task will be to eliminate the alkali and alkali earth metal traces from the ash. The investigation should focus on selective reaction and separation of these alkali metals. In the absence of the liquid forming constituents, the chlorination of aluminum is anticipated to proceed rapidly.
- (2) Attempts should be undertaken to study and compare the chlorination behaviour of coal ash of varying composition and origin. It is indicated in this study that coal ash characteristics vary significantly with the type and source of coal.
- (3) The separation of various metal chlorides, such as AlCl_3 from FeCl_3 , by fractional condensation should be investigated. Conventionally, the vapours are allowed to deposit on the cooler walls of a condenser. The collected solids are mechanically scraped. Since AlCl_3 is extremely corrosive, serious design and operating problems will be

inevitable.

- (4) Attempts should be undertaken to investigate the recycling of silicon tetrachloride experimentally. The feasibility of SiCl_4 recycle to suppress further chlorination of silicon has been demonstrated with equilibrium computations.
- (5) Complete utilization of ash particles of all sizes would require chlorination of finer fractions as well. Due to an excessive carry over of the fines with exit gases from the reactor, an efficient collection and recycling of these particles will be necessary. Once higher reaction yields are achieved for all particles, it would be of interest to study the process of ash chlorination on a pilot plant scale. This will provide the important and necessary data to be used for constructing large scale metals recovery plant.

REFERENCES

- (1) Wright, J.H. and Roffman, H.K., Coal Ash - A Potential Mineral Source, Proceedings of Institute of Environmental Science, 22nd Annual Meeting, p163-173 (1976).
- (2) Condry, L.Z., Recovery of Alumina from Coal Refuse - An Annotated Bibliography, Coal Research Bureau Report No. 130 (1976).
- (3) Peacey, J.G. and Davenport, W.G., Evaluation of Alternative Methods of Aluminum Production, Journal of Metals, 26, 7, p25-28 (1974).
- (4) -----, Alcan Pilots 2400F Process Equipment, Canadian Chemical Processing, 51, 2, p45-48 (1967).
- (5) Paige, J.I., Robidart, G.B., Harris, H.M. and Campbell, T.T., Recovery of Chlorine and Iron Oxide from Ferric Chloride, Journal of Metals, 27, 11, p12-16 (1975).
- (6) Mehrotra, A.K., Bishnoi, P.R. and Svrcek, W.Y., Metal Recovery From Coal Ash via Chlorination - A Thermodynamic Study, The Canadian Journal of Chemical Engineering, 57, 2, p 225-232 (1979).
- (7) Burnet, G., Murtha, M.J. and Wijatno, H., Recovery of Alumina from Fly Ash by High-Temperature Chlorination, Third Kentucky Coal Refuse Disposal and Utilization Seminar, Kentucky, May 11-12, p83-88 (1977).
- (8) Bibby, D.M., Composition and Variation of Pulverized Fuel Ash Obtained from the Combustion of Sub-bituminous Coals, New-Zealand, FUEL, 56, p427-431 (1977).
- (9) Kennerley, R.A., StJohn, D.A. and Eardley, R.P., Meremere Fly Ash as a Concrete Admixture, New Zealand Journal of Science, 16, p855-874 (1973).
- (10) O'Gorman, J.V. and Walker, P.L., Jr., Thermal Behaviour of Mineral Fractions Separated from Selected American Coals, FUEL, 52, 1, p71-79 (1973).
- (11) Karyakin, S.K., X-Ray Structural Investigation of the Mineral Fraction of Ash-Poor Berezovskii Coal, Solid Fuel Chemistry, 11, 6, p54-56 (1977).

- (12) Katell, S., The Potential Economics of the Recovery of Trace Elements in Coal Refuse, Coal Research Bureau Report No. 142 West Virginia University, Morgantown, West Virginia (1977).
- (13) Chakrabarti, J.N., Potential Uses of Pulverized Fuel Ash in India, Journal of Mines, Metals & Fuels, 25,3,p79-82 (1977).
- (14) Cavin, D.C., Klemm, W.A. and Burnet, G., Analytical Methods for Characterization of Fly Ash, Proceedings of Iowa Academy of Science, 81, pl30-134 (1974).
- (15) Chiu, A.S., Characterization of Submicron Fly Ash in Cyclone Fired Boilers, M.Sc. Thesis, University of New Hampshire, U.S.A. (1978).
- (16) Tibbetts, T.E., Evaluation of Canadian Commercial Coals: Saskatchewan, Alberta and British Columbia-1975, CANMET Report 76-41 (1976).
- (17) Fisher, G.L., Prentice, B.A., Silberman, D., Ondov, J.M., Ragaini, R.C., Bierman, A.H., McFarland, A.R. and Pawley, J.B., American Chemical Society, Division of Fuel Chemistry, 22, pl49 (1977).
- (18) Behie, S.W., Personal Communications (1977).
- (19) Bryers, R.W. and Taylor, T.E., An Examination of the Relationship between Ash Chemistry and Ash Fusion Temperatures in various Coal Size and Gravity Fractions using Polynomial Regression Analysis, Transactions of ASME, Journal of Engineering for Power, 98,4,p528-539 (1976).
- (20) Smith, R.D., Campbell, J.A. and Nielson, K.K., Mechanisms for Trace Element Enrichment in Fly Ash during Coal Combustion, American Chemical Society, Division of Fuel Chemistry, 23,1, pl96-201 (1978).
- (21) Piccolo, L., Chirga, M. and Calcagno, B., Gas-Solid Reactor: Effects of Chemical and Fluidynamic Parameters on Alumina Chlorination Process, Chimie et Industrie-Genie Chimique, 104,19,p2485-2489 (1971).
- (22) Goroshchenko, Ya.G. and Pishchai, I.Ya., Chlorination of Aluminum Oxide in the Presence of Carbon at 1200-1450C, Journal of Applied Chemistry of USSR, 44,8,pl894-1896 (1971).
- (23) Spinella, A.L., Yean, D.H. and Riter, J.R., Jr., High Temperature Heterogeneous Equilibria in the Unit Activity Approximation 1. Alumina-Carbon-Chlorine System, Metallurgical Transactions, 4, Aug, p2002-2003 (1973).

- (24) Holliday, R.D. and Milne, D.J., Experimental Evaluation of Routes for Purification of Bauxite by Gas-Solid Reactions, Industrial & Engineering Chemistry, Process Design Development, 14,4,p447-452 (1975).
- (25) Foley, E. and Tittle, K., Removal of Iron Oxides from Bauxite Ores, Proceedings of Australian Institute of Mining & Metallurgy No.239,p59-65 (1971).
- (26) Geisser, H., Baiker, A. and Richarz, W., Comparison of Alumina Chlorination Processes, 6th International Congress of Chemical Engineering, Aug 21-25 (1978).
- (27) Storozhenko, V.N., Determination of Aluminum Oxide in Aluminum Powders by Chlorination, Industrial Laboratory of USSR, (Translated from Zavodskaya Laboratoriya, 38,11,p1317-1319, Nov.,1972), p1663-1665 (1973).
- (28) Landsberg, A., Chlorination Kinetics of Aluminum Bearing Minerals, Metallurgical Transactions B, 6B, June,p207-214 (1975).
- (29) Brin, V.G. and Eremin, N.I., Removal of Iron and Titanium from Kaolins by Chlorination, Journal of Applied Chemistry of USSR, 42,8,p1776-1778 (1969).
- (30) Dunn, W.E., Jr., High Temperature Chlorination of TiO_2 Bearing Minerals, Transactions of the Metallurgical Society of American Institute of Mining Engineers, 218, Feb,p6-12 (1960).
- (31) Mehra, O.K., Hussain, S.Z. and Jena, P.K., Kinetics of the Chlorination of Niobium Pentoxide with Chlorine in Presence of Excess of Graphite Powder, Transactions of the Indian Institute of Metals, 19, March,p53-56 (1966).
- (32) Mehra, O.K. and Jena, P.K., Kinetics of the Chlorination of Tantalum-pentaoxide with Chlorine in Presence of Excess Graphite Powder, Transactions of the Indian Institute of Metals 20,p210-212 (1967).
- (33) Skeaff, J.M., Chlorination of Uranium Ore for Extraction of Uranium, Thorium and Radium and for pyrite Removal, Canadian Institute of Mining Bulletin, Aug.,p120-125 (1979).
- (34) Olsen, R.S. and Block, F.E., The Chlorination of Columbite in a Fluidized-bed Reactor, Fluidization Fundamentals and Applications, Chemical Engineering Progress Symposium Series 66,105,p225-228 (1970).
- (35) Milliken, T.H., Jr., Recovery of Metallic Aluminum from Aluminous Ores, U.S. Patent 2,813,786, Nov.19 (1957).

- (36) Othmer, D.F., Method for Producing Aluminum Metal directly from Ore, U.S. Patent 3,861,904, Jan.21 (1975).
- (37) King, L.K. and Jarrett, N., Selective Recycle Production of Aluminum Chloride, U.S. Patent 3,929,975, Dec.20 (1975).
- (38) Ujhidy, A., Szepvolgyi, J. and Borlai, O., Application of Fluidized Bed Reactor to Chlorination at High Temperatures, p565-568, Fluidization Technology II, Edited by Keairns, D.L., Hemisphere Publishing Corporation, Washington (1975).
- (39) Roy, N.K., Murtha, M.J. and Burnet, G., Recovery of Iron Oxide from Power Plant Fly Ash by Magnetic Separation, IS-M-153 (1978).
- (40) Murtha, M.J. and Burnet, G., Recovery of Alumina from Coal Fly Ash by High Temperature Chlorination, Proceedings of Iowa Academy of Science, 83, pl25-129 (1976).
- (41) Milne, D.J., Chlorination of Bauxite in the Presence of Silicon Tetrachloride, Metallurgical Transactions B, 6B, 3, p486-488 (1975).
- (42) Abel, K.H. and Rancitelli, L.A., Instrumental Neutron Activation Analysis, Trace Elements in Fuels, Edited by Babu, S.P., Advances in Chemistry Series, 141, pl32-133 (1975).
- (43) van Zeggeren, F. and Storey, S.H., Computation of Chemical Equilibria, Cambridge University Press, Cambridge, U.K. (1970).
- (44) Dluzniewski, J.H. and Adler, S.B., Calculation of Complex Equilibria Problems, Institution of Chemical Engineers, 50th Annual Technical Meeting, London (1972).
- (45) White, W.B., Johnson, S.M. and Dantzig, G.B., Chemical Equilibrium in Complex Mixtures, Journal of Chemical Physics, 28, 5, p751-755 (1958).
- (46) Horton, W.S., An Algorithm and BASIC Computer Program for Calculating Simple Coal Gasification Equilibria, NBSIR-78-1509 (PB-291-241) (1978).
- (47) Balzhiser, R.E., Samuels, M.R. and Eliassen, J.D., Chemical Engineering Thermodynamics: The Study of Energy, Entropy and Equilibrium, Prentice-Hall, Englewood Cliff, N.J. (1972).

- (48) Milne, D.J. and Holliday, R.D., Thermodynamics of Gas-Solid Reactions for Purification of Bauxite at Moderate Temperatures, Industrial & Engineering Chemistry, Process Design Development, 14,4,p442-447 (1975).
- (49) Stull, D.R. and Prophet, H., JANAF Thermochemical Tables, NSRDS-NBS 37, Second Edition, The Dow Chemical Co., Midland, Mich., U.S.A. (1971).
- (50) Chase, M.W., Curnutt, J.L., Hu, A.T., Prophet, H., Syverud, A.N. and Walker, L.C., JANAF Thermochemical Tables - 1974 Supplement, Journal of Physical and Chemical Data, 3,p311 (1974).
- (51) Chase, M.W., Curnutt, J.L., Prophet, H., McDonald, R.A., and Syverud, A.N., JANAF Thermochemical Tables - 1975 Supplement, Journal of Physical and Chemical Data, 4,pl (1975).
- (52) Fletcher, R. and Powell, M.J.D., A Rapidly Convergent Descent Method for Minimization, Computer Journal, 6,2,pl63-168 (1963).
- (53) Mehrotra, A.K., Svrcek, W.Y. and Bishnoi, P.R., Extraction of Metals as their Chlorides from Fly Ash, Proceedings of Coal & Coke Sessions, 28th Canadian Chemical Engineering Conference, Halifax, Nova Scotia Canada (1978).
- (54) Bishnoi, P.R., Svrcek, W.Y. and Mehrotra, A.K., The Effect of Recycling Silicon Chloride on the Chlorination of Coal Ash, Canadian Journal of Chemical Engineering, accepted for publication, Nov. (1979).
- (55) Gregory, G.A., Applied Statistical Methods in Research and Production, Parts I & II, The University of Calgary, Calgary, Canada (1973).
- (56) Medlin, J.H., Suhr, N.H. and Bodkin, J.B., Atomic Absorption Analysis of Silicates Employing LiBO_3 Fusion, Atomic Absorption Newsletter, 8,2,p25-29 (1969).
- (57) Perry, R.H. and Chilton, C.H., Chemical Engineers' Handbook, Fifth Ed., McGraw-Hill (1973).
- (58) Kunii, D. and Levenspiel, O., Fluidization Engineering, John Wiley & Sons, U.S.A. (1969).
- (59) McCabe, W.L. and Smith, J.C., Unit Operations of Chemical Engineering, Third Ed., McGraw-Hill (1976).

- (60) Levenspiel, O., Chemical Reaction Engineering, Second Edition, John Wiley & Sons, U.S.A. (1972).
- (61) Mamantov, G., Molten Salts - Characterization and Analysis, Marcel Dekker, Inc., U.S.A. (1969).
- (62) Danckwerts, P.V., Gas Liquid Reactions, McGraw Hill, Inc. (1970).
- (63) Janz, G.J. et al., Molten Salts: Vol. 1 Electrical Conductance, Density and Viscosity Data, NSRDS-NBS-15 October (1968).
- (64) Sundheim, B.R., Fused Salts, McGraw Hill Book Co., U.S.A. (1964).
- (65) Bird, R.B., Stewart, W.E. and Lightfoot, E.N., Transport Phenomena, International Edition, John Wiley & Sons (1960).

A _ P _ P _ E _ N _ D _ I _ C _ E _ S

APPENDIX I

Mathematics of Free Energy Minimization

I.1 The Derivation

A system for the minimization of free energy computations is defined by specifying the following:

- (a) temperature and pressure of the system, and
- (b) the amounts of all reactants.

The contribution to the total gas phase free energy function F by any component i for an ideal case (ideal gas and ideal gas mixture) at 1 atmosphere pressure is

$$F_i = n_i \left\{ \frac{G_i}{RT} \right\} + \ln \left[\frac{n_i}{n} \right] \quad i = S+1, S+1, \dots, C \quad (I.1)$$

For the condensed species, due to the assumption of pure phase, the ratio (n_i/n) is unity. Thus Equation (I.1) for the condensed species simplifies as

$$F_i = n_i \left\{ \frac{G_i}{RT} \right\} \quad i = 1, 2, \dots, S \quad (I.2)$$

In the above formulation it was arbitrarily decided to list all the condensed species first followed by the gaseous ones. The set of expressions given by Equations (I.1) and (I.2) can be combined to yield a general expression for the total free energy of the system

$$F = \sum_{i=1}^S n_i \left\{ \frac{G_i}{RT} \right\} + \sum_{i=S+1}^C n_i \left\{ \frac{G_i}{RT} \right\} + \ln \left[\frac{n_i}{n} \right] \quad (I.3)$$

$$\text{where, } n = \sum_{i=S+1}^C n_i$$

The function, F, given by Equation (I.3) is to be minimized subject to the conditions that all molecular amounts, n_i 's, are non-negative and that all elemental balances are satisfied, i.e.

$$n_i \geq 0 \quad i = 1, 2, \dots, S, S+1, \dots, C \quad (I.4)$$

and,

$$\sum_{i=1}^C a_{ji} n_i = B_j \quad j = 1, 2, \dots, M \quad (I.5)$$

By using Lagrangian multipliers, $\bar{\pi}$, and following the procedure outlined by Balzhiser et al (47), a set of (M+S+1) linear algebraic equations with (M+S+1) unknowns for the k^{th} iteration is given as follows:

M equations are

$$\sum_{l=1}^M \bar{\pi}_l \left[\sum_{i=S+1}^C a_{ji} a_{li} n_i^k + \sum_{i=1}^S a_{ji} n_i^{k+1} + n^{k+1} \sum_{i=S+1}^C a_{ji} \frac{n_i^k}{n^k} \right] = b_j + \sum_{i=S+1}^C a_{ji} n_i^k \left\{ \frac{G_i}{RT} \right\} + \ln \left[\frac{n_i^k}{n^k} \right] \quad 1 \leq j \leq M \quad (I.6)$$

S equations are

$$\sum_{j=1}^M \bar{\pi}_j a_{ji} = \frac{G_i}{RT} \quad 1 \leq i \leq S \quad (I.7)$$

and, the last equation is

$$\sum_{j=1}^M \pi_j B_j = \sum_{i=1}^S n_i^k \left\{ \frac{G_i}{RT} \right\} + \ln \left[\frac{n_i^k}{n^k} \right] \quad (\text{I.8})$$

The (M+S+1) unknowns in the above Equations (I.6), (I.7) and (I.8) are

- M unknowns - Lagrangian multipliers, π_j ,
- S unknowns - amounts of solids, n_i^{k+1} ,
- 1 unknown - total moles of gas phase.

It should be noted that at the overall system equilibrium, the free energy of gas phase would also be at minimum. The expression for calculating moles of individual gas phase constituents after the k^{th} iteration is:

$$n_i^{k+1} = n_i^k \left[\frac{n^{k+1}}{n^k} \right] + \sum_{j=1}^M \pi_j a_{ji} - \left\{ \frac{G_i}{RT} \right\} + \ln \left[\frac{n_i^k}{n^k} \right] \quad (\text{I.9})$$

$$i = S+1, S+2, \dots, C$$

I.2 Limitation on Number of Phases

A significant limitation of the free energy minimization calculations for heterogeneous systems is exposed by the Gibbs phase rule. The restriction is on the number of solid (or liquid) phases that may be included in a single computation. The degrees of freedom for a reactive system are given by the phase rule

as

$$f = x - \phi + 2 \quad (\text{I.10})$$

van Zeggeren and Storey (43) showed that for reactive systems, the number of components x can be replaced by the number of atomic species M in the system. The remaining $(x-M)$ components can be obtained simply by writing $(x-M)$ algebraic equations and solving them simultaneously. However, this is valid only if the chemical structures of the species do not contain any two or more elements in one proportion in all the species containing them. In a system with S condensed phases in equilibrium with one gas phase, the number of phases is

$$\phi = S + 1 \quad (\text{I.11})$$

Hence the phase rule for a heterogeneous system can be rewritten as

$$f = M - S + 1 \quad (\text{I.12})$$

The temperature and pressure of the system will be specified for the minimization calculations. The material balance for an element (or a set of elements) appearing as condensed species will not be essential for the gas phase. This is true because the amount of species in the condensed phase does not affect the calculation routine given by Equations (I.6), (I.7) and

(I.8). The number of moles of the species in the condensed phase is thus a reservoir for those elements. As long as the condensed phase is predicted to exist from the calculations, any amount of the species can be either added to or removed from the gas phase without affecting the computational process. For each element present in the condensed phase, one less element balance for the gas phase is required. The amount of an element that necessarily satisfies the mass balance condition, Equation (I.5), is called the abundance of that element (43).

From the preceding discussion, it is evident that the number of degrees of freedom is equal to the number of specified thermodynamic variables, i.e. temperature and pressure, plus the number of ratios of elemental abundances, n_r , that can be arbitrarily specified (43):

$$f = 2 + n_r \quad (I.13)$$

Equations (I.12) and (I.13), when combined, result in Equation (I.14):

$$S = M - n_r - 1 \quad (I.14)$$

Thus the maximum number of condensed species that can be considered for any one computation is restricted by the total number of atomic species present in the condensed phase. In order to include as many condensed

species with a total of M elements, the number of elemental abundances must go to the minimum, i.e. $n_r=0$, and

$$S_{\max} = M - 1 \quad (\text{I.15})$$

Equation (I.15) yields two important conclusions regarding the maximum number of solids that can be included for the calculations. These are:

- (i) The number of condensed phases can never exceed one less than the number of elements, and
- (ii) only one element balance, Equation (I.5), would suffice to compute the overall equilibrium.

While selecting a particular set of the condensed species, caution is needed in avoiding two compounds with composition vectors that are a linear combination of one another. An illustrative example will be given to make it more explicit. The inclusion of three solids, Al_2O_3 , SiO_2 and Al_2SiO_5 , in one calculation is not justified. The three composition vectors, a_{ji} 's, are (2, 0, 3), (0, 1, 2) and (2, 1, 5). Since the vector (2, 1, 5) can be obtained simply by adding the other two; having all three solids will result in a trivial solution of the computational process.

APPENDIX II

Design of 3-Factor Experiments

II.1 3-Factor Complete Factorial Experiments

In a Factorial Experiment, the effects of a number of independent variables, called factors, are investigated at a finite, and usually a small number of levels. In a complete factorial experiment, all possible combinations that can be formed by choosing one level for each factor, are studied.

It will be assumed that factor 'A' is to be investigated at 'a' levels, factor 'B' at 'b' levels, and factor 'C' at 'c' levels. The replication of experimental runs will not be considered in this study. A total of 'abc' trials must be performed at abc treatment combinations. Ideally, in any factorial experiment, the order in which each trial is performed should be randomized.

II.2 Interpretation of Experimental Data

The equations and procedure of the analysis are adopted from Gregory (55). The model for the 3-Factor experiment is given as

$$y_{ijk} = \mu + \theta_i^A + \theta_j^B + \theta_k^C + \theta_{ij}^{AB} + \theta_{ik}^{AC} + \theta_{jk}^{BC} + \theta_{ijk}^{ABC} \quad (II.1)$$

where, y_{ijk} = the observed response at the i th level of jk th block

μ = the overall population mean of all possible results

θ_m^M = correction to μ to account for m th level of M (has zero expectation)

θ_{mn}^{MN} = 2-factor interaction term (has zero expectation)

θ_{mno}^{MNO} = 3-factor interaction term (estimate of error variance).

The existence of a three-factor interaction is rather rare for most real systems (55). Consequently, the mean square associated with the three-factor interaction can be interpreted simply as the variation due to experimental error.

II.3 The Sum of Squares

The various sums of squares will be defined in this section.

II.3.1 Correction for the Mean

The correction for the mean is the square of grand total for all the observations divided by the total number of observations.

$$CM = \frac{[\sum_{i=1}^a \sum_{j=1}^b \sum_{k=1}^c y_{ijk}]^2}{abc} \quad (II.2)$$

II.3.2 Main Effect

The main effect sums of squares for the three factors are given as:

$$SSA = \frac{1}{bc} \sum_{i=1}^a [\sum_{j=1}^b \sum_{k=1}^c y_{ijk}]^2 - CM \quad (II.3)$$

$$SSB = \frac{1}{ac} \sum_{j=1}^b [\sum_{i=1}^a \sum_{k=1}^c y_{ijk}]^2 - CM \quad (II.4)$$

$$SSC = \frac{1}{ab} \sum_{k=1}^c [\sum_{i=1}^a \sum_{j=1}^b y_{ijk}]^2 - CM \quad (II.5)$$

II.3.3 Two-factor Interaction

The two-factor interaction sums of squares are defined by:

$$SS(AB) = \frac{1}{c} \sum_{i=1}^a \sum_{j=1}^b [\sum_{k=1}^c y_{ijk}]^2 - SSA - SSB - CM \quad (II.6)$$

$$SS(AC) = \frac{1}{b} \sum_{i=1}^a \sum_{k=1}^c [\sum_{j=1}^b y_{ijk}]^2 - SSA - SSC - CM \quad (II.7)$$

$$SS(BC) = \frac{1}{a} \sum_{j=1}^b \sum_{k=1}^c [\sum_{i=1}^a y_{ijk}]^2 - SSB - SSC - CM \quad (II.8)$$

II.3.4 Three-factor Interaction

As mentioned previously, the three-factor interaction term for this case will be interpreted as an estimate of the error variance. The three-factor interaction sum of squares is given by:

$$\begin{aligned} SS(ABC) = & \sum_{i=1}^a \sum_{j=1}^b \sum_{k=1}^c (y_{ijk})^2 - SSA - SSB - SSC \\ & - SS(AB) - SS(AC) - SS(BC) - CM \end{aligned} \quad (II.9)$$

II.3.5 Total Sum of Squares

The total sum of squares is the sum of the squares of all observations minus the correction for the mean and is represented by:

$$SST = \sum_{i=1}^a \sum_{j=1}^b \sum_{k=1}^c (y_{ijk})^2 - CM \quad (II.10)$$

The analysis of variance for complete three-factor factorial experiments is summarized in Table II.1.

Source	Sum of Squares	Degrees of Freedom	Error (Mean Square)
A	SSA	(a-1)	$\sigma_o^2 + bc \sigma_A^2$
B	SSB	(b-1)	$\sigma_o^2 + ac \sigma_B^2$
C	SSC	(c-1)	$\sigma_o^2 + ab \sigma_C^2$
AB	SS(AB)	(a-1)(b-1)	$\sigma_o^2 + c \sigma_{AB}^2$
AC	SS(AC)	(a-1)(c-1)	$\sigma_o^2 + b \sigma_{AC}^2$
BC	SS(BC)	(b-1)(c-1)	$\sigma_o^2 + a \sigma_{BC}^2$
ABC	SS(ABC)	(a-1)(b-1)(c-1)	$\sigma_o^2 + \sigma_{ABC}^2$

Table II.1 Analysis of Variance for Complete Three-Factor Factorial Experiments.

A p p e n d i x - I I I

Experimental Data Tables

Experimental Run # 1						
Ash Type: Fly Size: 194 μ m Mass: 250 gm						
Gas Flow (l/min): Chlorine: 4.6 CO: 11.9						
Fluid Coke: None						
Average Reaction Temperature: 430 $^{\circ}$ C						
Maximum Temperature Reached Initially: 431 $^{\circ}$ C						
Average Pressure Drop: not available						
Loss due to Carry over: 2 gm						
Sample No.	Time min	Temp. ($^{\circ}$ C)	% of Metal Recovered			
			Al	Fe	Si	Ti
1	0.0	425	0.00	0.0	--	--
2	15.0	430	0.13	5.9	--	--
3	30.0	432	0.13	5.9	--	--
4	45.0	435	0.13	5.2	--	--
5	60.0	431	0.13	8.3	--	--
6	60.0+	431	0.13	8.1	--	--

Table III.1 Experimental Data for Run Number 1.

Experimental Run # 2						
Ash Type: Fly Size: 164 μ m Mass: 385 gm						
Gas Flow (l/min): Chlorine: 4.2 CO: 10.8						
Fluid Coke: None						
Average Reaction Temperature: 522 $^{\circ}$ C						
Maximum Temperature Reached Initially: 534 $^{\circ}$ C						
Average Pressure Drop: 80 cm H ₂ O						
Loss due to Carry over: 8 gm						
Sample No.	Time min	Temp. ($^{\circ}$ C)	% of Metal Recovered			
			Al	Fe	Si	Ti
1	0.0	531.8	0.00	0.00	--	--
2	10.0	524.3	0.02	4.04	--	--
3	25.0	520.3	0.06	2.29	--	--
4	40.0	520.7	0.17	2.16	--	--
5	55.0	520.4	0.17	2.40	--	--
6	70.0	519.8	0.23	3.22	--	--
7	70.0+	---	0.23	3.13	--	--

Table III.2 Experimental Data for Run Number 2.

Experimental Run # 3							

Ash Type: Fly		Size: 164 μ m		Mass: 385 gm			
Gas Flow (l/min):		Chlorine: 3.5		CO: 7.2			
Fluid Coke: None							
Average Reaction Temperature: 648 $^{\circ}$ C							
Maximum Temperature Reached Initially: 660 $^{\circ}$ C							
Average Pressure Drop: 84 cm H ₂ O							
Loss due to Carry over: 6 gm							
Sample No.	Time min	Temp. ($^{\circ}$ C)	% of Metal Recovered				
			Al	Fe	Si	Ti	
1	0.0	650	0.0	0.0	--	--	
2	10.0	649.5	0.02	3.0	--	--	
3	20.0	647.3	0.13	4.0	--	--	
4	30.0	647.3	0.13	4.4	--	--	
5	45.0	646.7	0.18	4.9	--	--	
6	60.0	645.2	0.29	5.2	--	--	
7	60.0+	---	0.29	5.4	--	--	

Table III.3 Experimental Data for Run Number 3.

Experimental Run # 4							

Ash Type: Fly		Size: 164 μ m		Mass: 260 gm			
Gas Flow (l/min):		Chlorine: 3.3		CO: 7.0			
Fluid Coke: None							
Average Reaction Temperature: 758 $^{\circ}$ C							
Maximum Temperature Reached Initially: 765 $^{\circ}$ C							
Average Pressure Drop: 86 cm H ₂ O							
Loss due to Carry over: 7 gm							
Sample No.	Time min	Temp. ($^{\circ}$ C)	% of Metal Recovered				
			Al	Fe	Si	Ti	
1	0.0	762.0	0.0	0.0	--	--	
2	5.0	762.8	0.0	0.7	--	--	
3	15.0	758.0	0.0	1.1	--	--	
4	25.0	758.6	0.1	1.6	--	--	
5	40.0	757.5	0.1	2.3	--	--	
6	60.0	757.5	0.1	2.4	--	--	
7	80.0	---	0.1	2.5	--	--	

Table III.4 Experimental Data for Run Number 4.

Experimental Run # 5						

Ash Type: Fly		Size: 229 μ m	Mass: 390 gm			
Gas Flow (l/min):		Chlorine: 4.0	CO: 10.4			
Fluid Coke: None						
Average Reaction Temperature: 849 $^{\circ}$ C						
Maximum Temperature Reached Initially: 855 $^{\circ}$ C						
Average Pressure Drop: 121 cm H ₂ O						
Loss due to Carry over: 8 gm						
Sample No.	Time min	Temp. ($^{\circ}$ C)	% of Metal Recovered			
			Al	Fe	Si	Ti
1	0.0	849.2	0.0	0.0	--	--
2	5.0	848.6	0.0	10.6	--	--
3	10.0	847.1	0.1	10.2	--	--
4	20.0	849.3	0.2	13.6	--	--
5	30.0	848.8	0.4	16.8	--	--
6	45.0	849.9	0.6	20.6	--	--
7	60.0	849.9	0.9	23.1	--	--
8	70.0	---	0.9	27.4	--	--
9	70.0+	---	1.5	35.4	--	--

Table III.5 Experimental Data for Run Number 5.

Experimental Run # 6						

Ash Type: Bottom		Size: 212 μ m	Mass: 345 gm			
Gas Flow (l/min):		Chlorine: 2.7	CO: 7.1			
Fluid Coke: None						
Average Reaction Temperature: 902 $^{\circ}$ C						
Maximum Temperature Reached Initially: 906 $^{\circ}$ C						
Average Pressure Drop: 110 cm H ₂ O						
Loss due to Carry over: 3 gm						
Sample No.	Time min	Temp. ($^{\circ}$ C)	% of Metal Recovered			
			Al	Fe	Si	Ti
1	0.0	898.5	0.0	0.0	0.0	0.0
2	10.0	904.3	0.1	9.5	0.1	0.0
3	20.0	903.3	0.3	21.1	0.1	0.0
4	30.0	902.4	0.4	22.2	0.1	0.0
5	40.0	902.8	0.5	22.8	0.1	0.0
6	50.0	902.2	0.5	23.9	0.1	0.0
7	66.0	901.6	0.6	27.0	0.1	0.0
8	80.0	901.5	0.7	27.0	0.2	0.0
9	95.0	901.6	0.7	28.1	0.2	0.0
10	110.0	901.7	0.9	28.1	0.2	3.0
11	110.0+	---	0.9	29.6	0.2	3.0

Table III.6 Experimental Data for Run Number 6.

Experimental Run # 7						
Ash Type: Bottom		Size: 212 μ m	Mass: 320 gm			
Gas Flow (l/min):		Chlorine: 2.0	CO: 5.3			
Fluid Coke: None						
Average Reaction Temperature: 960 $^{\circ}$ C						
Maximum Temperature Reached Initially: 966 $^{\circ}$ C						
Average Pressure Drop: 98 cm H ₂ O						
Loss due to Carry over: 2 gm						
Sample No.	Time min	Temp. ($^{\circ}$ C)	% of Metal Recovered			
			Al	Fe	Si	Ti
1	0.0	960.0	0.0	0.0	0.0	0.0
2	10.0	952.8	0.0	25.1	0.0	0.0
3	20.0	953.0	0.0	27.0	0.0	0.0
4	35.0	962.9	0.3	28.8	0.0	0.0
5	50.0	961.8	0.7	32.4	0.0	0.0
6	65.0	961.1	0.8	32.4	0.1	0.0
7	85.0	961.4	1.4	39.5	0.1	0.0
8	105.0	961.7	1.8	40.3	0.2	0.0
9	120.0	961.4	2.5	48.9	0.2	10.7

Table III.7 Experimental Data for Run Number 7.

Experimental Run # 8						
Ash Type: Bottom		Size: 125 μ m	Mass: 220 gm			
Gas Flow (l/min):		Chlorine: 2.0	CO: 5.3			
Fluid Coke: None						
Average Reaction Temperature: 975 $^{\circ}$ C						
Maximum Temperature Reached Initially: 1020 $^{\circ}$ C						
Average Pressure Drop: 98 cm H ₂ O						
Loss due to Carry over: 8 gm						
Sample No.	Time min	Temp. ($^{\circ}$ C)	% of Metal Recovered			
			Al	Fe	Si	Ti
1	0.0	978.6	0.0	0.0	0.0	0.0
2	15.0	974.3	2.0	24.0	0.1	0.0
3	30.0	973.5	2.4	28.1	0.1	0.0
4	60.0	978.2	4.4	30.3	0.3	0.0
5	90.0	976.0	5.2	34.6	0.4	0.0
6	120.0	973.2	7.3	52.0	0.6	0.0
7	150.0	972.6	8.6	60.8	0.8	0.0
8	175.0	972.4	11.1	73.5	1.0	25.4
9	175.0+	---	11.0	74.0	1.0	25.4

Table III.8 Experimental Data for Run Number 8.

Experimental Run # 9							
Ash Type: Bottom		Size: 164 μ m	Mass: 390 gm				
Gas Flow (l/min):		Chlorine: 2.0	CO: 5.0				
Fluid Coke: None							
Average Reaction Temperature: 970 $^{\circ}$ C							
Maximum Temperature Reached Initially: 995 $^{\circ}$ C							
Average Pressure Drop: 99 cm H ₂ O							
Loss due to Carry over: 6 gm							
Sample No.	Time min	Temp. ($^{\circ}$ C)	% of Metal Recovered				
			Al	Fe	Si	Ti	
1	0.0	973.8	0.0	0.0	0.0	--	
2	15.0	968.7	1.8	29.2	0.1	--	
3	30.0	970.5	1.8	33.0	0.1	--	
4	60.0	969.9	2.9	36.7	0.2	--	
5	90.0	969.5	4.0	40.3	0.3	--	
6	120.0	969.8	4.7	43.9	0.5	--	
7	140.0	969.7	5.7	47.5	0.6	--	
8	160.0	970.2	5.7	47.5	0.8	--	
9	180.0	969.9	7.1	51.0	0.9	--	
10	180.0+	---	7.5	57.9	0.9	--	

Table III.9 Experimental Data for Run Number 9.

Experimental Run # 10							
Ash Type: Bottom		Size: 89 μ m	Mass: 460 gm				
Gas Flow (l/min):		Chlorine: 2.8	CO: 2.8				
Fluid Coke: None							
Average Reaction Temperature: 924 $^{\circ}$ C							
Maximum Temperature Reached Initially: 946 $^{\circ}$ C							
Average Pressure Drop: 75 cm H ₂ O							
Loss due to Carry over: 3 gm							
Sample No.	Time min	Temp. ($^{\circ}$ C)	% of Metal Recovered				
			Al	Fe	Si	Ti	
1	0.0	905.0	0.0	0.0	0.0	0.0	
2	15.0	932.0	3.4	52.8	0.1	5.7	
3	30.0	925.8	4.4	58.4	0.4	1.8	
4	45.0	925.4	5.2	65.7	0.5	7.8	
5	49.0	925.0	4.5	66.8	0.5	7.8	

Table III.10 Experimental Data for Run Number 10.

Experimental Run # 11						
Ash Type: Fly Size: 89µm Mass: 200 gm						
Gas Flow (l/min): Chlorine: 3.5 CO: 3.5						
Fluid Coke: None						
Average Reaction Temperature: 808°C						
Maximum Temperature Reached Initially: 822°C						
Average Pressure Drop: 67 cm H ₂ O						
Loss due to Carry over: 4 gm						
Sample No.	Time min	Temp. (°C)	% of Metal Recovered			
			Al	Fe	Si	Ti
1	0.0	802.0	0.0	0.0	0.0	0.0
2	10.0	805.6	0.5	11.5	0.0	0.0
3	20.0	808.0	0.9	13.6	0.2	2.9
4	30.0	811.1	1.3	15.6	0.3	2.9
5	45.0	811.6	1.9	19.7	0.6	2.9
6	60.0	809.9	2.5	23.7	0.6	5.6
7	75.0	808.4	3.1	26.7	0.7	5.6
8	90.0	808.0	3.7	29.6	1.0	5.6
9	105.0	807.6	4.5	32.5	1.2	5.6
10	120.0	806.5	5.4	35.4	1.3	5.6
11	140.0	806.0	6.3	39.2	1.3	5.6
12	160.0	806.2	7.2	42.9	1.8	8.2
13	180.0	805.8	7.6	46.6	2.2	5.7
14	180.0+	---	8.0	48.4	1.9	8.2

Table III.11 Experimental Data for Run Number 11.

Experimental Run # 12						
Ash Type: Fly Size: 125µm Mass: 270 gm						
Gas Flow (l/min): Chlorine: 4.1 CO: 4.1						
Fluid Coke: None						
Average Reaction Temperature: 802°C						
Maximum Temperature Reached Initially: 816°C						
Average Pressure Drop: 81 cm H ₂ O						
Loss due to Carry over: 6 gm						
Sample No.	Time min	Temp. (°C)	% of Metal Recovered			
			Al	Fe	Si	Ti
1	0.0	800.2	0.0	0.0	0.0	0.0
2	10.0	800.8	0.6	6.9	0.2	0.5
3	20.0	802.5	0.9	7.6	0.3	0.5
4	30.0	801.4	1.3	8.9	0.4	0.5
5	45.0	801.9	1.7	11.6	0.5	0.5
6	60.0	802.7	2.1	13.5	0.6	0.5
7	75.0	802.4	2.5	14.2	0.7	0.5
8	90.0	802.2	3.4	15.5	0.8	0.5
9	105.0	802.2	3.9	16.1	1.0	0.5
10	120.0	802.3	4.6	17.4	1.0	0.5
11	140.0	802.7	4.9	18.0	1.0	0.5
12	160.0	802.4	5.8	19.2	1.4	1.0
13	180.0	802.1	6.3	20.4	1.5	1.0
14	180.0+	---	6.5	22.8	1.7	1.0

Table III.12 Experimental Data for Run Number 12.

Experimental Run # 13						
Ash Type: Fly		Size: 89 μ m	Mass: 250 gm			
Gas Flow (l/min):		Chlorine: 5.2	CO: 2.6			
Fluid Coke: None						
Average Reaction Temperature: 811 $^{\circ}$ C						
Maximum Temperature Reached Initially: 836 $^{\circ}$ C						
Average Pressure Drop: 75 cm H ₂ O						
Loss due to Carry over: 5 gm						
Sample No.	Time min	Temp. ($^{\circ}$ C)	% of Metal Recovered			
			Al	Fe	Si	Ti
1	0.0	806.0	0.0	0.0	0.0	0.0
2	10.0	809.5	0.7	13.4	0.3	0.0
3	20.0	809.8	1.1	13.4	0.3	0.0
4	30.0	811.5	1.5	16.1	0.4	0.0
5	45.0	811.5	1.9	17.4	0.6	2.8
6	60.0	811.3	2.5	18.6	0.8	2.8
7	75.0	812.8	3.1	21.2	1.0	2.8
8	83.0	812.4	3.5	23.7	1.1	2.8
9	90.0	810.0	3.5	23.7	1.1	2.8

Table III.13 Experimental Data for Run Number 13.

Experimental Run # 14						
Ash Type: Fly		Size: 125 μ m	Mass: 100 gm			
Gas Flow (l/min):		Chlorine: 3.5	CO: 3.5			
Fluid Coke:		Size: 169 μ m	Mass: 300 gm			
Average Reaction Temperature: 808 $^{\circ}$ C						
Maximum Temperature Reached Initially: 847 $^{\circ}$ C						
Average Pressure Drop: 79 cm H ₂ O						
Loss due to Carry over: 6 gm						
Sample No.	Time min	Temp. ($^{\circ}$ C)	% of Metal Recovered			
			Al	Fe	Si	Ti
1	0.0	802.0	0.0	0.0	0.0	0.0
2	10.0	817.5	3.6	19.6	1.3	7.0
3	20.0	806.3	3.9	21.5	1.5	10.4
4	30.0	805.9	4.7	23.4	1.7	10.4
5	40.0	807.4	5.8	25.3	1.9	10.4
6	55.0	806.3	6.4	25.3	2.2	10.4
7	70.0	807.2	7.6	29.0	2.5	10.4
8	85.0	807.1	8.4	30.8	2.9	10.4
9	100.0	807.2	9.1	32.6	3.2	10.4
10	115.0	807.5	10.0	34.4	2.6	10.4
11	130.0	808.0	10.5	36.1	2.5	10.4
12	145.0	807.5	11.3	34.4	2.2	13.5
13	160.0	807.5	12.0	36.1	2.6	13.5
14	175.0	807.4	12.7	39.5	2.7	13.5
15	180.0	807.4	13.1	41.1	3.2	13.5

Table III.14 Experimental Data for Run Number 14.

Experimental Run # 15						
Ash Type: Fly		Size: 89 μ m	Mass: 75 gm			
Gas Flow (l/min):		Chlorine: 3.5	CO: 3.5			
Fluid Coke: Size: 125 μ m		Mass: 300 gm				
Average Reaction Temperature: 911 $^{\circ}$ C						
Maximum Temperature Reached Initially: 936 $^{\circ}$ C						
Average Pressure Drop: 113 cm H ₂ O						
Loss due to Carry over: 7 gm						
Sample No.	Time min	Temp. ($^{\circ}$ C)	% of Metal Recovered			
			Al	Fe	Si	Ti
1	0.0	909.2	0.0	0.0	0.0	0.0
2	5.0	925.0	8.3	60.8	1.6	14.2
3	10.0	916.2	8.1	63.5	1.4	14.2
4	23.0	909.0	12.2	68.6	2.1	21.1
5	30.0	909.5	13.3	71.2	2.1	21.1
6	45.0	909.3	15.3	76.2	2.7	21.1
7	60.0	909.4	17.3	81.1	3.0	21.1
8	75.0	910.0	18.1	81.2	2.6	27.7
9	90.0	910.2	20.8	86.0	3.5	27.7
10	105.0	910.2	22.0	86.0	3.5	27.7
11	120.0	909.9	23.7	90.8	3.2	27.7
12	135.0	909.7	25.0	93.1	3.7	27.7
13	150.0	910.5	26.3	97.7	4.1	27.7
14	165.0	910.0	27.2	97.7	5.0	33.8
15	180.0	909.5	27.9	99.8	5.3	27.7
16	180.0+	---	28.8	100.0	5.1	27.8

Table III.15 Experimental Data for Run Number 15.

Experimental Run # 16						
Ash Type: Fly		Size: 125 μ m	Mass: 100 gm			
Gas Flow (l/min):		Chlorine: 4.1	CO: 4.1			
Fluid Coke: Size: 89 μ m		Mass: 300 gm				
Average Reaction Temperature: 951 $^{\circ}$ C						
Maximum Temperature Reached Initially: 971 $^{\circ}$ C						
Average Pressure Drop: 102 cm H ₂ O						
Loss due to Carry over: 5 gm						
Sample No.	Time min	Temp. ($^{\circ}$ C)	% of Metal Recovered			
			Al	Fe	Si	Ti
1	0.0	950.1	0.0	0.0	0.0	0.0
2	5.0	965.6	4.9	61.3	1.4	8.1
3	10.0	959.4	5.7	63.7	1.4	8.1
4	20.0	949.2	7.1	68.5	1.4	8.1
5	30.0	949.6	8.4	68.5	1.2	12.1
6	40.0	949.8	9.8	75.5	1.7	12.1
7	50.0	950.0	10.8	77.8	1.9	12.1
8	60.0	950.2	12.0	80.1	2.2	12.1
9	75.0	949.5	13.5	82.3	2.2	15.8
10	90.0	950.5	15.6	89.0	2.8	15.8
11	105.0	950.0	17.4	91.2	2.9	15.8
12	120.0	950.4	18.6	95.6	3.5	15.8
13	135.0	950.8	20.6	97.7	3.6	19.4
14	150.0	950.3	21.9	99.8	4.2	19.4
15	160.0	950.4	22.9	99.8	4.4	22.9
16	160.0+	---	22.9	100.0	4.6	22.9

Table III.16 Experimental Data for Run Number 16.

Experimental Run # 17						
Ash Type: Fly		Size: 125 μ m	Mass: 100 gm			
Gas Flow (l/min):		Chlorine: 4.1	Nitrogen: 4.1			
Fluid Coke: Size: 169 μ m		Mass: 300 gm				
Average Reaction Temperature: 951 $^{\circ}$ C						
Maximum Temperature Reached Initially: 972 $^{\circ}$ C						
Average Pressure Drop: 116 cm H ₂ O						
Loss due to Carry over: 7 gm						
Sample No.	Time min	Temp. ($^{\circ}$ C)	% of Metal Recovered			
			Al	Fe	Si	Ti
1	0.0	951.2	0.0	0.0	0.0	0.0
2	5.0	967.0	3.4	47.0	1.0	4.2
3	10.0	959.8	4.0	52.4	1.1	4.2
4	20.0	950.0	4.6	54.1	1.2	4.2
5	30.0	949.9	5.2	57.6	1.2	8.2
6	40.0	950.0	5.5	61.1	1.2	8.2
7	50.0	950.5	5.9	64.5	1.3	8.2
8	60.0	950.4	6.2	66.2	1.3	8.2
9	75.0	950.3	6.8	69.5	1.4	8.2
10	90.0	950.6	7.2	76.0	1.3	8.2
11	105.0	949.7	7.5	79.2	1.4	8.2
12	120.0	950.2	7.8	80.8	1.5	8.2
13	135.0	949.8	8.2	87.1	1.5	11.8
14	150.0	949.8	8.6	94.8	1.5	11.8
15	165.0	950.4	8.7	95.0	1.5	11.8
16	175.0	950.5	8.8	97.0	1.5	11.8
17	175.0+	---	9.2	98.2	1.5	11.8

Table III.17 Experimental Data for Run Number 17.

Experimental Run # 18						
Ash Type: Fly		Size: 125 μ m	Mass: 40 gm			
Gas Flow (l/min):		Chlorine: 4.1	CO: 4.1			
Fluid Coke: Size: 225 μ m		Mass: 360 gm				
Average Reaction Temperature: 952 $^{\circ}$ C						
Maximum Temperature Reached Initially: 984 $^{\circ}$ C						
Average Pressure Drop: 106 cm H ₂ O						
Loss due to Carry over: 6 gm						
Sample No.	Time min	Temp. ($^{\circ}$ C)	% of Metal Recovered			
			Al	Fe	Si	Ti
1	0.0	952.0	0.0	0.0	0.0	0.0
2	5.0	977.5	6.2	42.8	1.2	9.1
3	10.0	960.5	6.5	46.3	1.3	9.1
4	20.0	948.7	7.2	46.3	1.4	9.1
5	30.0	950.2	8.3	49.7	1.7	17.9
6	40.0	950.4	9.6	53.1	1.8	17.9
7	50.0	950.5	11.0	56.5	2.0	17.9
8	60.0	950.6	12.0	59.8	2.2	17.9
9	75.0	950.3	13.7	63.0	2.5	17.9
10	90.0	950.5	15.3	66.3	2.7	17.9
11	105.0	950.7	16.9	69.5	3.0	17.9
12	120.0	950.8	18.2	72.6	3.2	17.9
13	135.0	950.2	19.8	81.9	3.4	17.9
14	150.0	950.5	20.7	97.2	3.5	17.9
15	150.0+	---	21.7	99.0	3.5	17.9

Table III.18 Experimental Data for Run Number 18:

Experimental Run # 19						

Ash Type: Fly		Size: 125 μ m	Mass: 100 gm			
Gas Flow (l/min):		Chlorine: 4.1	CO: 4.1			
Fluid Coke: Size: 169 μ m		Mass: 300 gm				
Average Reaction Temperature: 912 $^{\circ}$ C						
Maximum Temperature Reached Initially: 942 $^{\circ}$ C						
Average Pressure Drop: 99 cm H ₂ O						
Loss due to Carry over: 6 gm						
Sample No.	Time min	Temp. ($^{\circ}$ C)	% of Metal Recovered			
			Al	Fe	Si	Ti
1	0.0	913.0	0.0	0.0	0.0	0.0
2	5.0	938.0	5.7	36.6	1.3	7.3
3	10.0	922.8	6.4	36.6	1.3	10.9
4	20.0	909.3	7.6	39.7	1.9	10.9
5	30.0	910.0	9.3	42.7	2.0	10.9
6	40.0	911.0	10.2	44.3	2.3	10.9
7	50.0	910.6	11.3	47.3	2.5	10.9
8	60.0	910.2	12.5	48.7	2.6	14.4
9	70.0	910.9	13.3	51.7	2.9	14.4
10	80.0	909.9	14.5	53.1	3.3	14.4
11	90.0	910.0	15.5	57.4	3.4	14.4
12	100.0	910.0	16.5	60.2	3.7	14.4
13	110.0	910.0	17.7	65.8	3.8	14.4
14	120.0	910.2	18.7	69.9	4.0	17.5
15	130.0	910.4	19.8	76.7	4.1	17.5
16	140.0	909.9	20.7	83.3	4.6	17.5
17	150.0	909.5	21.3	88.6	4.6	17.5
18	150.0+	---	21.4	91.2	4.8	17.5

Table III.19 Experimental Data for Run Number 19.

Experimental Run # 20						

Ash Type: Fly		Size: 89 μ m	Mass: 100 gm			
Gas Flow (l/min):		Chlorine: 4.6	CO: 2.3			
Fluid Coke: Size: 125 μ m		Mass: 300 gm				
Average Reaction Temperature: 920 $^{\circ}$ C						
Maximum Temperature Reached Initially: 948 $^{\circ}$ C						
Average Pressure Drop: 89 cm H ₂ O						
Loss due to Carry over: 8 gm						
Sample No.	Time min	Temp. ($^{\circ}$ C)	% of Metal Recovered			
			Al	Fe	Si	Ti
1	0.0	910.6	0.0	0.0	0.0	0.0
2	5.0	937.6	7.7	44.5	1.6	19.0
3	12.0	925.0	8.4	46.7	1.7	19.0
4	15.0	920.5	8.4	46.7	2.2	19.0
5	20.0	916.0	8.7	46.7	2.1	19.0
6	30.0	913.5	10.0	48.8	2.6	19.0
7	33.0	912.8	10.2	50.9	2.6	19.0
8	35.0	---	10.8	50.9	2.3	27.9

Table III.20 Experimental Data for Run Number 20.

Experimental run # 21						

Ash Type: Fly		Size: 89µm	Mass: 100 gm			
Gas Flow (l/min):		Chlorine: 3.5	CO: 3.5			
Fluid Coke: Size: 125µm		Mass: 300 gm				
Average Reaction Temperature: 951°C						
Maximum Temperature Reached Initially: 975°C						
Average Pressure Drop: 90 cm H ₂ O						
Loss due to Carry over: 7 gm						
Sample No.	Time min	Temp. (°C)	% of Metal Recovered			
			Al	Fe	Si	Ti
1	0.0	947.3	0.0	0.0	0.0	0.0
2	5.0	964.4	6.8	43.5	1.3	10.8
3	10.0	951.4	7.0	45.1	1.3	10.8
4	20.0	949.4	8.5	46.7	1.8	16.1
5	30.0	950.0	9.6	49.8	2.4	16.1
6	40.0	950.7	11.0	52.8	2.5	21.3
7	50.0	950.3	12.1	54.3	2.5	21.3
8	60.0	951.2	13.1	55.8	2.6	21.3
9	70.0	951.0	15.1	60.3	3.0	21.3
10	80.0	950.8	15.4	60.3	3.0	21.3
11	90.0	951.2	17.2	58.8	3.7	26.2
12	102.0	950.7	19.1	64.5	3.7	26.2
13	110.0	950.8	19.7	65.9	3.9	26.2
14	120.0	950.1	20.7	71.5	4.4	26.2
15	131.0	950.8	22.2	76.9	4.4	30.8
16	140.0	950.5	22.7	86.4	4.5	30.8
17	150.0	950.4	23.5	90.4	5.1	30.8
18	150.0+	---	23:1	96.9	4.9	30.8

Table III.21 Experimental Data for Run Number 21.

Experimental Run # 22						

Ash Type: Fly		Size: 89µm	Mass: 100 gm			
Gas Flow (l/min):		Chlorine: 4.6	CO: 2.3			
Fluid Coke: Size: 125µm		Mass: 300 gm				
Average Reaction Temperature: 947°C						
Maximum Temperature Reached Initially: 981°C						
Average Pressure Drop: 92 cm H ₂ O						
Loss due to Carry over: 8 gm						
Sample No.	Time min	Temp. (°C)	% of Metal Recovered			
			Al	Fe	Si	Ti
1	0.0	951.8	0.0	0.0	0.0	0.0
2	5.0	970.9	6.8	44.7	2.4	15.6
3	10.0	952.5	7.9	44.7	2.6	15.6
4	20.0	949.7	9.9	50.9	2.9	15.6
5	30.0	958.0	11.8	50.9	2.9	20.6
6	40.0	949.8	12.9	52.9	3.6	20.6
7	50.0	949.3	15.6	54.9	3.7	25.5
8	60.5	944.0	16.3	56.9	4.1	25.5
9	70.0	943.8	17.0	58.9	4.0	25.5
10	80.0	942.5	18.8	62.7	4.4	25.5
11	90.0	939.8	19.4	64.6	5.0	25.5
12	100.0	938.6	20.9	72.1	4.4	25.5
13	110.0	940.6	22.3	75.9	4.8	25.5
14	120.0	940.6	24.9	86.8	5.0	25.5
15	130.0	940.5	26.4	90.0	5.3	29.9
16	130.0+	---	25.9	94.0	5.3	29.9

Table III.22 Experimental Data for Run Number 22.

Experimental Run # 23						
Ash Type: Fly Size: 125 μ m Mass: 100 gm Gas Flow (l/min): Chlorine: 5.2 CO: 2.6 Fluid Coke: Size: 169 μ m Mass: 300 gm Average Reaction Temperature: 912 $^{\circ}$ C Maximum Temperature Reached Initially: 951 $^{\circ}$ C Average Pressure Drop: 76 cm H ₂ O Loss due to Carry over: 6 gm						
Sample No.	Time min	Temp. ($^{\circ}$ C)	% of Metal Recovered			
			Al	Fe	Si	Ti
1	0.0	912.0	0.0	0.0	0.0	0.0
2	5.0	945.1	8.0	45.7	1.8	10.0
3	10.0	923.6	9.1	45.7	1.9	13.3
4	20.0	909.7	10.5	47.5	2.3	13.3
5	30.0	909.9	11.1	47.5	2.6	13.3
6	40.0	910.0	12.5	51.0	2.8	13.3
7	50.0	910.4	14.1	52.7	3.2	16.4
8	60.0	910.4	15.4	54.4	3.4	16.4
9	70.5	910.6	16.8	57.7	3.7	16.4
10	80.0	910.3	17.1	54.4	3.7	19.4
11	90.0	910.7	19.5	57.7	4.2	19.4
12	100.0	910.8	20.5	56.1	4.3	19.4
13	110.0	910.6	21.5	59.3	4.6	19.4
14	120.0	910.8	21.9	60.8	4.9	19.4
15	130.0	910.7	23.0	60.8	4.3	19.4
16	130.0+	---	23.0	60.9	4.8	19.4

Table III.23 Experimental Data for Run Number 23.

Experimental Run # 24						
Ash Type: Fly Size: 89 μ m Mass: 100 gm Gas Flow (l/min): Chlorine: 5.2 CO: 2.6 Fluid Coke: Size: 125 μ m Mass: 300 gm Average Reaction Temperature: 912 $^{\circ}$ C Maximum Temperature Reached Initially: 959 $^{\circ}$ C Average Pressure Drop: 91 cm H ₂ O Loss due to Carry over: 8 gm						
Sample No.	Time min	Temp. ($^{\circ}$ C)	% of Metal Recovered			
			Al	Fe	Si	Ti
1	0.0	909.5	0.0	0.0	0.0	0.0
2	5.0	945.0	8.5	47.0	2.2	15.3
3	10.0	920.5	9.2	47.0	2.3	15.3
4	20.0	910.1	10.5	45.1	2.5	15.3
5	30.0	910.7	11.8	45.1	2.7	15.3
6	40.0	911.5	12.9	45.1	2.8	15.3
7	50.0	910.9	14.4	46.9	3.0	15.3
8	60.0	910.6	15.5	50.4	3.0	15.3
9	70.0	910.8	16.4	57.3	3.2	15.3
10	80.0	910.6	17.4	60.7	3.5	15.3
11	90.0	910.9	18.6	65.7	3.7	15.3
12	100.0	910.1	19.6	72.4	3.8	15.3
13	110.0	910.2	21.1	75.7	4.1	15.3
14	120.0	909.7	22.3	83.8	4.5	19.6
15	130.0	909.9	23.4	88.5	4.6	19.6
16	130.0+	---	23.6	98.0	4.7	19.6

Table III.24 Experimental Data for Run Number 24.

Experimental Run # 25						

Ash Type: Fly		Size: 125 μ m	Mass: 100 gm			
Gas Flow (l/min):		Chlorine: 5.2	CO: 2.6			
Fluid Coke: Size: 169 μ m		Mass: 300 gm				
Average Reaction Temperature: 951 $^{\circ}$ C						
Maximum Temperature Reached Initially: 974 $^{\circ}$ C						
Average Pressure Drop: 100 cm H ₂ O						
Loss due to Carry over: 7 gm						
Sample No.	Time min	Temp. ($^{\circ}$ C)	% of Metal Recovered			
			Al	Fe	Si	Ti
1	0.0	952.2	0.0	0.0	0.0	0.0
2	5.0	969.5	7.3	50.2	2.2	7.1
3	10.0	956.1	7.6	50.2	2.0	10.6
4	20.0	950.4	9.4	53.8	2.5	10.6
5	30.0	950.6	10.3	57.4	2.5	14.0
6	40.0	950.6	12.4	59.2	2.7	14.0
7	50.0	950.5	13.2	64.4	3.3	14.0
8	60.0	950.7	13.6	64.4	3.6	17.3
9	70.0	950.5	15.3	66.2	3.5	17.3
10	80.0	949.5	17.0	67.8	3.8	17.3
11	90.5	950.0	17.8	67.8	4.0	20.5
12	100.0	949.8	18.6	71.1	4.3	17.4
13	111.0	950.3	19.7	74.3	4.9	20.5
14	120.0	950.0	21.2	74.3	6.2	17.4
15	130.0	949.8	23.2	80.6	5.8	20.4
16	130.0+	---	22.8	83.7	5.8	20.4

Table III.25 Experimental Data for Run Number 25.

Appendix IV

Gaseous Diffusion in Molten Salts

Sample calculations will be performed to demonstrate the slow rates of diffusion of a gas through a film of molten salt. The diffusion of chlorine, in particular, is estimated in a micro layer of molten NaCl over a spherical particle. The results will be compared with an actual gas consumption rate for the case of fly ash chlorination. Though the computations are done only for Cl₂-NaCl system, similar results can be obtained for other salts as well.

The solubility of chlorine in molten chlorides seems to involve an interaction between the dissolved gas and the melt (61). Such interaction will introduce serious non-idealities to the the problem at hand. Simplifying assumptions will be made where data are lacking. The following procedure will only give approximate estimates accurate to an order of magnitude.

IV.1 Physical Properties Estimation

The diffusivity, D , of a gas through a liquid film is approximated by Wilke-Chang equation (62). The diffusion of chlorine in molten NaCl is calculated at 950°C.

$$D = 7.4 \times 10^{-8} \frac{T(y \text{ MW})^{0.5}}{\mu_{cp} V^{0.6}} \quad (\text{IV.1})$$

where, D = Diffusivity, cm²/s

MW = Mole weight of solvent

T = Temperature, K

μ_{cp} = Viscosity of solvent, cp

V = Molar volume of solvent, cm³/mol

y = an association factor.

A viscosity correlation for molten NaCl is given by Janz et al (63).

$$\mu_{cp} = 81.9 - 0.1856T + 1.428 \times 10^{-3} T^2 - 3.7 \times 10^{-8} T^3 \quad (\text{IV.2})$$

The calculated μ_{NaCl} is 1923 cp at 1223 K. The association factor, y, is assumed 1.0, and V = 48.4 is given by Danckwerts (62). With these values, the diffusivity of Cl₂ in NaCl is calculated using Equation (IV.1) to be:

$$D = 7.4 \times 10^{-8} \frac{(1223)(58.5)^{0.5}}{(1923)(48.4)^{0.6}}$$

$$= 3.5 \times 10^{-8} \text{ cm}^2/\text{s}$$

The solubility of chlorine in molten NaCl is calculated using Henry's constant (64) given as 0.83 x 10⁻⁷ mol Cl₂/(mol NaCl Pa). The solubility will be calculated for chlorine fraction of 50% in a gas mixture at atmospheric pressure (660 mmHg).

$$c = 0.83 \times 10^{-7} \times 1.013 \times 10^5 \times 0.5 \times \frac{660}{760}$$
$$= 0.365 \times 10^{-2} \text{ mol Cl}_2/\text{mol NaCl}$$

The density is calculated from the correlation given by Janz et al (63):

$$P_{\text{NaCl}} = 2.14 - 0.543 \times 10^{-3} \times T \quad (\text{IV.3})$$
$$= 1.48 \text{ g/cm}^3$$

Hence, the molar density = $\frac{1.48}{58.5} = 2.53 \times 10^{-2} \text{ mol/cm}^3$

The solubility on a volumetric basis is

$$c = 0.365 \times 10^{-2} \times 2.53 \times 10^{-2}$$
$$= 0.924 \times 10^{-4} \text{ mol Cl}_2/\text{cm}^3$$

IV.2 Rate of Diffusion

The rate of diffusion of chlorine is calculated using a model described by Bird et al (65) for the diffusion of a gas through a spherical film shell. The model is shown as Figure 8.4. Very briefly, the procedure is as follows:

Mass balance on a spherical film shell leads to

$$\frac{d}{dr} \{ r^2 N_a \} = 0 \quad (\text{IV.4})$$

The appropriate substitution of N_a for the case where counter diffusion is absent leads to

$$\frac{d}{dr} \left\{ r^2 \frac{c D}{(1-X_a)} \frac{dX_a}{dr} \right\} = 0 \quad (\text{IV.5})$$

At constant temperature, Equation (IV.5) is integrated to give

$$\left[\frac{(1-X_a)}{(1-X_a)_1} \right] = \left[\frac{(1-X_a)_2}{(1-X_a)_1} \right]^{\frac{(1/r_1 - 1/r)}{(1/r_1 - 1/r_2)}} \quad (\text{IV.6})$$

The molar flux is N_a multiplied by the shell area for the flow.

$$\begin{aligned} W_a &= 4\pi r^2 N_a \quad \text{at } r=r_1 \quad (\text{IV.7}) \\ &= \frac{4 \pi c D}{(1/r_1) - (1/r_2)} \ln \frac{(1-X_a)_2}{(1-X_a)_1} \end{aligned}$$

The flux calculated by this equation gives the rate of gas flow assuming there is no other resistance to the flow. Hence, $X_{a2} = 0$ (at the reaction surface) and $X_{a1} = c$ (the solubility of gas in molten salt). It will be assumed that the diameter of particle is $125\mu\text{m}$ and a film thickness of $0.1\mu\text{m}$ is present on the particle surface. The corresponding values of r_1 and r_2 are $62.6\mu\text{m}$ and $62.5\mu\text{m}$ respectively. With the values of c and D calculated earlier, the molar flux is now calculated using Equation (IV.7):

$$\begin{aligned} W_a &= \frac{4 \pi 0.924 \times 10^{-4} \times 3.5 \times 10^{-8}}{((1/62.6) - (1/62.5)) \times 10^4} \ln \left[\frac{(1-0.00367)}{1} \right] \\ &= 0.585 \times 10^{-12} \text{ mol/s} \quad \text{or, } 2.1 \times 10^{-9} \text{ mol/h} \end{aligned}$$

The rate of diffusion of chlorine through a $0.1\mu\text{m}$ thick film of molten NaCl is 2.1×10^{-9} mol/h. Similar values are calculated for other film thicknesses as well.

When the film thicknesses are $1\mu\text{m}$ and $5\mu\text{m}$, the molar fluxes are 2.13×10^{-10} and 4.5×10^{-12} mol/h, respectively.

These rates are based on a stationary spherical particle surface. It can be seen that the rate is an inverse function of the film thickness. The concentration of gas in melt and the diffusivity terms have a direct proportionality with the rate term. It is reiterated that the calculations are based on the assumption of no other resistance to mass transfer. With the presence of other resistances, the resultant flux will be even smaller. The rate will increase, however, if the particle is non-spherical or has larger surface area available.

IV.3 Comparison with Experimental Rates

The experimental data in terms of the yields of metal chlorides from one of the runs with coke and CO will be used for the comparison. The data of experiment #16 are chosen to calculate the composite rate of chlorine consumption. This particular run was made with $125\mu\text{m}$ particles at 950°C and with 50% Cl_2 in the feed gas. It is important to note that the diffusion through molten salts appears most dominating where the

yield curve is a straight line. It will be assumed, once again, that this diffusion step is considered to be the rate controlling step. The chlorine consumption for only Al, Si, Fe and Ti is being considered. The yield data at 1-hour and 2-hour periods are obtained for these 4 metals graphically. It is assumed that complete chlorination of all other metallic species has occurred within 1 hour.

The computations of total chlorine consumption in one hour are presented in Table IV.1. The amount of chlorine required to achieve the experimental chlorination is 6.77 g Cl₂/h. On a molar rate basis, this is equivalent to 0.0954 mol Cl₂/h.

It is shown in Chapter 5 that the ash particles are not simple solid spheres. The ratio of actual area to the calculated area for spheres is 170 for 125µm diameter fly ash particles. The molar flux value, calculated previously in Section IV.2, should be multiplied by this ratio to obtain a more realistic approximation of the rate of diffusion. In addition, the flux calculation is for one ash particle. The experimental rate is based on 100 gram of ash sample. Assuming that the density of fly ash is 2.2 g/cm³, there are approximately 4.45×10^7 particles of 125µm diameter in 100 gram of ash.

Element	Yield, %		Fraction in Ash %	Mass of each Metal Chlorinated in 1 hour Basis: 100 gm ash	Chlorine Required gm/h
	1-hour	2-hour			
Aluminum	11.5	19.5	16.0	1.20	4.73
Iron	81.0	95.0	1.3	0.18	0.34
Silicon	2.3	3.5	27.4	0.33	1.67
Titanium	12.1	15.8	0.4	0.01	0.03
Total	--	--	--	--	6.77

Table IV.1 Calculation of Chlorine Consumption Rate.

Hence the modified value of the calculated flux for 1 μ m film thickness is

$$\begin{aligned} W_a &= 2.1 \times 10^{-10} \times 4.45 \times 10^7 \times 170 \\ &= 0.161 \text{ mol/h} \end{aligned}$$

Similarly, the flux corresponding to a 5 μ m film thickness is 0.034 mol/h.

The chlorine consumption rate from the experimental data is 0.0954 mol/h. Clearly, the experimental rate falls within the two flux values calculated above, and a film thickness of the order of 1 to 5 μ m is predicted. Similar calculations can be repeated for other salts such as CaCl₂, KCl and MgCl₂. The flux in each case is expected to be of the same order of magnitude.

The complications will arise, however, when a mixture of the molten salts is considered. The diffusion of chlorine in molten chlorides is not clearly understood. As mentioned previously, the dissolution of chlorine involves an interaction between the gas and the liquid phases (61). The estimation of diffusivity of chlorine and other physical properties for a complex mixture will present serious difficulties.